● REVIEW ●

A Review on Development, Challenges, and Future Perspectives of Ensemble Forecast

Jing CHEN[1,2*], Yuejian ZHU[1,2], Wansuo DUAN[3], Xiefei ZHI[4], Jinzhong MIN[4], Xiaoli LI[1,2], Guo DENG[1,2], Huiling YUAN[5], Jie FENG[6], Jun DU[7], Qiaoping LI[1,2], Jiandong GONG[1,2], Xueshun SHEN[1,2], and Mu MU[6]

1 *CMA Earth System Modeling and Prediction Centre (CEMC), China Meteorological Administration (CMA), Beijing* 100081, *China*
2 *State Key Laboratory of Severe Weather Meteorological Science and Technology (LaSW), CEMC, Beijing* 100081, *China*
3 *Institute of Atmospheric Physics, Chinese Academy of Sciences, Beijing* 100029, *China*
4 *Nanjing University of Information Science & Technology, Nanjing* 210044, *China*
5 *Nanjing University, Nanjing* 210008, *China*
6 *Fudan University, Shanghai* 200433, *China*
7 *National Centers for Environmental Predictions, National Oceanic and Atmospheric Administration, Maryland* 20740, *USA*

(Received 5 January 2025; in final form 5 March 2025)

ABSTRACT

This paper reviews the development of ensemble weather forecast and the primary techniques employed in the main ensemble prediction systems (EPSs) designed by China and other countries. Here, the emphasis is placed on the advancements in the China Meteorological Administration (CMA) global and regional ensemble prediction systems (i.e., CMA-GEPS and CMA-REPS), with particular attention to operational technologies such as initial and model perturbation methods and the applications of ensemble forecast. Through comparative verification with EPSs from other leading international numerical weather prediction (NWP) centers, CMA's EPSs demonstrate forecast skills comparable to its global counterparts. As EPSs progress to convective scales and coupled systems between sea, land, air, and ice, the paper addresses some key challenges in ensemble forecast technologies across the aspects of operation, science, integration of artificial intelligence (AI), merging of weather and climate models, and challenging user requirements. Finally, a summary of conclusions and future perspectives on ensemble forecast are provided.

Key words: ensemble forecast, method, China Meteorological Administration (CMA) ensemble forecast, review

Citation: Chen, J., Y. J. Zhu, W. S. Duan, et al., 2025: A review on development, challenges, and future perspectives of ensemble forecast. *J. Meteor. Res.*, **39**(3), 534–558, https://doi.org/10.1007/s13351-025-4909-4.

1. Introduction

Numerical weather prediction (NWP) is one of the greatest scientific advancements of the 20th century, often described as a "quiet revolution" (Bauer et al., 2015; Shen et al., 2020). Among its key achievements, four-dimensional variational data assimilation (4DVar) and ensemble forecasting are regarded as two major milestones. The atmospheric system is inherently nonlinear, characterized by chaos that is sensitive to minor initial perturbations. Even with ideal numerical models, uncertainties in the initial states—arising from errors in observations and assimilation systems—lead to significant forecast errors as the forecast lead time increases (Lorenz, 1963; Chou, 1986; Mu et al., 2003, 2011). Additionally, numerical models employ discretization schemes, sub-grid parameterizations, and other approximations to represent the dynamical and physical processes of the atmosphere. Consequently, single deterministic NWP has inherent forecast uncertainty (Li et al., 2000; Arakawa, 2004; Chen et al., 2004). Quantifying this uncertainty has thus become a critical focus for NWP. The ensemble prediction system (EPS), which may transform single deterministic numerical forecasts into probability density function (PDF) distributions and estimate the uncertainty of deterministic numerical forecasts, was first developed through the Monte Carlo method (Epstein, 1969; Leith, 1974).

Theoretically, the evolution of the PDF over time can be described by the Liouville equation. However, solving this equation is highly challenging and practically in-

Supported by the National Natural Science Foundation of China (U2242213 and 42341209).

*Corresponding author: chenj@cma.gov.cn

feasible, even for a nonlinear system with only a few degrees of freedom. To address this issue, the ensemble forecasting method was developed (Molteni et al., 1996). This method utilizes specific mathematical techniques to generate a set of initial conditions, each potentially representing the true state of the atmosphere. These initial conditions are then integrated by a numerical model to produce an ensemble of forecasts, from which the PDF distribution of future weather variables can be derived. When the initial condition ensemble accurately captures the distribution of initial analysis errors and the model has adequate precision, the ensemble forecast can reliably approximate the atmospheric state's PDF.

The core challenge in ensemble forecasting lies in appropriately representing error sources and accurately estimating uncertainties in NWP. The well-documented sources of NWP errors originate from both initial conditions and the model's inherent limitations. Correspondingly, ensemble forecasting methods are derived from the first (initial condition) and second (model) predictability theories. Various perturbation methods are designed to represent initial condition errors and model uncertainties, leading to the development of initial condition and model perturbation methods (Chen et al., 2002; Du et al., 2018). In terms of initial condition perturbation, methods such as the singular vector (SV; Buizza, 1997), the breeding of growing mode (BGM; Toth and Kalnay, 1993), the perturbed observations (Houtekamer and Derome, 1995), the ensemble transform Kalman filter (ETKF; Wang and Bishop, 2003; Wei et al., 2006), the ensemble transform with rescaling (ETR; Wei et al., 2008), the ensemble square root filter (EnSRF; Whitaker and Hamill, 2002; Zhou et al., 2022), and hybrid perturbations combining SV perturbations with ensemble data assimilation (EDA; Isaksen et al., 2010) have been developed. In terms of model perturbation, proposed methods include the multi-physics scheme (Chen et al., 2003), the stochastically perturbed parameterization tendencies (SPPT; Buizza et al., 1999; Tan et al., 2013), the stochastic kinetic energy backscatter scheme (SKEB; Shutts, 2005; Peng et al., 2019), and the stochastically perturbed parameterization (SPP; Jankov et al., 2019; Xu et al., 2019). These studies have significantly contributed to the continuous improvement of operational EPSs in terms of overall performance and reliability.

Since the 1990s, significant progress has been made in operational ensemble forecasting, driven by advancements in ensemble forecasting theory and technology. In 1992, the ECMWF and the NCEP established the first global medium-range EPS, marking a major milestone in operational ensemble forecasting (Toth and Kalnay, 1993; Molteni et al., 1996; Buizza, 1997). Following remarkable improvements in model technology and computer power, ECMWF took a pioneering step in June 2023 by upgrading its operational NWP system. The traditional EPS combined a high-resolution deterministic model with a lower-resolution ensemble forecast model. The new system, however, employs high-resolution models for both deterministic and ensemble forecasts, offering a more accurate representation of forecast uncertainty at higher resolutions. In 2006, the World Meteorological Organization (WMO) launched the Observing System Research and Predictability Experiment (THORPEX) Interactive Grand Global Ensemble (TIGGE) as an important component of the THORPEX initiative (Jiao, 2010). In recent years, ensemble forecasting has expanded to fields such as data assimilation, physical process parameterization, flood forecasting, severe weather prediction, and typhoon track forecasting. The ensemble forecasting approach has become an integral part of the entire operational NWP process (Buizza et al., 2018).

Chinese scientists have also been actively engaged in ensemble forecasting research and operations since the early stages (Li et al., 1997; Chen et al., 2002; Li and Chen, 2002). In terms of initial condition perturbation, methods such as conditional nonlinear optimal perturbation (CNOP; Mu et al., 2003; Duan and Huo, 2016), the heterogeneous physical mode method (Chen et al., 2005), nonlinear local Lyapunov vectors (NLLV; Feng et al., 2014), multi-scale hybrid initial perturbation (Zhang et al., 2015), and multi-scale SV (Ye et al., 2020) have been proposed. Regarding model perturbation, studies have focused on methods such as the multi-physics scheme (Chen et al., 2003), SPPT (Tan et al., 2013), nonlinear forcing SV (NFSV; Duan et al., 2013), SPP (Xu et al., 2019), and a model tendency perturbation method combining systematic and random errors (Han et al., 2023). China's operational EPS has evolved from initially relying on imported spectral models to the self-developed GRAPES-EPS (Chen and Li, 2020). The initial perturbation methods have advanced from the ETKF (Ma X. L. et al., 2008; Long et al., 2011; Zhang et al., 2017) to the multi-scale SV initial perturbation method (Liu et al., 2011; Ye et al., 2020). Furthermore, a combination of SPPT and SKEB has been implemented to generate model perturbations. These advancements collectively represent a milestone in the development of China's EPSs (Chen and Li, 2020; Shen et al., 2020).

This paper first reviews the ensemble weather forecasting methods and the primary techniques employed in

the main EPSs designed by China and other countries, emphasizing the development of China Meteorological Administration (CMA) global EPS (CMA-GEPS) and regional EPS (CMA-REPS), including operational technologies, initial and model perturbation methods, and the applications of ensemble forecast. Besides, a comparison of the EPS settings and verification results between the CMA-GEPS and other major international NWP centers is presented. Furthermore, the paper addresses some of the key challenges in ensemble forecast technologies from the aspects of operation, science, integration with artificial intelligence (AI), merging of weather and climate models, and challenging user requirements. The summaries and future perspectives of ensemble forecast are concluded at the end.

2. Review of ensemble forecast methods

2.1 *Sources of initial errors and advances in initial perturbation methods*

Initial errors play a critical role in numerical simulations, primarily arising from inaccuracies in observation, as well as errors introduced during the processes of data assimilation. The initial condition perturbation (ICP) method, which aims to describe errors in model initial conditions, has been developed within global medium-range EPSs. The development of ICP methods has gone through several stages, from the initial human-generated random perturbations to statistically-based perturbation techniques, such as the Monte Carlo, BGM, SV, ETKF, and CNOP. These methods have been widely applied in the construction of various EPSs, providing effective information about forecasting uncertainty and enhancing prediction skill.

2.1.1 *Initial perturbation for estimating assimilation analysis errors*

The primary function of these methods is to estimate the error probability distribution in assimilated analyses. For instance, the Monte Carlo random perturbation method generates initial conditions by superimposing random noise or perturbations on control fields (Hollingsworth, 1979), while the time-lagged average method utilizes analyses from different past times as perturbed initial conditions (Hoffman and Kalnay, 1983). As an example, the initial version of the GEPS developed by the Canadian Meteorological Centre (CMC) employed Monte Carlo-based random perturbations of observations to create ensemble initial conditions (Houtekamer et al., 1996). With the development of data assimilation systems and EPSs, ensemble Kalman filter (EnKF) initial perturbation method, which randomly perturbed observation data, is used by Canada's EPS (Houtekamer and Mitchell, 2005) and the NCEP (Zhou et al., 2016). While these perturbation methods demonstrate advantages in effectively representing uncertainties in initial analysis errors and enabling generation of substantial ensemble members, they exhibit limitations including constrained growth of initial perturbation energy, insufficient ensemble spread, and inadequate characterization of forecast uncertainties. Recent innovations by Pan et al. (2021) and Wang et al. (2023) introduced an analysis-constrained method that effectively incorporates characteristics of assimilation analysis increments. This method improved initial perturbation quality and the consistency between ensemble spread and forecast error.

2.1.2 *Estimation of initial perturbations with the fastest error growth*

These types of initial perturbations are based on research findings in atmospheric predictability. By analyzing the direction and speed of numerical prediction error growth in phase space, perturbations are introduced along the most unstable directions in initial conditions. Representative methods include the SV developed based on nonlinear dynamical finite-time instability theory (Molteni et al., 1996; Yang et al., 2002; Liu et al., 2011) and the BGM employed by NCEP, in which random perturbations are cycled through a nonlinear model and scaled to generate the final fields (Toth and Kalnay, 1993). Both the two methods aim to capture initial errors in atmospheric baroclinic instability regions, representing the forecast uncertainty of large-scale unstable waves. The SV, often developed in conjunction with a 4D variational system, has clear physical significance and can achieve favorable results. It has been successfully applied in medium-range weather ensemble forecasting by ECMWF, Japan, China, and others. Moreover, Zhang et al. (2020) proposed an initial perturbation method combining ensemble sensitivity analysis (ESA) and BGM to represent the characteristics of initial analysis errors. The distribution of perturbations, which is derived from sensitivity modes and rapidly growing perturbations calculated by BGM, adapts to changes in weather conditions and provides accurate simulations of the location and intensity of convective systems. The BGM method is favored by operational forecasting centers due to its effectiveness, simplicity, and low computational cost. Additionally, the NCEP developed the ETR (Wei et al., 2008), a method similar to the BGM but with perturbation structures that are nearly orthogonal and may reduce the correlation among ensemble members.

The SV method has achieved significant success in

operational ensemble forecasting. However, since it relies on a linear approximation of the nonlinear model, it fails to fully capture the impact of nonlinear physical processes, which limits further improvements in ensemble forecast skill. Mu et al. (2003) proposed the CNOP method, which comprehensively considers the effects of nonlinear processes and identifies the fastest-growing initial perturbations in nonlinear models, thereby addressing the limitations of the SV. Duan and Huo (2016) extended the CNOP to different perturbation phase spaces, developing an orthogonal scheme for ensemble forecast initial perturbations. This method has been successfully applied in the study of typhoon track ensemble forecasting, demonstrating that the initial perturbations generated by orthogonal CNOP significantly improve the typhoon track forecasting skill, especially for abnormal tracks, compared to those generated by the SV and the BGM methods (Zhang H. et al., 2023).

To address the rapid growth of errors caused by convective instability in meso- and small-scale systems, Chen et al. (2005) proposed a new method, known as the Heterogeneous Physical Mode Method, for constructing initial perturbations in ensemble forecasting that targets convective instability and exhibits mesoscale motion characteristics. By identifying forecast deviations from different cumulus convective parameterization schemes, this method identifies regions sensitive to convection, extracts perturbation variables, structures, and magnitudes, and constructs perturbed initial conditions. Unlike traditional initial perturbation methods such as the BGM or SV, this approach perturbs the initial values in convectively unstable regions, thereby promoting rapid growth of the unstable perturbations related to convection.

2.1.3 *Estimating initial perturbations for multi-scale system errors*

Despite the continuous improvement in numerical weather prediction resolution, the rapid growth of multi-scale initial errors continues to significantly impact forecast skill. Limited-area models face dual challenges, i.e., insufficient large-scale initial error information and inadequate characterization of small-scale errors from dynamical downscaling. In response to these issues, Chinese scientists developed the hybrid initial condition perturbation method for enhanced ensemble perturbation generation (Wang Y. et al., 2014; Zhang et al., 2015; Zhuang et al., 2017; Ma et al., 2018). This method uses filtering and spectral analysis techniques to extract small-scale perturbations from regional ensemble forecasts and large-scale perturbations from global ensemble forecasts, and combines the two to generate the growth ICPs. The hybrid ICPs effectively represent both large- and small-scale uncertainties in the analysis, aligning more closely with the lateral boundary perturbations provided by global EPSs, thereby significantly improving the forecast skill of regional EPSs. Furthermore, the CMA (Ye et al., 2020; Liu et al., 2024) and the Japan Meteorological Agency (JMA; Ono et al., 2021) have conducted research on multiscale SV ICP methods based on regional and global ensemble prediction models. These studies have generated ICPs containing multiscale initial uncertainty, which more effectively reflect the multiscale variations in initial errors and improve both regional and global ensemble prediction performance.

In general, ensemble forecasts based on ICPs formed by analysis errors tend to show slightly higher forecast accuracy but a lower spread, while ensemble forecasts based on initial perturbations derived from dynamical instability growth theory generally exhibit an inverse pattern, i.e., a slightly higher spread but marginally lower accuracy (Pauluis and Schumacher, 2013).

2.2 *Model error sources and development of model perturbation methods*

Early ensemble forecasting studies primarily focused on initial perturbations. However, as research advanced, it became evident that addressing initial condition uncertainty alone could lead to drawbacks such as insufficient ensemble spread, which further results in systematically biased forecasts (Palmer et al., 2009). Therefore, it is necessary to consider the uncertainty caused by model errors or defects in ensemble forecasting. The model errors primarily originate from inadequate representations of both physical and dynamical processes in the numerical model (Mu et al., 2011). Currently, the predominant model errors considered by ensemble forecasting systems stem from imperfect representations of subgrid-scale parameterization processes.

2.2.1 *Estimation of model uncertainty*

The uncertainty of the physical process of the model is described by a combination of different physical parameterization schemes within the framework of a single model (Houtekamer et al., 1996), which is called a multi-physics scheme. This scheme was applied to the global EPS of Environment Canada in the early days. It has also been commonly used in regional ensemble forecasting in recent years (Stensrud et al., 2000; Chen et al., 2003; Zhi et al., 2013) to improve the probabilistic forecasting skill. Another model perturbation method is the multi-model method (Krishnamurti et al., 1999), which can represent the systematic bias in the forecasts of different models, so that the ensemble members can produce a larger ensemble spread, which greatly improves the accuracy of

medium-term forecasts and small- and medium-scale ensemble forecasts in limited areas (Zhang et al., 2017). However, since the ensemble members in multi-model or multi-physics schemes employ different models or physical processes, their physical consistency is compromised. This makes it challenging to satisfy the equal-likelihood requirement for members and increases the complexity of determining member weights for probability calculations (Berner et al., 2015). Consequently, the model perturbation method has been increasingly developed in recent years to estimate the uncertainty of the parameterization scheme of the model physical process.

2.2.2 *Estimation of physical parameterization scheme uncertainty*

Stochastic physical perturbation is now a standard technique for assessing physical parameterization uncertainty in modeling. The theoretical basis is to introduce a random process or factor to perturb some parameter values or related terms of a model (such as tendency and diffusion) to characterize the uncertainty of the model. This type of perturbation scheme mainly includes methods such as the stochastically perturbed physics parameterization tendency term (SPPT; Buizza et al., 1999; Yuan et al., 2016), stochastic kinetic energy backscattering (SKEB; Shutts, 2005), random parameters (RP; Bowler et al., 2008), and stochastically perturbed parameterization (SPP; Chen et al., 2003; Tan et al., 2013; Jankov et al., 2017).

The SPPT scheme employs spatiotemporally continuous random numbers conforming to a uniform distribution to multiplicatively perturb parameterized subgrid physical tendencies. By applying distinct perturbation values to different tendency terms, this method effectively enhances ensemble spread and improves probabilistic forecast reliability in ensemble forecasting systems (Li et al., 2008). The SPPT is currently the most widely adopted method among global NWP centers (Charron et al., 2010; Sanchez et al., 2016; Peng et al., 2020), yet it also has some drawbacks. For instance, perturbation amplitude may cause discontinuity and energy non-conservation in model top and near-surface fluxes, and the long-term integration will produce systematic bias (Leutbecher et al., 2017). Yuan et al. (2016) introduces SPPT technology to the CMA-REPS, which significantly improves the precipitation forecast of heavy rainfall in the late medium-range forecast. Qiao et al. (2017) developed a novel parameterization scheme for stochastic perturbation dissipation based on the uncertainty of the model dissipation term. It follows the same procedure as the SPPT method, but uses a recursive filter to generate smooth perturbations. It also uses horizontal and vertical localization to maintain the influence of perturbation in regions with strong wind shear, which effectively improves the systematically weak vortex intensity. Similar results have been demonstrated in perturbation studies of microphysical processes (Qiao et al., 2018).

The SKEB scheme targets excessive momentum dissipation errors in the numerical model's dynamic framework at truncated scales, compensating for dissipated energy effects on resolvable scales through stochastic perturbations. It has been applied in global medium-range ensemble forecasting (Berner et al., 2009; Zhou et al., 2017) and is being progressively implemented in regional convective ensemble forecasting (Cai et al., 2017; Yang et al., 2024). Peng et al. (2020) found that the combined application of the SKEB and the SPPT in the GRAPES global ensemble forecast can effectively improve the ensemble spread in the tropics. The SKEB scheme can excite possible instabilities in atmospheric motion (Berner et al., 2015), thereby producing larger ensemble spread and capturing low-probability events. However, due to the higher computational cost of the SKEB compared to the SPPT and the unsatisfactory balance between spread and root mean square error (RMSE), the usefulness of the SKEB scheme has gradually decreased. It is reported that the ECMWF has discontinued the operational implementation of this scheme (Chen C. H. et al., 2021).

The RP/SPP method characterizes model uncertainty by performing random perturbations of subjective empirical and semi-empirical parameters within physical parameterization schemes (Bowler et al., 2008), which represents the predicted uncertainty of small-scale system changes. Although this method improves the ensemble forecasting, it has certain irrationalities. For instance, the parameter values will change suddenly at a certain time (Jankov et al., 2019). In addition, it is found that the SPP method has a more significant effect on the parameters in cumulus convection and planetary boundary layer schemes (Xu et al., 2019). However, the RP/SPP method yields inadequate ensemble spread for medium- and extended-range forecasts (Leutbecher et al., 2017).

Beyond these three prevalent stochastic physical perturbation schemes, researchers have developed various approaches to address uncertainty sources in other model components, such as the stochastic trigger of convection (STC; Li et al., 2015), stochastic boundary-layer humidity (SHUM; Tompkins and Berner, 2008), vorticity confinement (VC; Steinhoff and Underhill, 1994), meso- and medium-scale terrain perturbation schemes (Li et al., 2017), and model tendency perturbation methods combining model systematic bias and random errors (Han et

al., 2023). Zhao and Torn (2022) applied an independent stochastic perturbation parameterization scheme to a single parametric perturbation, and the results showed that turbulent mixed stochastic perturbation can increase the ensemble standard deviation of typhoon intensity, while the impact of stochastic perturbation on microphysics, radiation, and cumulus tendencies is negligible. The SHUM scheme improves the consistency between ensemble spread and forecast error in the tropical regions, and reduces the ensemble mean forecast error. The SHUM is applied to the ensemble data assimilation module of the NCEP global forecast system EnKF/3DVar. The VC method is applied to the NCEP GEPS, which increases the subtropical ensemble spread. The model tendency perturbation method combining model systematic bias and random error reduces the systematic bias of the model, which is applied to the CMA-GEPS.

2.2.3 *Estimation of nonlinear characteristics of model error growth*

Accurately characterizing the nonlinear nature of model error growth remains a critical challenge for cutting-edge high-resolution ensemble forecasting systems. Wang et al. (2020) implemented the CNOP perturbation (CNOP-P) method in the GRAPES model for convection-scale ensemble forecasting. The experiments demonstrated enhanced ensemble spread in tropospheric humidity and temperature predictions, along with improved forecast reliability for near-surface variables and precipitation. Xu et al. (2022a) applied a nonlinear forcing SV method (NFSV), also known as CNOP forcing (CNOP-F). Duan and Zhou (2013) described the combined effects of model errors from different sources by superimposing NFSV perturbations with specific structures on top of SPPT perturbations, which better characterizes the impact of model uncertainty on convection-scale ensemble forecasting (Xu et al., 2022b). In addition, Zhang Y. C. et al. (2023) extended the NFSV to the orthogonal subspace of inclined perturbations and developed an orthogonal NFSV-based ensemble prediction model perturbation method. When applied to typhoon intensity ensemble prediction, this method demonstrated significantly higher forecasting skill than the SPPT and the SKEB, particularly in providing earlier warning information for predicting typhoon rapid intensification processes.

In summary, the multi-model and multi-physics schemes have been gradually eliminated due to the average error of members, the inequality of meteorological significance, and the complexity of probability calculation, while the stochastic physics perturbation method has received more and more attention. However, whether the representativeness and flow dependence of reasonable stochastic functions and their spatiotemporal correlation scales of random noises truly reflect the uncertainty of physical processes still need to be studied.

2.3 *Post-processing and verification assessment of ensemble forecast uncertainty information*

The EPS generates a vast array of data products. In contrast to a single deterministic forecast, ensemble forecasting can provide a probability distribution of possible future atmospheric states and characteristics of forecast uncertainty, demonstrating superior advantages in the early warning of extreme weather events (Du and Chen, 2010; Gao et al., 2019). The critical task in the post-processing of ensemble forecasts is to design appropriate post-processing techniques that provide meteorologically meaningful interpretations of the distribution of ensemble forecast products, as well as to extract similarities, discrepancies, and extreme information among the ensemble forecast members (Williams et al., 2014). The primary techniques currently employed in ensemble forecast post-processing include obtaining probabilistic forecast information to describe forecast uncertainty, correcting systematic model errors, and extracting extreme weather forecast information from the tails of the ensemble forecast probability distribution.

2.3.1 *Probability forecast information based on ensemble prediction*

The ensemble mean and ensemble spread are two fundamental products of ensemble forecasting. The ensemble mean represents the primary level of information in ensemble forecast products. It filters out unpredictable elements from the ensemble members, providing an overall forecast trend. However, due to its inherent smoothing effect, the ensemble mean might not completely retain extreme values in weather events. The ensemble spread is a measure of the uncertainty in ensemble forecasting or the amplitude of variation of ensemble members relative to the ensemble mean. It can be measured by the standard deviation of the ensemble members relative to the ensemble mean forecast, or by the average anomaly correlation coefficient (ACC) of each member relative to the overall mean field. The spread, to some extent, can represent the skill of ensemble forecasting. Generally speaking, a smaller spread indicates higher forecast confidence with potentially higher forecast skill; however, a larger spread indicates lower forecast confidence but does not necessarily imply lower forecast skill.

Probabilistic forecast of weather elements is a crucial ensemble forecast product. By calculating the forecast probabilities for different thresholds of weather elements such as precipitation, temperature, and wind, it repres-

ents the occurrence likelihood of specific weather conditions. For instance, probability of precipitation exceeding 1, 5, 10, and 20 mm day^{-1}, or that of a specific weather element (e.g., snow) to occur at certain stations can be provided. Another probabilistic forecast product is the spaghetti plot, which involves selecting a specific characteristic contour line and plotting forecasted contours from all ensemble members on the same chart. Generally, the degree of divergence among contour lines roughly indicates forecast confidence, and more concentrated contours correspond to higher confidence.

Ensemble forecast clustering products utilize clustering analysis to classify ensemble member forecasts into distinct clusters, offering various possible outputs. Common clustering algorithms include hierarchical, non-hierarchical, and tubing clustering approaches. Through clustering classification, the number of members in each cluster can be compared, allowing for determination of the most probable weather scenarios. Additionally, two commonly used visualization tools, i.e., plume chart and spaghetti chart, apply clustering analysis principles to classify 500-hPa geopotential height patterns, providing forecasters with operationally actionable guidance.

2.3.2 *Post-processing methods for systematic error correction in ensemble forecasting*

Common post-processing methods for systematic bias in ensemble forecasting can be broadly categorized into parametric and non-parametric approaches (Mylne et al., 2022). Parametric post-processing methods generally assume that the target variable follows a specific probability distribution and conduct regression on its parameters. Examples include ensemble model output statistics (EMOS), Bayesian model averaging (BMA), and Bayesian joint probability (BJP). Additionally, correction methods based on different probability distributions have been developed for various physical quantities. For instance, Gaussian distribution is used for temperature and pressure, truncated normal distribution and lognormal distribution for wind, and Gamma (and truncated Gamma) distribution for precipitation. Furthermore, ensemble forecast correction based on precipitation categories has been proposed and applied to improve the forecast skill for different levels of precipitation, particularly extreme precipitation (Ji et al., 2023).

Non-parametric post-processing methods eliminate the need for predefined probability distributions of target variables, thereby providing enhanced flexibility. Common non-parametric methods include quantile mapping (QM), frequency matching (FM), probability matching (PM), member by member (MBM), the optimal percentile method, and isotonic distributional regression (IDR).

Meanwhile, by combining effective forecast information obtained from multiple models for multi-model ensemble forecasting, non-equal-weight ensemble methods based on error analysis, such as super ensemble and Kalman filtering, have been developed (Zhi et al., 2013; Zhu et al., 2021). The concept of a sliding training period (Zhi et al., 2012) has been widely applied in the correction of forecasts for tropical cyclones, temperature, precipitation, wind, and other variables. To reduce the positional and structural biases in the target system forecasts, various post-processing methods based on spatial features have been proposed, such as neighborhood methods, model projection methods, and object-based correction techniques (Ji et al., 2020).

In recent years, machine learning techniques have been widely adopted due to their high nonlinearity and strong robustness. Deep learning algorithms, such as random forests, support vector machines, convolutional neural networks, long short-term memory neural networks, and U-Net neural networks, have also been extensively applied to the post-processing of EPSs, achieving remarkable results (Zhi et al., 2020; Yang et al., 2022; Lyu et al., 2023). At the same time, by integrating machine learning algorithms with traditional statistical methods, hybrid machine learning and statistical approaches have been designed to further enhance the reliability of ensemble forecasting. Detailed descriptions of the aforementioned systematic error post-processing methods can be found in the ensemble forecast guidance manual published by the WMO (Mylne et al., 2022).

2.3.3 *Extreme forecast information extraction based on ensembles*

To extract early warning information for extreme weather from ensemble forecasts, the Extreme Forecast Index (EFI) developed through ECMWF ensemble forecast results was established (Lalaurette, 2003). This index characterizes the continuous difference between the cumulative probability distribution of the ensemble forecast results and the model climate cumulative probability distribution. The larger the value, the greater the deviation of the forecast from the model climate. Such deviations indicate a higher probability of extreme forecasts, and consequently, an increased probability of extreme weather occurring in reality. The NCEP has also conducted studies on extreme weather forecasting based on EFI. Guan and Zhu (2017) pointed out that the EFI index based on the NCEP global ensemble forecasts has certain medium-range forecasting ability for extreme precipitation and extreme low-temperature weather in the U.S. during the winter of 2013/14. In addition to conventional weather elements such as temperature, precipitation, and

10-m wind, the EFI index can also be applied to diagnostic quantities such as convective parameters (e.g., convective available potential energy) and total column water vapor flux (Tsonevsky et al., 2018). The application range of the EFI index has gradually expanded from large-scale medium-range ensemble forecasts to convective-scale and sub-seasonal to seasonal ensemble forecasts (Dutra et al., 2013; Raynaud et al., 2018). Many domestic scholars have also studied the EFI index (Xia and Chen, 2012; Liu et al., 2018; Peng et al., 2024). Research on extreme weather forecasting methods based on the EFI using the CMA-GEPS has shown that the EFI has certain recognition ability for extreme low temperatures and extreme heavy precipitation in China, with good medium-range forecasting skill. Another similar method is the Ensemble Anomaly Forecasting by ranking ensemble forecasts relative to observed climatology rather than model climatology (Du et al., 2014).

2.3.4 *Verification and evaluation metrics*

The accuracy and reliability of ensemble forecasting are crucial in meteorological prediction, driving the continuous development and refinement of verification and evaluation methods for ensemble forecasts. The works of Wilks (2011) and Jolliffe and Stephenson (2012) comprehensively summarize the verification methods for meteorological forecasts, covering deterministic, probabilistic, and qualitative forecasts, along with their applications. For deterministic forecasts based on ensemble means or individual ensemble members, commonly used verification metrics include the RMSE and spatial correlation coefficients. In the realm of probabilistic forecast verification, primary evaluation methods encompass the Brier skill score (BSS), continuous ranked probability skill score (CRPSS; Hersbach, 2000), reliability diagrams, relative operating characteristics (ROC) curve, and potential economic value (Zhu et al., 2002).

To quantify uncertainty, ensemble spread and the Talagrand distribution are key metrics. The spread–error relationship, commonly referred to as the spread–skill relationship, is often employed to evaluate the predictability of EPSs. However, real-world systems often exhibit under-dispersion in ensemble spread, particularly in quantitative precipitation forecasting (Li, 2001; Li et al., 2009; Su et al., 2014). Uncertainty quantification typically relies on the bootstrapping method (Hamill, 1999), with error bars representing the confidence intervals of the scores. Additionally, Torn and Hakim (2008) introduced the ESA method to assess the sensitivity of forecast outcomes to minor changes in initial conditions or other input parameters.

Su et al. (2014) proposed an area-weighted verification method, applying spatial weighting to probabilistic precipitation forecast scores. In the field of precipitation forecasting, some researchers have integrated these spatial verification methods into ensemble forecast evaluation. For instance, Ji et al. (2020) explored the integration of the Method for Object-based Diagnostic Evaluation (MODE) with ensemble forecasting techniques, finding significant advantages in evaluating and improving the spatial structural characteristics of precipitation forecasts. Chen et al. (2018) investigated the spatial relationship between ensemble spread and forecast error for Meiyu precipitation forecasts in the Yangtze–Huaihe region using the precipitation consistency scale method, revealing the impact of positional errors on forecast skill under different precipitation thresholds. Furthermore, Du and Deng (2020) introduced two new forecast evaluation metrics, i.e., the measure of forecast challenge (MFC) and the predictability horizon diagram index (PHDX). The MFC, which may comprehensively consider forecast error and uncertainty, serves as a novel metric for assessing forecast difficulty. The PHDX further investigates how the temporal evolution of forecasts influences decision-making processes, aiming to better represent the dynamic nature of ensemble forecast information.

It is important to note that the accuracy of scores in ensemble forecast verification may be influenced by reference values. For example, the calculation of BSS by using high-frequency grid-based climatological samples could potentially lead to score underestimation (Hamill and Juras, 2006). Additionally, the uncertainty and quality of verification data can significantly impact evaluation outcomes, particularly in precipitation forecast verification (Yuan et al., 2005). With the ongoing advancement of high-resolution ensemble forecasting and observational data, ensemble forecast verification methods are expected to become more refined and scientifically robust in the future.

3. Chinese operational EPS and its applications

3.1 *Development history of GEPS and REPS*

3.1.1 *GEPS of spectral model*

In the 1990s, the National Meteorological Centre (NMC) of CMA developed the GEPS (Li et al., 1997). In 1996, a T63L16 EPS had been implemented using the time-lagged method, consisting of 12 ensemble members with a 10-day forecast lead time. In 1999, a T106L19 EPS was developed by the SV method (Li and Chen, 2002), which includes 32 ensemble members with a 10-day forecast lead time. In 2007, based on the BGM

method (Tian et al., 2007), a T213 EPS was established, which includes 15 ensemble members with a 10-day forecast lead time. The year 2014 saw the upgrade of CMA's operational EPS from T213 to T639, which for the first time incorporated SPPT to generate model perturbations (Tan et al., 2013).

3.1.2 *REPS*

Exploratory efforts toward REPS commenced in the early 21st century. In 2005, based on the mesoscale model MM5, a heterogeneous physical mode method was proposed to generate initial perturbation (Chen et al., 2005), alongside experimental studies incorporating multi-physics configurations and stochastic physical parameter perturbations (Chen et al., 2003; Feng et al., 2006; Wang et al., 2007). By 2006, the NMC developed a regional mesoscale EPS over China using the Weather Research and Forecasting (WRF) model, integrating the BGM method and multi-physics ensemble method (Deng et al., 2010). This system became operational EPS on 15 November 2010, operating at a horizontal resolution of 15 km with 15 ensemble members and running 4 daily forecast cycles (Ma Q. et al., 2008).

3.1.3 *GRAPES-based GEPS and REPS*

The GRAPES model is a new-generation numerical weather prediction system developed through self-innovation by the CMA (Chen et al., 2008). Since 2005, research and development efforts have been dedicated to advancing ensemble forecast techniques within the GRAPES framework. The Chinese Academy of Meteorological Sciences has successively implemented both the BGM and ETKF methods to investigate GRAPES regional ensemble prediction techniques and systems (Tan and Chen, 2007; Tian and Zhuang, 2008; Ji et al., 2011), ultimately developing its REPS (GRAPES-REPS). The model's version 1.0 became operational in 2014 at NMC, utilizing ETKF for initial condition perturbations and superseding the WRF REPS. This system featured a 15-km horizontal resolution with 15 ensemble members. In 2015, the initial condition perturbation scheme was upgraded to a multi-scale blending (MSB) method (Zhang et al., 2015) that combined large-scale initial perturbations derived from the T639 EPS by using the BGM method with meso-scale initial perturbations obtained through the ETKF method within the GRAPES-REPS. This upgrade culminated in the release of version 2.0. In September 2019, the lateral boundary perturbations for the new GRAPES-REPS were sourced from the GRAPES-GEPS. The parallel enhancement of initial condition perturbation and model perturbation methods led to the operational system's evolution to version 3.0 (Chen and Li, 2020).

Development of the GRAPES-GEPS began in 2008, with initial research focused on the global ETKF method (Ma X. L. et al., 2008). With the advancement of the GRAPES global 4DVar data assimilation technology, the GRAPES SV ICP technique was developed (Li and Liu, 2019). In December 2018, the GRAPES global medium-range EPS, based on the SV ICP, became operational and replaced the T639 EPS. This achievement represents China's first successful implementation of both global and regional operational EPSs utilizing fully independent and self-controlled technologies (Chen and Li, 2020).

To characterize uncertainties in the GRAPES model, researchers have investigated multiple model perturbation methods through GRAPES's REPS and GEPS, building upon prior studies of the NMC's T213 and T639 global medium-range ensemble models. The methods used include the multi-physics (MP; Feng et al., 2006), SPPT (Yuan et al., 2016), SKEB (Peng et al., 2019), and SPP (Xu et al., 2019). The SPPT scheme became operational in the GRAPES-REPS in 2015, followed by implementation of both the SPPT and the SKEB in the GEPS in 2018 (Chen and Li, 2020).

Since 2018, significant methodological improvements have been achieved in the tropical cyclone SV technique, blended SV-EDA perturbation scheme, and sea surface temperature perturbation scheme (Huo et al., 2020; Qi et al., 2022). Based on the GRAPES-REPS forecast model, extensive advancements in initial condition and model perturbations include stochastic parameter perturbation (Xu et al., 2019), conditional typhoon vortex relocation (Wu et al., 2020), radar reflectivity algorithm (Chen Y. X. et al., 2021), and model tendency perturbation combined with systematic bias and random errors (Han et al., 2023).

Since 2020, active research on convective-scale ensemble forecasting has been conducted using the GRAPES-Meso 3-km model. Researchers have performed various experiments involving both model and initial condition perturbations, including multi-scale initial condition perturbation experiments (Ma et al., 2023) and the construction of model perturbations through conditional nonlinear optimal perturbations combined with stochastic physical perturbations (Xu et al., 2022a, b). The established 3-km regional ensemble forecast experimental system has been applied in major events such as the Beijing Winter Olympics and the Hangzhou Asian Games. Under the WMO Research Demonstration Project for the Hangzhou Asian Games, a fully independent 3-km convective-scale ensemble prediction system was successfully developed and implemented in Hangzhou, providing ensemble forecast services for the broader East China

region. This system commenced operational service on 21 May 2023, delivering comprehensive probabilistic forecasts and multifaceted decision-support capabilities to forecasters.

3.2 *Technology of CMA EPSs*

3.2.1 *Global/regional integrated multi-scale SV initial perturbation technique*

The SV initial perturbations effectively capture both the primary error information and the sensitive features of analysis errors that grow and intensify within the basic flow. The development of the Tangent Linear Model (TLM) and Adjoint Model (ADM) within the CMA global 4DVar system has provided the necessary foundation for the research and advancement of SV perturbation techniques in the CMA-GEPS (Liu et al., 2017). The SV initial perturbation calculation scheme for the CMA-GEPS is composed of two parts, i.e., calculations of SVs for the extratropical regions and for tropical cyclones, respectively. The specific mathematical treatment scheme is outlined as follows.

3.2.1.1 SV calculation scheme for extratropical regions

In the CMA-GEPS, the SV calculation can be mathematically formulated as maximizing the ratio of the evolved perturbation vector norm to the initial perturbation vector norm, as shown in Eq. (1):

$$\left(\boldsymbol{E}^{-1/2}\boldsymbol{L}^{\mathrm{T}}\boldsymbol{P}^{\mathrm{T}}\boldsymbol{E}\boldsymbol{P}\boldsymbol{L}\boldsymbol{E}^{-1/2}\right)x(t_0)=\lambda^2 x(t_0), \tag{1}$$

where $\boldsymbol{L}$ represents TLM in the CMA global 4DVar assimilation system, $\boldsymbol{L}^{\mathrm{T}}$ indicates the corresponding adjoint model, $\boldsymbol{E}$ is the weight matrix that measures the perturbation magnitude, x denotes the SV, λ is the corresponding singular value, and $\boldsymbol{P}$ stands for a projection operator that sets the SV perturbations outside the target region to zero. From Eq. (1), it is evident that the SV structure is influenced by three key factors.

(1) Definition of the weight matrix $\boldsymbol{E}$. This matrix determines the relative importance of different components of the perturbation vector.

(2) Characteristics of the TLM ($\boldsymbol{L}$) and ADM ($\boldsymbol{L}^{\mathrm{T}}$). These models primarily involve the use of linearized physical process parameterization schemes.

(3) Integration of time length for the TLM ($\boldsymbol{L}$) forward and the ADM ($\boldsymbol{L}^{\mathrm{T}}$) backward, referred to as the optimal time interval.

The CMA global SVs employ the dry total energy norm to define the weight matrix $\boldsymbol{E}$ (Liu et al., 2013). Let the prognostic variables of the CMA global TLM and ADM include the horizontal wind components (i.e., u and v), perturbation potential temperature (θ'), and perturbation dimensionless pressure (Π'). The corresponding perturbation quantities can be expressed as u', v', $(\theta')'$, and $(\Pi')'$. The total energy norm $\boldsymbol{E}$ is calculated as follows:

$$E=\iiint_V\left\{\frac{\rho_{\mathrm{r}}\cos\phi}{2}(u')^2+\frac{\rho_{\mathrm{r}}\cos\phi}{2}(v')^2+\frac{\rho_{\mathrm{r}}\cos\phi C_p T_{\mathrm{r}}}{(\theta_{\mathrm{r}})^2}[(\theta')']^2+\frac{\rho_{\mathrm{r}}\cos\phi C_p T_{\mathrm{r}}}{(\Pi_{\mathrm{r}})^2}[(\Pi')']^2\right\}\mathrm{d}V. \tag{2}$$

In Eq. (2), the sums of the first two and last two terms represent the perturbation kinetic energy (KE) and the perturbation potential energy (PE) norms, respectively. The third and fourth terms correspond to the contributions of perturbation potential temperature and perturbation dimensionless pressure to the PE norm. Meanwhile, $\mathrm{d}V=\mathrm{d}\lambda\mathrm{d}\varphi\mathrm{d}\widehat{z}$, among which $\widehat{z}$ denotes the terrain-following coordinate, and λ and φ represent longitude and latitude in the spherical coordinate system of the model. In addition, C_p is the specific heat capacity of dry air at constant pressure; and T_{r}, θ_{r}, Π_{r}, and ρ_{r} denote the reference temperature, reference potential temperature, reference dimensionless pressure, and reference density, respectively.

Based on the aforementioned CMA global SV calculation technique, three types of SVs with different scales are defined by varying resolutions and optimal time intervals. Large-scale SV (LSV) has a horizontal resolution of 2.5° and an optimal time interval of 48 h. It is computed by using dry linearized physical processes and is primarily used to capture uncertainty information at the synoptic scale. Mesoscale SV (MSV), with a horizontal resolution of 1.5° and an optimal time interval of 24 h, also employs dry linearized physical processes and is designed to capture uncertainty at the meso-α scale. Small-scale SV (SSV), which has a horizontal resolution of 0.5° and an optimal time interval of 6 h, incorporates moist linearized physical processes in its computation compared to LSV and MSV, and is mainly used to capture uncertainty at the meso-β scale. The specific configurations of the CMA global/regional integrated multi-scale SVs are summarized in Table 1.

3.2.1.2 Tropical cyclone SV calculation scheme

Considering the unique characteristics of tropical cyclones, a specialized tropical cyclone SV calculation scheme has been developed for the CMA-GEPS (Huo et al., 2020). Specifically, for tropical cyclone cases, the target region for SV computation is defined as a 10° × 10° (latitude × longitude) domain centered on the cyclone position. A maximum of six tropical cyclone SVs can be calculated.

As a result, the target regions for SV computation in the CMA-GEPS consist of the extratropical regions of

Table 1. The settings of calculation for multi-scale SVs

	LSV	MSV	SSV
Target region	30°–80°N; 30°–80°S	30°–80°N; 30°–80°S	20°–50°N, 105°–125°E
TLM resolution/optimization time	2.5°/48 h	1.5°/24 h	0.5°/6 h
Energy norm	Dry energy	Dry energy	Dry energy
Linearized physical process	Subgrid topographic drag, vertical diffusion	Subgrid topographic drag, vertical diffusion	Subgrid topographic drag, vertical diffusion, large-scale condensation
Number of SVs	10	10	10

the Northern and Southern Hemispheres and the tropical cyclone region. This approach not only captures the development of baroclinically unstable perturbations in the mid-to-high latitudes of both hemispheres but also accounts for the evolution of tropical cyclones when they are present.

Based on the initial SV computed for the Northern and Southern Hemispheres as well as tropical cyclones, Gaussian sampling techniques are employed to construct the initial perturbation fields for the CMA-GEPS. Additionally, a scaling amplification factor σ is applied to normalize the amplitudes of all initial perturbations, ensuring that their magnitudes are consistent with the actual analysis error levels. Finally, by adding and subtracting the initial perturbations to/from the assimilation analysis initial conditions in pairs, the perturbed initial conditions for the CMA-GEPS are generated.

3.2.2 *MSB initial perturbation techniques in short-range regional ensembles*

Due to the resolution limitations of GEPSs, the dynamical downscaling method fails to fully capture uncertainties at smaller scales that can be resolved by regional models. However, meso- and small-scale initial perturbations are essential for accurately capturing uncertainties in local severe weather. Therefore, the CMA-REPS has developed an MSB initial perturbation technique based on the ETKF scheme.

3.2.2.1 ETKF initial perturbation method

The ETKF method is an initial perturbation scheme developed based on Kalman filter theory. It rapidly estimates analysis errors from ensemble forecast perturbations and observational error variances (Long et al., 2011), thereby effectively capturing uncertainties in meso- and small-scale initial conditions.

In the CMA-REPS, the forecast perturbation vector $\boldsymbol{X}^{\mathrm{f}}$ is transformed into the analysis perturbation vector $\boldsymbol{X}^{\mathrm{a}}$ through the transformation matrix $\boldsymbol{T}$, as shown in Eq. (3). Specifically, the analysis perturbations at the current time are derived by linearly combining the forecast perturbation vector using the transformation matrix $\boldsymbol{T}$.

$$\boldsymbol{X}^{\mathrm{a}} = \boldsymbol{X}^{\mathrm{f}}\boldsymbol{T}. \tag{3}$$

The core of the ETKF initial perturbation method lies in obtaining the transformation matrix $\boldsymbol{T}$. In the ETKF scheme of CMA-REPS, the transformation matrix $\boldsymbol{T}$ is defined using the method proposed by Wang and Bishop (2003). To centralize the perturbed members relative to the ensemble mean, we employ a spherical simplex centralization scheme. In the operational version of the CMA-REPS, simulated observations are derived by interpolating the analysis fields from the GEPS to the observational space (Wang et al., 2018). The variables used to compute the transformation matrix $\boldsymbol{T}$ include meridional wind v and zonal wind u, and the variables for calculating the amplification factor are u, v, and specific humidity q. The system applies a 6-h cycling perturbation scheme to provide forecast perturbation fields for the ETKF cycle. The model runs 4 times per day at 0000, 0600, 1200, and 1800 UTC, among which the 0000 and 1200 UTC cycles are integrated for 84-h forecasts, and the other two (i.e., 0600 and 1800 UTC cycles) for 6-h forecasts.

3.2.2.2 MSB initial perturbation method

Practical experience has shown that the initial perturbation fields in regional ensemble prediction, derived from the dynamical downscaling of global ensemble prediction, contain more large-scale perturbation information. Since 2016, the CMA-REPS has adopted an MSB initial perturbation technique (Zhang et al., 2015; Xia et al., 2019). This method employs the two-dimensional discrete cosine transform (2D-DCT; Denis et al., 2002) to filter the initial perturbations from both the ETKF method in regional ensemble prediction and the dynamical downscaling of the T639 global ensemble prediction. Subsequently, through the 2D-DCT inverse transformation, the initial perturbation fields are reconstructed by integrating large-scale perturbations from the global ensemble prediction with meso- and small-scale perturbations from the regional ensemble prediction, with more multiscale initial condition uncertainties.

3.2.2.3 Conditional typhoon vortex relocation technique in ensemble forecasting

To more reasonably describe the uncertainty in the positioning of typhoon vortex centers in ensemble forecasting, Wu et al. (2020) applied the best track data of typhoons from the CMA and the JMA during 2009 and 2018. They analyzed the uncertainties of typhoon vortex

center positioning in these best tracks and developed a conditional typhoon vortex relocation method. Additionally, they established procedures for threshold discrimination of typhoon vortex relocation for ensemble members, as well as mathematical treatment processes for typhoon vortex separation and vortex relocation.

By analyzing and comparing the best typhoon vortex center locations from the CMA and the JMA during the study period, it was found that the maximum annual average positioning error was 17.18 km (in 2009), while the minimum was 11.98 km (in 2015). Given the 10-km horizontal resolution of the CMA-REPS, a critical threshold of 15 km was established to determine whether conditional typhoon vortex relocation should be performed for ensemble members. Specifically, if the distance between the typhoon vortex center in an ensemble member's initial field and the best track exceeds 15 km, the typhoon vortex positioning in that member's initial condition is deemed beyond the range of analyzed uncertainties, requiring conditional vortex relocation. Otherwise, the error is considered within the range of analyzed uncertainties, making relocation unnecessary. The relocation method utilizes the typhoon vortex separation technique developed by the U.S. Geophysical Fluid Dynamics Laboratory to isolate the typhoon vortex from the initial fields of ensemble members requiring relocation. The separated typhoon is then shifted to the observed position through interpolation. This scheme was implemented in the CMA-REPS v3.0 in 2019.

3.2.3 *Stochastic model perturbation technique for subgrid physical processes*

The EPS relying solely on initial perturbations suffers from insufficient divergence among ensemble members and inadequate reliability. In a complete system, incorporating model perturbation techniques is essential to effectively characterize model uncertainty and account for model errors (Palmer et al., 2009). Therefore, CMA's GEPS and REPS should introduce such techniques to represent uncertainties arising from model imperfections. At present, the SPPT and the SKEB model perturbation techniques are mainly used in the CMA's forecast system, which are briefly introduced below.

3.2.3.1 SPPT scheme

The SPPT scheme in CMA's GEPS and REPS shares the same fundamental design principles as ECMWF's implementation (Buizza et al., 1999). Specifically, during numerical integration, the model integration term can be decomposed into the integral term of non-parametric (dynamic) processes, and the integral tendency term of parametric physical processes. The model integral tendency term perturbed by the SPPT scheme can then be expressed as:

$$e_j(t_e) = \int_0^{t_e} \left[A(e_j,t) + \Psi(\lambda,\phi,t)P(e_j,t)\right] \mathrm{d}t, \tag{4}$$

where $\Psi(\lambda,\phi,t)$ is a three-dimensional random field with spatiotemporal correlation features. A stretch function is introduced to implement a range of custom perturbations (Li et al., 2008), which is defined as:

$$\Psi(\lambda,\phi,t) = \mu + \left\{ 2 - \frac{1-\exp\left[\beta\left(\frac{\psi-\mu}{\Psi_{\max-\mu}}\right)\right]^2}{1-\exp(\beta)} \right\}(\psi-\mu), \tag{5}$$

where β is a constant with a value of -1.27 and $\mu = (\Psi_{\max} + \Psi_{\min})/2$; $\Psi_{\max}$ and $\Psi_{\min}$ represent the upper and lower bounds of the random field $\Psi(\lambda,\phi,t)$, respectively; and ψ is a three-dimensional random field with spatiotemporal correlated characteristics, defined as:

$$\psi(\lambda,\phi,t) = \mu + \sum_{l=1}^{L}\sum_{m=-l}^{l} \alpha_{l,m}(t)\, Y_{l,m}(\lambda,\phi), \tag{6}$$

where λ, ϕ, and t represent the longitude, latitude, and time, respectively; and $Y_{l,m}$ is the spherical harmonic function, L is the horizontal truncation scale of the random field, l and m are the total wavenumber and latitude wavenumber in the horizontal direction, and $\alpha_{l,m}(t)$ is the spectral coefficient of the random field. The correlation of the stochastic spectral coefficient $\alpha_{l,m}(t)$ in the time dimension is realized by the first-order Markov chain stochastic process (also known as the first-order autoregressive stochastic process), as shown in the following formula:

$$\alpha_{l,m}(t+\Delta t) = \mathrm{e}^{-\Delta t/\tau}\alpha_{l,m}(t) + \sqrt{\frac{4\pi\sigma^2(1-\mathrm{e}^{-2\Delta t/\tau})}{L(L+2)}} R_{l,m}(t), \tag{7}$$

where Δt is the specific time interval that can correspond to the integration step of the model in the CMA's EPS; τ is the timescale of the random field decorrelation; and $R_{l,m}(t)$ is a Gaussian distribution stochastic process that obeys a variance of 1 and a mean of 0. The stochastic pattern constructed by the above formula features time–space scale correlation and controllable perturbation amount. In the CMA's GEPS and REPS, perturbations are applied only to the net tendency terms of potential temperature, horizontal wind components, and humidity variables.

Considering the different integration times and forecast objects of global and regional models, the parameter settings of the SPPT scheme in the CMA's GEPS and REPS are different. In the CMA-REPS, the SPPT perturbation amplitude ranges from 0.2 to 1.8 with a mean

of 1.0. The scheme uses a decorrelation time scale of 6 h, a maximum wavenumber of 24, and a standard deviation σ of 0.27. In the CMA-GEPS, to ensure operational stability, the stochastic function's perturbation amplitude is constrained to 0.5–1.5. The vertical profile of tendency perturbations is introduced at both the near-surface layer and atmospheric top, where physical tendencies either remain unperturbed or receive only minimal-amplitude perturbations. The SPPT scheme can significantly improve the ensemble spread and missing rate of temperature and wind speed forecasts, improve the probabilistic forecasting skills of heavy precipitation, and significantly increase the ensemble spread of various elements (altitude field, temperature field, and wind speed) forecasts in tropical areas, which makes up for the lack of perturbation in tropical areas by SV initial perturbation technique (Peng et al., 2020).

3.2.3.2 SKEB scheme

The main purpose of the SKEB scheme is to represent the stochastic process and uncertainty of subgrid-scale energy upscaling transitions in the model (Shutts, 2005). The SKEB scheme in the CMA-GEPS addresses excessive energy dissipation by employing a random flow function forcing with specific spatiotemporal correlations and local dynamic dissipation rates (Peng et al., 2019). The random stream function forcing F_ψ is defined as follows.

$$F_\psi = \frac{\alpha \Delta x}{\Delta t} \Psi(\lambda,\varphi,t) \sqrt{\Delta t D(\lambda,\varphi,\eta,t)}. \tag{8}$$

In Eq. (8), $\Psi(\lambda,\varphi,t)$ is a random type, and its generation method is the same as the definition of the random type of SPPT, as shown in Eq. (5); and $D(\lambda,\varphi,\eta,t)$ is the dissipation rate of local dynamic energy. At present, the SKEB scheme in the CMA-GEPS constructs the local dynamic energy dissipation rate based on the explicit horizontal scheme.

$$D(\lambda,\varphi,\eta,t) = -k \times \boldsymbol{u} \times \boldsymbol{u}', \tag{9}$$

where k is a constant factor greater than 1, $\boldsymbol{u}$ is the horizontal wind speed, and $\boldsymbol{u}'$ is the change in the horizontal wind speed before and after the application of the horizontal diffusion scheme. Based on the relationship between the stream function and the rotational component of the horizontal wind field, the perturbation forcing terms of the CMA-GEPS in horizontal wind field are constructed as S_u and S_v. These stochastic forcing terms are then added to the tendency terms of the model's horizontal wind field.

$$S_u = -\frac{1}{\alpha}\frac{\partial F_\psi}{\partial \phi}, \tag{10}$$

$$S_v = \frac{1}{\alpha \cos\phi}\frac{\partial F_\psi}{\partial \lambda}. \tag{11}$$

In the CMA-GEPS, the minimum and maximum truncation wavenumbers $L_{\min}$ and $L_{\max}$ of the Ψ random pattern of the SKEB scheme are 10 and 80, the decorrelation time scale τ is 6 h, the mean μ is 0, the standard deviation σ is 0.27, and the maximum $\Psi_{\max}$ (minimum $\Psi_{\min}$) is 0.8 (−0.8). The application of the SKEB scheme can improve the simulation ability of the CMA-GEPS on the atmospheric kinetic energy spectrum, and significantly enhance the relationship between the ensemble mean error and the ensemble spread of the wind field forecast in the tropics.

3.2.4 *Systematic bias and extreme information extraction*

In addition to the aforementioned initial perturbation and model perturbation techniques, the CMA's GEPS and REPS have innovatively developed a suite of ensemble post-processing techniques and extreme weather forecasting applications. These include an ensemble dynamical method for correcting bias (Chen et al., 2020), the radar reflectivity factor for subgrid-scale precipitation (Chen Y. X. et al., 2021), and the model of extreme weather index. These techniques addressed the challenges of extracting extreme forecast signals from the tails of probabilistic forecast distributions and correcting systematic model biases, leading to notable improvements in probability density distributions and enhanced extreme weather prediction capabilities in CMA's GEPS and REPS. A brief overview of these technologies is as follows.

3.2.4.1 Ensemble forecasting dynamic correction method based on subtracting model systematic bias in tendency term

Current ensemble prediction techniques primarily address model stochastic errors. However, under pronounced model systematic biases, sole dependence on either initial perturbation or model perturbation methods is inadequate to optimize the error–spread relationship in ensemble forecasts. Following the research on the impacts of CMA global/regional model systematic biases on ensemble probability density distributions, an ensemble forecasting method was developed, applying dynamic correction through subtraction of model systematic bias in the tendency term. This approach removes bias tendencies from both dynamical and physical tendency terms during model integration, as shown in Eq. (12) (Chen et al., 2020; Han et al., 2023).

$$e_j(t_e) = \int_0^{t_e} \left[A(e_j,t) + P(e_j,t) - \hat{B}_l(e_0) \right] \mathrm{d}t. \tag{12}$$

In the equation, $e_j(t)$ is the total tendency, $A(e_j,t)$ is

the dynamic tendency, $P(e_j,t)$ is a physical tendency, and $\hat{B}_l(e_0)$ is the subtracted bias. A linear bias coefficient is derived by linear regression and systematically removed from tendency terms at each model integration step. This method significantly enhances both the first- (ensemble mean) and second-order moment (ensemble spread) of the ensemble forecast probability density distribution, thereby improving the probabilistic prediction skill for surface meteorological elements.

3.2.4.2 A new calculated method of radar reflectivity factor for subgrid-scale precipitation

Since radar reflectivity can reveal the characteristics of strong convective weather events, forecasters pay close attention to uncertainty in model forecasts. To better quantify radar reflectivity uncertainties, we developed and implemented a new radar reflectivity calculation method for subgrid-scale precipitation in the CMA-REPS, as presented in Eq. (13). This addresses the current limitation where simulated radar reflectivity fails to represent precipitation from the Kain–Fritsch cumulus parameterization scheme (Chen Y. X. et al., 2021).

$$Z_{\text{total}} = Z_{\text{micro}} + AR_{\text{cu}}^{b}. \tag{13}$$

In the equation, Z_{total} is the new radar reflectivity, Z_{micro} is the radar reflectivity from the cloud microphysics parameterization scheme, R_{cu} is the subgrid precipitation, and A and b are empirical parameters of the Z–R relationship for the radar quantitative precipitation estimation. The methodology operates by subtracting the downdraft evaporation rate from the subgrid precipitation rate, followed by layer-wise estimation of radar reflectivity using the radar-derived reflectivity–rainfall (i.e., Z–R) relationship. This new reflectivity is then integrated with microphysics-simulated radar echoes to generate a novel three-dimensional radar reflectivity field. The new reflectivity fields improved diagnostic capability for precipitation generated by the cumulus parameterization scheme, particularly under conditions dominated by subgrid convective processes. It can better simulate the radar reflectivity related to subgrid precipitation of a single ensemble member and then improve the probabilistic prediction technique of radar reflectivity in CMA-REPS.

3.2.4.3 Extreme weather prediction product

Based on the forecast, model climate, and historical climate data of 31 ensemble members of the CMA-GEPS, extreme weather prediction products are developed, including EFI of ground elements, 2-m temperature anomaly probability forecast product, and medium anomaly probability forecast product based on the Kalman filter bias correction technology.

(1) Ground elements EFI product based on climate probability of CMA-GEPS. With the development of deterministic and ensemble forecasting for each forecasting element (precipitation, wind, temperature, and cloud cover), forecasters aim to utilize EPS for generating early warning signals of extreme events. However, it is difficult to directly compare the difference between the observed meteorological elements and the forecast output of the model. Therefore, based on the CMA-GEPS, a CMA ensemble forecast method of extreme weather called EFI was developed. The principle is to calculate the difference between the cumulative model climate probability distribution and the ensemble forecast probability distribution. The calculation of the model climate percentile is a crucial step in calculation of the EFI, but the CMA-GEPS has less historical data. Thus, the model climate percentile was calculated by using a 15-day sliding time window (±7 days centered on the target date) and a spatial window comprising the target grid point and its 9 nearest neighbors. The daily model climate sequence was constructed from this spatiotemporal sampling, and percentiles (1, 2, ..., 99, 100) of the forecast field were extracted to form the model's climate percentile distribution (Wang J. Y. et al., 2014; Peng et al., 2024).

(2) Medium anomaly probability forecast product based on Kalman filter bias correction technology. The medium anomaly probability forecast products based on Kalman filter bias correction technology are developed, including atmospheric circulation anomaly probability products of 500-hPa geopotential height (Z500), 850-hPa temperature, and 850-hPa wind. These products help to better grasp the characteristics of extreme disaster weather and improve the probability forecasting skills of extreme disaster weather.

3.3 *China's GEPS and REPS and their comparison with international systems*

3.3.1 *China's GEPS and REPS*

In response to the characteristics of initial and model errors in CMA's GEPS and REPS, Chinese technicians have independently developed key technologies for ensemble forecast, thereby overcoming the bottlenecks in initial perturbation, model perturbation, and ensemble forecast application technologies. They have developed an independent and controllable GEPS with a horizontal resolution of 50 km for 0–15-day forecasts, along with a REPS featuring 10-km resolution and a convective-scale EPS with 3-km resolution, both for 0–3-day forecasts. These systems provide robust scientific and technological support for global ensemble prediction, propelling China's numerical prediction operations to achieve remarkable progress and reach an advanced level. The operational implementation of the CMA's GEPS and REPS

marks a significant milestone in advancing China's NWP capabilities. Beyond daily forecasting services and major meteorological support, the products from the CMA's GEPS and REPS continue to supply a wide range of forecast data to the TIGGE Center. They also provide core support for the World Meteorological Centre (WMC) Beijing and the WMO Severe Weather Forecasting Demonstration Programme for Southeast Asia (SWFDP-SeA) website, further elevating China's role in global meteorological science. Table 2 illustrates the parameter settings of the CMA's GEPS, REPS, and convective-scale ensemble forecast (CAEF) in detail.

The CMA-GEPS integrates SV initial perturbation, model random physical perturbation, and generation technologies for extreme medium-range probabilistic forecast products. It features a horizontal resolution of 0.5°, a forecast range of 0–15 days, and 31 ensemble members. Leveraging ecFlow technology (a client/server workflow package of ECMWF that enables users to run a large number of programs in a controlled environment), the operational process of the CMA-GEPS has been established, enabling daily operations at 0000 and 1200 UTC. The system provides 29 types of products, including conventional forecasts and probabilistic forecasts for extreme weather events over the 0–15-day period.

The CMA-REPS v3.0 integrates a suite of advanced techniques, including the ETKF, multi-scale blended initial perturbation, SPPT, blended dynamic perturbations of lateral boundary conditions (LBCs), Conditional Typhoon Vortex Relocation (CTVR), and a new sub-grid scale precipitation radar echo reflectivity algorithm. The system operates with 15 ensemble members and runs 4 times daily, with a forecast duration of 84 h for the 0000 and 1200 UTC cycles, and 6 h for the 0600 and 1800 UTC cycles. The system primarily supports the ETKF forecast cycle, preparing data for ETKF calculations and generating forecast perturbations. The system offers 49 types of ensemble products, with a focus on probabilistic forecasts for localized severe weather and tropical cyclones.

3.3.2 *Analysis of international major numerical prediction centers*

3.3.2.1 Comparison on key techniques and systems of ensemble prediction

Table 3 is a comprehensive comparison of major international EPSs. The main technical characteristics of the CMA are demonstrated as follows.

(1) The SV initial perturbation technique, a core component of the CMA-GEPS, has been innovatively enhanced with advanced algorithms for perturbation energy modulus, parallel computing, scaling, and linear sampling of initial perturbations based on a Gaussian distribution in a three-dimensional structure. This technique effectively captures the growth of large-scale baroclinic instability perturbation energy, significantly improving the accuracy and reliability of global ensemble forecasts. Given its high technical complexity, the SV initial perturbation technique is employed by only a few leading GEPSs, including those of ECMWF, the French Meteorological Service, and the JMA. The successful implementation of this technique marks CMA's entry into the global forefront of meteorological forecasting, with its

Table 2. The parameter configuration for CMA's GEPS, REPS, and CAEF

	CMA-GEPS	CMA-REPS	CMA-CAEF
Model version	CMA-GFS v3.1	CMA-MESO v4.3	CMA-MESO v5.1
Horizontal resolution	0.5°	0.1°	0.03°
Vertical level	87	50	50
Domain	90°S–90°N, 180°W–180°E	10°–60°N, 70°–145°E	10°–60°N, 70°–145°E
Initial perturbation of control member	Upscaled from analysis field via CMA-GFS 4DVAR	Downscaled from CMA-GEPS	Generated from analysis field via 3DVAR
Initial perturbation scheme	SVs	ETKF	Multi-scale blending based on SVs
Model perturbation scheme	SPPT, SKEB	SPPT	SPPT
Lateral boundary perturbation scheme	/	From CMA-GEPS	Blended dynamic lateral boundary perturbations
Number of members	31	15	15
Forecast length	360 h (0000/1200 UTC)	84 h (0000/1200 UTC) 6 h (0600/1800 UTC)	72 h (0600/1800 UTC)
Output interval	0–84 h (3 h), 84–360 h (6 h)	1 h	1 h
Postprocessing product	GRIB2 data, ensemble prediction products for normal, extreme weather and typhoon	GRIB2 data, ensemble prediction products for normal, emergency service and typhoon	GRIB2 data, ensemble prediction products for normal, emergency service and typhoon

Note: GRIB2 refers to the Gridded Binary Format Edition 2, which is a standard encoding format sponsored by the WMO for the transmission of gridded data between the national meteorological centers.

technical level matching that of the world's most advanced NWP centers.

(2) The CMA-REPS incorporates several cutting-edge techniques, including the ETKF for initial perturbations, the MSB, and the CTVR. These advancements have significantly improved the accuracy of probabilistic precipitation forecasts in China. The ETKF method is based on the same principles and framework as the local ensemble transform Kalman filter (LETKF), which is operationally used by both the Meteorological Service of Canada and the JMA. Meanwhile, the MSB and CTVR techniques are originally developed by the CMA, showcasing the agency's innovation in REPS.

(3) The stochastic perturbation methods for physical processes, such as the SPPT and the SKEB, utilize a first-order autoregressive stochastic process and spherical harmonic function expansion. These methods produce random functions and key parameters that are temporally and spatially correlated and normally distributed. By introducing stochastic perturbations to the tendencies of physical processes and the dissipation of small-scale kinetic energy, these techniques provide a realistic characterization of the stochastic error growth in sub-grid physical process parameterizations. This approach is consistent with the stochastic perturbation schemes employed by leading meteorological centers in Europe (e.g., ECMWF and the UK) and North America (e.g., the U.S. and Canada).

(4) Aiming at ensemble forecast applications, we have designed techniques for extracting extreme information, dynamically correcting systematic biases, and developing algorithms that consider radar reflectivity for model convective precipitation. Additionally, we have developed technologies for generating probabilistic forecast products such as extreme weather forecast indices. These advancements provide valuable reference information for extreme weather forecasts.

(5) An independent and proprietary operational system for ensemble forecast has been established in China, encompassing global medium-range forecasts (0–15 days), regional short-range forecasts (0–72 h), and convective-scale EPS. These advancements have significantly propelled progress in China's numerical weather prediction capabilities. A comparison of ensemble forecast techniques and system parameters across various international NWP centers reveals that global ensemble prediction resolutions typically range from 9 to 50 km, with ensemble members varying from 18 to 51. China's GEPS aligns closely with these international standards, featuring a horizontal resolution of 50 km and 31 ensemble members. In the realm of REPS, countries with smaller land areas, such as the UK, France, and Germany, have achieved resolutions of approximately 2.5 km, supported by 10–20 ensemble members. In contrast, countries with vast territories, like Canada, the U.S., and China, have generally established both regional meso- and convective-scale EPSs. China's REPS has a horizontal resolution of 10 km, while its convective-scale ensemble forecasting system achieves an even finer resolution of 3 km. Such a dual-system approach highlights China's commitments to enhancing forecast accuracy and resolution.

In summary, unique technical methods and products with independent intellectual property rights have been developed in China in the aspects of system parameters and construction schemes for CMA's GEPS and REPS.

3.3.2.2 Forecast capability comparison between CMA's GEPS and REPS and major international NWP centers

Based on data provided by the JMA from the Interna-

Table 3. Technical status of international major operational EPSs

Country	GEPS/horizontal resolution (number of members)/technology	REPS/horizontal resolution (number of members)/technology
USA	Spectral model/25 km (31)/ETKF, SPPT, SKEB	WRF, NMMB/16 km (26, North America)/3 km (11, key areas)/hybrid ensemble Kalman filter with BGM, dynamical downscaling, multi-physics
UK	Grid-point model MOGREPS-G/20 km (18)/EDA, SPPT, SKEB	Grid-point model MOGREPS-UK/2.2 km (3 perturbations, 18 lagged ensemble members)/Dynamical Downscaling
France	Spectral model/7.5–37 km (35)/SVs, EDA, MP	Spectral model AROME-EPS/2.5 km (16)/EDA, SPP
Germany	Grid-point model GEPS/40 km (40)/LETKF, SPP	Grid-point model COSMO-DE/2.2 km (20)/LETKF, SPP
Canada	Grid-point model/39 km (21)/LETKF, SPP, SKEB	Limited area model HREPS/15 km (21)/dynamical downscaling, physics perturbation
Japan	Spectral model/27–40 km (27)/SVs, LETKF, SPPT	Grid-point model/5 km (21)/multi-scale SVs
EU	Spectral model/9 km (51)/SVs, EDA, SPPT	/
China	Grid-point model GRAPES/50 km (31)/SVs, SPPT, SKEB	Grid-point model GRAPES/10 (15, China) and 3 km (15, China)/ETKF, MSB, multi-scale SVs, SPPT

Note: MOGREPS refers to the Met Office Global and Regional Ensemble Prediction System, and "G" in MOGREPS-G stands for "global"; NMMB indicates the Nonhydrostatic Mesoscale Model on the B-grid developed by NOAA; AROME denotes the Application of Research to Operations at Mesoscale; and COSMO-DE is a short for the Consortium for Small-scale Modeling Deutschland ("Germany" in English) Edition operated by the Deutscher Wetterdienst (DWD) of Germany.

tional Global Ensemble Forecast Verification Center, Fig. 1 presents a comparison of the continuous ranked probability score (CRPS) for the day 6 of ensemble forecast and the average RMSE for the day 10 of ensemble forecast of the 500-hPa geopotential height field from multiple centers over the period of 2012–2024. The verification data mainly include the GEPSs of several numerical centers, such as the ECMWF, the NCEP, the United Kingdom Met Office (UKMO), the CMC, the Bureau of Meteorology, Australia (BOM), the JMA, the Korea Meteorological Administration (KMA), and the CMA. It can be seen that since the operational implementation of the CMA-GEPS in December 2018, its forecast skill for medium-range forecasts has been comparable to that of the GEPSs of Europe and the U.S.

4. Challenges and prospects in the development of ensemble forecast

4.1 *Scientific challenges: Spatiotemporal variability of predictability in convective-scale models*

The predictability of convective-scale models exhibits significant spatiotemporal variability. First, the predictability of convective-scale models is influenced by the interactions of circulations across different spatiotemporal scales. Even if the magnitude of initial errors is sufficiently small, these errors can rapidly saturate and undergo upscale growth, thereby affecting the predictability of large-scale weather systems (Zhang et al., 2007). The growth of initial errors in convective-scale models has the characteristics of strong nonlinearity, with the error growth rate being approximately 10 times that of synoptic-scale models (Hohenegger and Schar, 2007). Second, convective-scale models typically employ more sophisticated and complex parameterization schemes such as cloud microphysics and turbulent diffusion. However, these approaches are subject to numerous assumptions and empirical parameters, as well as errors arising from finite-difference methods and computational truncation, all of which contribute to the strongly nonlinear growth of initial errors in convective-scale models (Mu et al., 2011; Yano et al., 2018). Third, the growth of initial errors at different scales and their impact on precipitation are closely related to environmental forcing conditions (Johnson, 2014; Zhuang et al., 2021). The relative importance of initial errors at different scales depends on the quantity and type of moist convection, with more moist convection leading to greater growth of small-scale error perturbation energy (Nielsen, 2016). Consequently, convective-scale ensemble forecast techniques are facing significant challenges.

4.2 *Frontier exploration of a combination of ensemble forecast and AI*

In recent years, AI has achieved groundbreaking progress in meteorological forecast applications. The computational cost of deep learning-based large-scale meteorological models is only 1×10^{-4} of that of traditional numerical models, offering a new potential pathway for the development of large-sample ensemble forecast. However, this also introduces new challenges. First, the sources of uncertainty in AI models differ from those in traditional numerical models, and the impact of these uncertainties on the forecast skill and performance of AI models requires further in-depth investigation. Second, the uncertainty characteristics of deep learning models differ from those of traditional numerical forecast, and how to appropriately describe the uncertainty features of deep learning models remains an urgent issue to be addressed. Third, the physical consistency and interpretability of AI-based ensemble forecast models remain debated, necessitating corresponding research and improvements alongside the development of AI models. Furthermore, the advancement of AI has brought new challenges and opportunities to ensemble forecast. The framework and concepts of ensemble forecast may also need to undergo transformations in the future. For instance, (1) ensemble forecast may revert to probabilistic forecast, with the core objective of obtaining the PDF of variables, which conceptually derives from seeking the probability distribution of forecast errors. (2) The significance of representative perturbations may decrease. As machine learning models can rapidly generate tens of thousands of ensemble forecasts, a broader spectrum of forecast possibilities can be explored, which provides better probabilistic and statistical characteristics. (3) Partial replacement of dynamical models may occur, as smaller-scale structures in the atmosphere require high-resolution dynamical models for identification. Here, dynamical models essentially act as effective but time-consuming random perturbation generators. Whether machine learning models can learn and generate such perturbations is a topic worthy of further research.

4.3 *Operational challenges: Inapplicability of traditional ensemble forecast techniques*

In recent years, operational ensemble forecasting development has encountered three fundamental limitations. First, global and regional operational ensemble forecast is moving toward convective-scale resolution. Under the convective-scale modeling framework, the multi-scale structures of initial condition and model errors, along with their nonlinear evolution and interac-

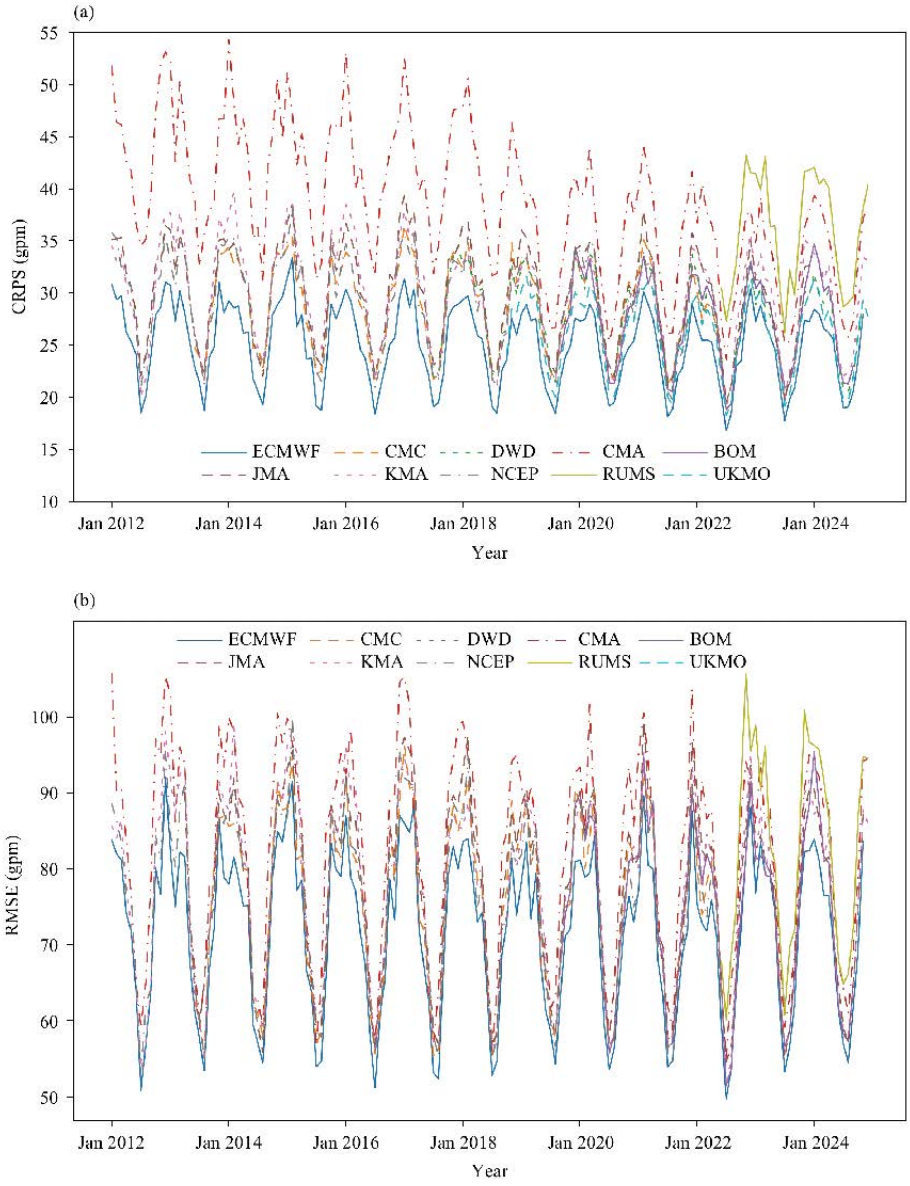

Fig. 1. The ensemble mean (a) continuous ranked probability score (CRPS) and (b) RMSE of the 500-hPa geopotential height (Z500) forecasts at 144 (day 6) and 240 h (day 10) from major international global EPSs, averaged monthly from January 2012 to December 2024. Different colors represent different NWP centers. RUMS refers to the regional unified model system.

tions, remain key scientific challenges in understanding the mechanisms of forecast error growth. How to construct ensemble perturbation methods is a technical bottleneck in the development of convective-scale ensemble forecast. Second, earth system models are evolving toward seamless weather–climate integrated EPSs, while traditional ensemble forecast techniques have been developed separately for temporal and spatial scales, making them inadequate for seamless spatiotemporal ensemble forecasting requirements. Third, ensemble forecast is gradually transitioning toward earth system ensemble forecast. Yet, traditional ensemble forecast techniques primarily address the uncertainty in forecasting derived from the error growth of dynamically unstable atmospheric systems. The understanding of error characteristics from coupled component models and coupled data assimilation remains insufficient, requiring the development of ensemble forecast techniques suitable for multi-component coupled models.

5. Conclusions

In recent years, ensemble forecasting in China has achieved remarkable development and progress, from theoretical methods to operational applications, making China a world leader in operational ensemble forecasting. However, there is still a certain gap compared to the performance of EPSs at the most advanced operational

centers such as the ECMWF. Currently, ensemble forecasting has been intentionally developed to gradually replace deterministic forecasting, emerging as the primary form and important trend in operational forecasting. The concept of probabilistic forecasting is also gradually being popularized and accepted among researchers, forecasters, and the public. Below, we briefly summarize and discuss the challenges facing the future development of ensemble forecasting, which are also key issues that need to be addressed in the scientific research and operational development of ensemble forecasting in China.

(1) The ensemble members of global ensemble forecasting systems will advance towards convective-scale resolution in the future. This will facilitate the sampling of fine-scale features from mesoscale to convective scale and the estimation of uncertainties in ensemble forecasting on a global scale. ECMWF is at the forefront of this development, targeting a global ensemble forecast at a resolution of 5 km by 2025. Higher resolution not only poses a significant challenge to the high-performance computing resources of major operational centers but also raises highly challenging scientific and engineering questions regarding how to effectively generate multi-scale initial ensemble perturbations and model physics perturbations, while ensuring the physical consistency of these perturbations.

(2) It is important to develop integrated ensemble forecasting for global medium-range to subseasonal-seasonal (S2S) predictions. As the sources of uncertainty in subseasonal and seasonal predictions become increasingly diverse and complex, conducting ensemble forecasting for S2S is an international frontier issue. The current trend among major international operational centers is to use integrated atmosphere–land–ocean coupled models for ensemble forecasting of short- to medium-range and subseasonal predictions. The main frontier scientific questions in this area are how to construct initial ensemble perturbations for the atmosphere–ocean coupled system and how to account for the impact of external forcing uncertainties on S2S ensemble forecasts.

(3) With the increasing resolution of global ensemble forecasting, it is necessary to reconsider the developmental positioning and key scientific issues of REPSs. Regional ensemble forecast requires enhanced spatial resolutions than global ensemble forecast, potentially advancing towards sub-kilometer resolution in the future. Its forecasting targets may also gradually encompass smaller urban-scale meteorological elements. Moreover, how to more effectively consider the coordination and nonlinear interactions of initial, lateral boundary, and model process multi-source perturbations remains a critical scientific issue in regional ensemble forecasting.

(4) The rise of AI technology presents unprecedented challenges and opportunities for ensemble forecasting. The essence of ensemble forecasting lies in statistical sampling, while AI tools excel in constructing statistical characteristics of variables and their nonlinear relationships. How to effectively apply AI technology to ensemble forecasting is a vast and cutting-edge scientific and engineering issue. Future developments in this area hold the promise of significantly advancing the level of ensemble forecasting.

REFERENCES

Arakawa, A., 2004: The cumulus parameterization problem: Past, present, and future. *J. Climate*, **17**, 2493–2525, https://doi.org/10.1175/1520-0442(2004)017<2493:RATCPP>2.0.CO;2.

Bauer, P., A. Thorpe, and G. Brunet, 2015: The quiet revolution of numerical weather prediction. *Nature*, **525**, 47–55, https://doi.org/10.1038/nature14956.

Berner, J., G. J. Shutts, M. Leutbecher, et al., 2009: A spectral stochastic kinetic energy backscatter scheme and its impact on flow-dependent predictability in the ECMWF ensemble prediction system. *J. Atmos. Sci.*, **66**, 603–626, https://doi.org/10.1175/2008JAS2677.1.

Berner, J., K. R. Fossell, S. Y. Ha, et al., 2015: Increasing the skill of probabilistic forecasts: Understanding performance improvements from model-error representations. *Mon. Wea. Rev.*, **143**, 1295–1320, https://doi.org/10.1175/MWR-D-14-00091.1.

Bowler, N. E., A. Arribas, K. R. Mylne, et al., 2008: The MOGREPS short-range ensemble prediction system. *Quart. J. Roy. Meteor. Soc.*, **134**, 703–722, https://doi.org/10.1002/qj.234.

Buizza, R., 1997: Potential forecast skill of ensemble prediction and spread and skill distributions of the ECMWF Ensemble Prediction System. *Mon. Wea. Rev.*, **125**, 99–119, https://doi.org/10.1175/1520-0493(1997)125<0099:PFSOEP>2.0.CO;2.

Buizza, R., M. Milleer, and T. N. Palmer, 1999: Stochastic representation of model uncertainties in the ECMWF ensemble prediction system. *Quart. J. Roy. Meteor. Soc.*, **125**, 2887–2908, https://doi.org/10.1002/qj.49712556006.

Buizza, R., J. Du, Z. Toth, et al., 2018: Major operational ensemble prediction systems (EPS) and the future of EPS. *Handbook of Hydrometeorological Ensemble Forecasting*, Q. Y. Duan, F. Pappenberger, A. Wood, et al., Eds., Springer, Berlin and Heidelberg, 1–43, https://doi.org/10.1007/978-3-642-40457-3_14-1.

Cai, W. C., J. Z. Min, and X. R. Zhuang, 2017: Comparison of different stochastic physics perturbation schemes on a storm-scale ensemble forecast in a heavy rain event. *Plateau Meteor.*, **36**, 407–423, https://doi.org/10.7522/j.issn.1000-0534.2016.00024. (in Chinese)

Charron, M., G. Pellerin, L. Spacek, et al., 2010: Toward random sampling of model error in the Canadian ensemble prediction system. *Mon. Wea. Rev.*, **138**, 1877–1901, https://doi.org/10.1175/2009MWR3187.1.

Chen, C. H., Y. Wang, H. R. He, et al., 2021: Review of the ensemble prediction using stochastic physics. *Adv. Meteor. Sci. Technol.*, **11**, 48–57, https://doi.org/10.3969/j.issn.2095-1973.2021.03.007. (in Chinese)

Chen, D. H., J. S. Xue, X. S. Yang, et al., 2008: New generation of multi-scale NWP system (GRAPES): General scientific design. *Chinese Sci. Bull.*, **53**, 3433–3445, https://doi.org/10.1007/s11434-008-0494-z.

Chen, J., and X. L. Li, 2020: The review of 10 years development of the GRAPES global/regional ensemble prediction. *Adv. Meteor. Sci. Technol.*, **10**, 9–18, 29, https://doi.org/10.3969/j.issn.2095-1973.2020.02.003. (in Chinese)

Chen, J., D. H. Chen, and H. Yan, 2002: A brief review on the development of ensemble prediction system. *J. Appl. Meteor. Sci.*, **13**, 497–507, https://doi.org/10.3969/j.issn.1001-7313.2002.04.013. (in Chinese)

Chen, J., J. S. Xue, and H. Yan, 2003: The uncertainty of mesoscale numerical prediction of South China heavy rain and the ensemble simulations. *Acta Meteor. Sinica*, **61**, 432–446, https://doi.org/10.11676/qxxb2003.042. (in Chinese)

Chen, J., J. S. Xue, and H. Yan, 2004: Impacts of diabatic physics parameterization schemes on mesoscale heavy rainfall short-range simulation. *Acta Meteor. Sinica*, **18**, 51–72. Available online at http://jmr.cmsjournal.net/en/article/id/943. Accessed on 6 May 2025.

Chen, J., J. S. Xue, and H. Yan, 2005: A new initial perturbation method of ensemble mesoscale heavy rain prediction. *Chinese J. Atmos. Sci.*, **29**, 717–726, https://doi.org/10.3878/j.issn.1006-9895.2005.05.05. (in Chinese)

Chen, J., J. Z. Wang, J. Du, et al., 2020: Forecast bias correction through model integration: A dynamical wholesale approach. *Quart. J. Roy. Meteor. Soc.*, **146**, 1149–1168, https://doi.org/10.1002/qj.3730.

Chen, X., H. L. Yuan, and M. Xue, 2018: Spatial spread-skill relationship in terms of agreement scales for precipitation forecasts in a convection-allowing ensemble. *Quart. J. Roy. Meteor. Soc.*, **144**, 85–98, https://doi.org/10.1002/qj.3186.

Chen, Y. X., J. Chen, D. H. Chen, et al., 2021: A simulated radar reflectivity calculation method in numerical weather prediction models. *Wea. Forecasting*, **36**, 341–359, https://doi.org/10.1175/WAF-D-20-0030.1.

Chou, J. F., 1986: Some general properties of the atmospheric model in H space, R space, point mapping, cell mapping. Proceedings of International Summer Colloquium on Nonlinear Dynamics of the Atmosphere, 10–20 August, Beijing. Science Press, Beijing, 187–189.

Deng, G., J. D. Gong, L. T. Deng, et al., 2010: Development of mesoscale ensemble prediction system at national meteorological center. *J. Appl. Meteor. Sci.*, **21**, 513–523, https://doi.org/10.3969/j.issn.1001-7313.2010.05.001. (in Chinese)

Denis, B., J. Côté, and R. Laprise, 2002: Spectral decomposition of two-dimensional atmospheric fields on limited-area domains using the discrete cosine transform (DCT). *Mon. Wea. Rev.*, **130**, 1812–1829, https://doi.org/10.1175/1520-0493(2002)130<1812:SDOTDA>2.0.CO;2.

Du, J., and J. Chen, 2010: The corner stone in facilitating the transition from deterministic to probabilistic forecasts-ensemble forecasting and its impact on numerical weather prediction. *Meteor. Mon.*, **36**, 1–11, https://doi.org/10.7519/j.issn.1000-0526.2010.11.001. (in Chinese)

Du, J., and G. Deng, 2020: An introduction to "measure of forecast challenge" and "predictability horizon diagram index". *Adv. Meteor. Sci. Technol.*, **10**, 75–77, https://doi.org/10.3969/j.issn.2095-1973.2020.02.009. (in Chinese)

Du, J., R. H. Grumm, and G. Deng, 2014: Ensemble anomaly forecasting approach to predicting extreme weather demonstrated by extremely heavy rain event in Beijing. *Chinese J. Atmos. Sci.*, **38**, 685–699, https://doi.org/10.3878/j.issn.1006-9895.2013.13218. (in Chinese)

Du, J., J. Berner, R. Buizza, et al., 2018: Ensemble methods for meteorological predictions. *Handbook of Hydrometeorological Ensemble Forecasting*, Q. Y. Duan, F. Pappenberger, A. Wood, et al., Eds., Springer, Berlin and Heidelberg, 1–52, https://doi.org/10.1007/978-3-642-40457-3_13-1.

Duan, W. S., and F. F. Zhou, 2013: Non-linear forcing singular vector of a two-dimensional quasi-geostrophic model. *Tellus A*, **65**, 18452, https://doi.org/10.3402/tellusa.v65i0.18452.

Duan, W. S., and Z. H. Huo, 2016: An approach to generating mutually independent initial perturbations for ensemble forecasts: Orthogonal conditional nonlinear optimal perturbations. *J. Atmos. Sci.*, **73**, 997–1014, https://doi.org/10.1175/JAS-D-15-0138.1.

Duan, W. S., R. Q. Ding, and F. F. Zhou, 2013: Several dynamical methods used in predictability studies for numerical weather forecasts and climate prediction. *Climatic Environ. Res.*, **18**, 524–538, https://doi.org/10.3878/j.issn.1006-9585.2012.12009. (in Chinese)

Dutra, E., L. Magnusson, F. Wetterhall, et al., 2013: The 2010–2011 drought in the Horn of Africa in ECMWF reanalysis and seasonal forecast products. *Int. J. Climatol.*, **33**, 1720–1729, https://doi.org/10.1002/joc.3545.

Epstein, E. S., 1969: Stochastic dynamic prediction. *Tellus A*, **21**, 739–759, https://doi.org/10.3402/tellusa.v21i6.10143.

Feng, H. Z., J. Chen, G. B. He, et al., 2006: Simulation and test of short-range ensemble prediction system for heavy rainfall in the upper reach of Changjiang River. *Meteor. Mon.*, **32**, 12–16, https://doi.org/10.3969/j.issn.1000-0526.2006.08.002. (in Chinese)

Feng, J., R. Q. Ding, D. Q. Liu, et al., 2014: The application of nonlinear local Lyapunov vectors to ensemble predictions in Lorenz systems. *J. Atmos. Sci.*, **71**, 3554–3567, https://doi.org/10.1175/JAS-D-13-0270.1.

Gao, L., J. Chen, J. W. Zheng, et al., 2019: Progress in researches on ensemble forecasting of extreme weather based on numerical models. *Adv. Earth Sci.*, **34**, 706–716, https://doi.org/10.11867/j.issn.1001-8166.2019.07.0706. (in Chinese)

Guan, H., and Y. J. Zhu, 2017: Development of verification methodology for extreme weather forecasts. *Wea. Forecasting*, **32**, 479–491, https://doi.org/10.1175/WAF-D-16-0123.1.

Hamill, T. M., 1999: Hypothesis tests for evaluating numerical precipitation forecasts. *Wea. Forecasting*, **14**, 155–167, https://doi.org/10.1175/1520-0434(1999)014<0155:HTFENP>2.0.CO;2.

Hamill, T. M., and J. Juras, 2006: Measuring forecast skill: Is it real skill or is it the varying climatology? *Quart. J. Roy. Meteor. Soc.*, **132**, 2905–2923, https://doi.org/10.1256/qj.06.25.

Han, Y. M., J. Chen, F. Peng, et al., 2023: A model tendency per-

turbation method that combines systematic bias of potential temperature and random errors in global ensemble prediction. *Acta Meteor. Sinica*, **81**, 592–604, https://doi.org/10.11676/qxxb2023.20220203. (in Chinese)

Hersbach, H., R. Mureau, J. D. Opsteegh, et al., 2000: A short-range to early-medium-range ensemble prediction system for the European area. *Mon. Wea. Rev.*, **128**, 3501–3519, https://doi.org/10.1175/1520-0493(2000)128<3501:ASRTEM>2.0.CO;2.

Hoffman, R. N., and E. Kalnay, 1983: Lagged average forecasting, an alternative to Monte Carlo forecasting. *Tellus A*, **35A**, 100–118. Available online at https://onlinelibrary.wiley.com/doi/abs/10.1111/j.1600-0870.1983.tb00189.x. Accessed on 6 May 2025.

Hohenegger, C., and C. Schar, 2007: Atmospheric predictability at synoptic versus cloud-resolving scales. *Bull. Amer. Meteor. Soc.*, **88**, 1783–1794, https://doi.org/10.1175/BAMS-88-11-1783.

Hollingsworth, A., 1979: An experiment in Monte Carlo forecasting. Proceedings of ECMWF Workshop on Stochastic Dynamic Forecasting, ECMWF, Reading, 65–85. Available online at https://www.ecmwf.int/en/elibrary/74849-experiment-monte-carlo-forecasting. Accessed on 6 May 2025.

Houtekamer, P. L., and J. Derome, 1995: Methods for ensemble prediction. *Mon. Wea. Rev.*, **123**, 2181–2196, https://doi.org/10.1175/1520-0493(1995)123<2181:MFEP>2.0.CO;2.

Houtekamer, P. L., and H. L. Mitchell, 2005: Ensemble Kalman filtering. *Quart. J. Roy. Meteor. Soc.*, **131**, 3269–3289, https://doi.org/10.1256/qj.05.135.

Houtekamer, P. L., L. Lefaivre, J. Derome, et al., 1996: A system simulation approach to ensemble prediction. *Mon. Wea. Rev.*, **124**, 1225–1242, https://doi.org/10.1175/1520-0493(1996)124<1225:ASSATE>2.0.CO;2.

Huo, Z. H., Y. Z. Liu, J. Chen, et al., 2020: The preliminary appliation of tropical cyclone targeted singular vectors in the GRAPES global ensemble forecasts. *Acta Meteor. Sinica*, **78**, 48–59, https://doi.org/10.11676/qxxb2020.006. (in Chinese)

Isaksen, L., M. Bonavita, R. Buizza, et al., 2010: Ensemble of Data Assimilations at ECMWF. Technical Memorandum No.636, ECMWF, 42 pp. Available online at https://www.ecmwf.int/en/elibrary/74969-ensemble-data-assimilations-ecmwf. Accessed on 6 May 2025.

Jankov, I., J. Berner, J. Beck, et al., 2017: A performance comparison between multiphysics and stochastic approaches within a North American RAP ensemble. *Mon. Wea. Rev.*, **145**, 1161–1179, https://doi.org/10.1175/MWR-D-16-0160.1.

Jankov, I., J. Beck, J. Wolff, et al., 2019: Stochastically perturbed parameterizations in an HRRR-based ensemble. *Mon. Wea. Rev.*, **147**, 153–173, https://doi.org/10.1175/MWR-D-18-0092.1.

Ji, L. Y., X. F. Zhi, C. Simmer, et al., 2020: Multimodel ensemble forecasts of precipitation based on an object-based diagnostic evaluation. *Mon. Wea. Rev.*, **148**, 2591–2606, https://doi.org/10.1175/MWR-D-19-0266.1.

Ji, Y., X. F. Zhi, L. Y. Ji, et al., 2023: Conditional ensemble model output statistics for postprocessing of ensemble precipitation forecasting. *Wea. Forecasting*, **38**, 1707–1718, https://doi.org/10.1175/WAF-D-22-0190.1.

Jiang, Y. M., J. Chen, M. Y. Jiao, et al., 2011: The preliminary experiment of GRAPES-MESO ensemble prediction based on TIGGE data. *Meteor. Mon.*, **37**, 392–402. (in Chinese)

Jiao, M. Y., 2010: Progress on the key technology development in application of ensemble prediction products associated with TIGGE. *J. Meteor. Res.*, **24**, 136. Available online at http://jmr.cmsjournal.net/en/article/id/1240. Accessed on 6 May 2025.

Johnson, A., 2014: Optimal design of a multi-scale ensemble system for convective scale probabilistic forecasts: Data assimilation and initial condition perturbation methods. Ph.D. dissertation, University of Oklahoma, USA, 156 pp.

Jolliffe, I. T., and D. B. Stephenson, 2012: *Forecast Verification: A Practitioner's Guide in Atmospheric Science*. 2nd ed. Wiley-Blackwell, Chichester, 274 pp.

Krishnamurti, T. N., C. M. Kishtawal, T. E. LaRow, et al., 1999: Improved weather and seasonal climate forecasts from multimodel superensemble. *Science*, **285**, 1548–1550, https://doi.org/10.1126/science.285.5433.1548.

Lalaurette, F., 2003: Early detection of abnormal weather conditions using a probabilistic extreme forecast index. *Quart. J. Roy. Meteor. Soc.*, **129**, 3037–3057, https://doi.org/10.1256/qj.02.152.

Leith, C. E., 1974: Theoretical skill of Monte Carlo forecasts. *Mon. Wea. Rev.*, **102**, 409–418, https://doi.org/10.1175/1520-0493(1974)102<0409:TSOMCF>2.0.CO;2.

Leutbecher, M., S.-J. Lock, P. Ollinaho, et al., 2017: Stochastic representations of model uncertainties at ECMWF: State of the art and future vision. *Quart. J. Roy. Meteor. Soc.*, **143**, 2315–2339, https://doi.org/10.1002/qj.3094.

Li, C., 2001: An integrated decision-making model of ecological and environmental management for sustainable development in the Yangtze River Basin. Ph.D. dissertation, China Institute of Water Resources and Hydropower Research, China. (in Chinese)

Li, J., J. Du, M. H. Wang, et al., 2009: Experiments of perturbing initial conditions in the development of mesoscale ensemble prediction system for heavy rainstorm forecasting. *Plateau Meteor.*, **28**, 1365–1375. (in Chinese)

Li, J., J. Du, and Y. Liu, 2015: A comparison of initial condition-, multi-physics- and stochastic physics-based ensembles in predicting Beijing "7.21" excessive storm rain event. *Acta Meteor. Sinica*, **73**, 50–71, https://doi.org/10.11676/qxxb2015.008.

Li, J., J. Du, Y. Liu, et al., 2017: Similarities and differences in the evolution of ensemble spread using various ensemble perturbation methods including topography perturbation. *Acta Meteor. Sinica*, **75**, 123–146, https://doi.org/10.11676/qxxb2017.011. (in Chinese)

Li, J. P., Q. C. Zeng, and J. F. Chou, 2000: Computational uncertainty principle in nonlinear ordinary differential equations. I. Numerical results. *Sci. China Ser. E*, **43**, 449–460. Available online at https://www.sciengine.com/Sci%20China%20Tech%20Sci%20E/doi/10.1360/ye2000-43-5-449. Accessed on 6 May 2025.

Li, X. L., and Y. Z. Liu, 2019: The improvement of GRAPES global extratropical singular vectors and experimental study. *Acta Meteor. Sinica*, **77**, 552–562, https://doi.org/10.11676/qxxb2019.020. (in Chinese)

Li, X. L., M. Charron, L. Spacek, et al., 2008: A regional ensemble prediction system based on moist targeted singular vectors and stochastic parameter perturbations. *Mon. Wea. Rev.*, **136**, 443–462, https://doi.org/10.1175/2007MWR2109.1.

Li, X. Q., J. D. Liu, and Y. H. Wang, 1997: The ensemble prediction and its application in medium range weather forecast. *Meteor. Mon.*, **23**, 3–9. (in Chinese)

Li, Z. C., and D. H. Chen, 2002: The development and application of the operational ensemble prediction system at National Meteorological Center. *J. Appl. Meteor. Sci.*, **13**, 1–15, https://doi.org/10.3969/j.issn.1001-7313.2002.01.001. (in Chinese)

Liu, L., J. Chen, and J. Y. Wang, 2018: A study on medium-range objective weather forecast technology for persistent heavy rainfall events based on T639 ensemble forecast. *Acta Meteor. Sinica*, **76**, 228–240, https://doi.org/10.11676/qxxb2018.002. (in Chinese)

Liu, X., J. Chen, Y. Z. Liu, et al., 2024: An initial perturbation method for the multiscale singular vector in global ensemble prediction. *Adv. Atmos. Sci.*, **41**, 545–563, https://doi.org/10.1007/s00376-023-3035-4.

Liu, Y. Z., X. S. Yang, and H. Q. Wang, 2011: Research on GRAPES singular vectors and application to heavy rain ensemble prediction. *Acta Sci. Nat. Univ. Pekinensis*, **47**, 271–277, https://doi.org/10.13209/j.0479-8023.2011.039. (in Chinese)

Liu, Y. Z., X. S. Shen, and X. L. Li, 2013: Research on the singular vector perturbation of the GRAPES global model based on the total energy norm. *Acta Meteor. Sinica*, **71**, 517–526, https://doi.org/10.11676/qxxb2013.043. (in Chinese)

Liu, Y. Z., L. Zhang, and Z. Y. Jin, 2017: The optimization of GRAPES global tangent linear model and adjoint model. *J. Appl. Meteor. Sci.*, **28**, 62–71, https://doi.org/10.11898/1001-7313.20170106. (in Chinese)

Long, K. J., J. Chen, X. L. Ma, et al., 2011: The preliminary study on ensemble prediction of GRAPES-meso based on ETKF. *J. Chengdu Univ. Inf. Technol.*, **26**, 37–46, https://doi.org/10.3969/j.issn.1671-1742.2011.01.008. (in Chinese)

Lorenz, E. N., 1963: Deterministic nonperiodic flow. *J. Atmos. Sci.*, **20**, 130–141, https://doi.org/10.1175/1520-0469(1963)020<0130:DNF>2.0.CO;2.

Lyu, Y., S. P. Zhu, X. F. Zhi, et al., 2023: Improving subseasonal-to-seasonal prediction of summer extreme precipitation over southern China based on a deep learning method. *Geophys. Res. Lett.*, **50**, e2023GL106245, https://doi.org/10.1029/2023GL106245.

Ma, Q., J. D. Gong, L. Li, et al., 2008: Study on the 2nd moment spread-correction of mesoscale ensemble forecast system. *Meteor. Mon.*, **34**, 15–21, https://doi.org/10.7519/j.issn.1000-0526.2008.11.003. (in Chinese)

Ma, X. L., J. S. Xue, and W. S. Lu, 2008: Preliminary study on ensemble transform Kalman filter-based initial perturbation scheme in GRAPES global ensemble prediction. *Acta Meteor. Sinica*, **66**, 526–536, https://doi.org/10.11676/qxxb2008.050. (in Chinese)

Ma, X. L., Y. X. Ji, B. Y. Zhou, et al., 2018: A new scheme of blending initial perturbation of the GRAPES regional ensemble prediction system. *Trans. Atmos. Sci.*, **41**, 248–257, https://doi.org/10.13878/j.cnki.dqkxxb.20160104001. (in Chinese)

Ma, Y. N., J. Chen, Z. Z. Xu, et al., 2023: Evolution characteristics of initial perturbation energy at different scales in convection-permitting ensemble prediction of GRAPES. *Chinese J. Atmos. Sci.*, **47**, 1541–1556, https://doi.org/10.3878/j.issn.1006-9895.2202.21242. (in Chinese)

Molteni, F., R. Buizza, T. N. Palmer, et al., 1996: The ECMWF Ensemble Prediction System: Methodology and validation. *Quart. J. Roy. Meteor. Soc.*, **122**, 73–119, https://doi.org/10.1002/qj.49712252905.

Mu, M., W. S. Duan, and B. Wang, 2003: Conditional nonlinear optimal perturbation and its applications. *Nonlinear Proc. Geophys.*, **10**, 493–501, https://doi.org/10.5194/npg-10-493-2003.

Mu, M., B. Y. Chen, F. F. Zhou, et al., 2011: Methods and uncertainties of meteorological forecast. *Meteor. Mon.*, **37**, 1–13. Available online at http://qxqk.nmc.cn/qx/ch/reader/view_abstract.aspx?file_no=20110101&flag=1. Accessed on 6 May 2025. (in Chinese)

Mylne, K., J. Chen, A. Erfani, et al., 2022: Guidelines for Ensemble Prediction System. WMO-1254, World Meteorological Organization, 40 pp.

Nielsen, E. R., 2016: Using convection-allowing ensembles to understand the predictability of extreme rainfall. Master dissertation, Colorado State University, USA, 178 pp.

Ono, K., M. Kunii, and Y. Honda, 2021: The regional model-based mesoscale ensemble prediction system, MEPS, at the Japan Meteorological Agency. *Quart. J. Roy. Meteor. Soc.*, **147**, 465–484, https://doi.org/10.1002/qj.3928.

Palmer, T. N., R. Buizza, F. Doblas-Reyes, et al., 2009: Stochastic Parametrization and Model Uncertainty. ECMWF Technical Memoranda 598, ECMWF, 42 pp, https://doi.org/10.21957/ps8gbwbdv.

Pan, X., Q. P. Wang, Y. Zhang, et al., 2021: Analysis constraints scheme of initial perturbation of ensemble prediction. *Chinese J. Atmos. Sci.*, **45**, 1327–1344. Available online at http://www.iapjournals.ac.cn/dqkx/article/doi/10.3878/j.issn.1006-9895.2103.21029. Accessed on 6 May 2025. (in Chinese)

Pauluis, O., and J. Schumacher, 2013: Radiation impacts on conditionally unstable moist convection. *J. Atmos. Sci.*, **70**, 1187–1203, https://doi.org/10.1175/JAS-D-12-0127.1.

Peng, F., X. L. Li, J. Chen, et al., 2019: A stochastic kinetic energy backscatter scheme for model perturbations in the GRAPES global ensemble prediction system. *Acta Meteor. Sinica*, **77**, 180–195, https://doi.org/10.11676/qxxb2019.009. (in Chinese)

Peng, F., X. L. Li, and J. Chen, 2020: Impacts of different stochastic physics perturbation schemes on the GRAPES global ensemble prediction system. *Acta Meteor. Sinica*, **78**, 972–987, https://doi.org/10.11676/qxxb2020.074. (in Chinese)

Peng, F., J. Chen, X. L. Li, et al., 2024: Development of the CMA-GEPS extreme forecast index and its application to verification of summer 2022 extreme high temperature forecasts. *Acta Meteor. Sinica*, **82**, 190–207, https://doi.org/10.11676/qxxb2024.20230017. (in Chinese)

Qi, Q. Q., Y. J. Zhu, J. Chen, et al., 2022: Error diagnosis and assessment of sub-seasonal forecast using GRAPES-GFS model. *Chinese J. Atmos. Sci.*, **46**, 327–345. Available online at http://www.iapjournals.ac.cn/dqkx/article/doi/10.3878/j.issn.1

006-9895.2008.20157. Accessed on 6 May 2025. (in Chinese)

Qiao, X. S., S. Z. Wang, and J. Z. Min, 2017: A stochastic perturbed parameterization tendency scheme for diffusion (SP PTD) and its application to an idealized supercell simulation. *Mon. Wea. Rev.*, **145**, 2119–2139, https://doi.org/10.1175/MWR-D-16-0307.1.

Qiao, X. S., S. Z. Wang, and J. Z. Min, 2018: The impact of a stochastically perturbing microphysics scheme on an idealized supercell storm. *Mon. Wea. Rev.*, **146**, 95–118, https://doi.org/10.1175/MWR-D-17-0064.1.

Raynaud, L., B. Touzé, and P. Arbogast, 2018: Detection of severe weather events in a high-resolution ensemble prediction system using the extreme forecast index (EFI) and shift of tails (SOT). *Wea. Forecasting*, **33**, 901–908, https://doi.org/10.1175/WAF-D-17-0183.1.

Sanchez, C., K. D. Williams, and M. Collins, 2016: Improved stochastic physics schemes for global weather and climate models. *Quart. J. Roy. Meteor. Soc.*, **142**, 147–159, https://doi.org/10.1002/qj.2640.

Shen, X. S., J. J. Wang, Z. C. Li, et al., 2020: China's independent and innovative development of numerical weather prediction. *Acta Meteor. Sinica*, **78**, 451–476, https://doi.org/10.11676/qxxb2020.030. (in Chinese)

Shutts, G., 2005: A kinetic energy backscatter algorithm for use in ensemble prediction systems. Quart. *J. Roy. Meteor. Soc.*, **131**, 3079–3102, https://doi.org/10.1256/qj.04.106.

Steinhoff, J., and D. Underhill, 1994: Modification of the Euler equations for "vorticity confinement": Application to the computation of interacting vortex rings. *Phys. Fluids*, **6**, 2738–2744, https://doi.org/10.1063/1.868164.

Stensrud, D. J., J. W. Bao, and T. T. Warner, 2000: Using initial condition and model physics perturbations in short-range ensemble simulations of mesoscale convective systems. *Mon. Wea. Rev.*, **128**, 2077–2107, https://doi.org/10.1175/1520-0493(2000)128<2077:UICAMP>2.0.CO;2.

Su, X., H. L. Yuan, Y. J. Zhu, et al., 2014: Evaluation of TIGGE ensemble predictions of Northern Hemisphere summer precipitation during 2008–2012. *J. Geophys. Res. Atmos.*, **119**, 7292–7310, https://doi.org/10.1002/2014JD021733.

Tan, N., J. Chen, and H. Tian, 2013: Comparison between two global model stochastic perturbation schemes and analysis of perturbation propagation. *Meteor. Mon.*, **39**, 543–555. Available online at http://qxqk.nmc.cn/qx/ch/reader/view_abstract.aspx?flag=1&file_no=20130502&journal_id=qx. Accessed on 7 May 2025. (in Chinese)

Tan, Y., and D. H. Chen, 2007: Meso-scale ensemble forecasts on physical perturbation using a non-hydrostatic model. *J. Appl. Meteor. Sci.*, **18**, 396–406, https://doi.org/10.3969/j.issn.1001-7313.2007.03.017. (in Chinese)

Tian, H., G. Deng, J. K. Hu, et al., 2007: Introduction to the global T213 numerical ensemble forecast service system. *Meteor. Mon*., **34**, 2658–2662. (in Chinese)

Tian, W. H., and S. Y. Zhuang, 2008: Application of ETKF method to regional ensemble forecasts. *Meteor. Mon.*, **34**, 35–39, https://doi.org/10.7519/j.issn.1000-0526.2008.08.005. (in Chinese)

Tompkins, A. M., and J. Berner, 2008: A stochastic convective approach to account for model uncertainty due to unresolved humidity variability. *J. Geophys. Res.*, **113**, D18101, https://doi.org/10.1029/2007JD009284.

Torn, R. D., and G. J. Hakim, 2008: Performance characteristics of a pseudo-operational ensemble Kalman filter. *Mon. Wea. Rev.*, **136**, 3947–3963, https://doi.org/10.1175/2008MWR2443.1.

Toth, Z., and E. Kalnay, 1993: Ensemble forecasting at NMC: The generation of perturbations. *Bull. Amer. Meteor. Soc.*, **74**, 2317–2330, https://doi.org/10.1175/1520-0477(1993)074<2317:EFANTG>2.0.CO;2.

Tsonevsky, I., C. A. Doswell III, and H. E. Brooks, 2018: Early warnings of severe convection using the ECMWF extreme forecast index. *Wea. Forecasting*, **33**, 857–871, https://doi.org/10.1175/WAF-D-18-0030.1.

Wang, C. X., J. Q. Yao, and X. D. Liang, 2007: The comparing experiment of improving the operational ensemble prediction system for Shanghai regional precipitation. *J. Meteor. Sci.*, **27**, 481–487, https://doi.org/10.3969/j.issn.1009-0827.2007.05.002. (in Chinese)

Wang, J. Y., J. Chen, L. Liu, et al., 2014: The sensitivity of the extreme precipitation forecast index on climatological cumulative probability distribution. *Torrential Rain Disaster*, **33**, 313–319, https://doi.org/10.3969/j.issn.1004-9045.2014.04.002. (in Chinese)

Wang, J. Z., J. Chen, Z. R. Zhuang, et al., 2018: Characteristics of initial perturbation growth rate in the regional ensemble prediction system of GRAPES. *Chinese J. Atmos. Sci.*, **42**, 367–382, https://doi.org/10.3878/j.issn.1006-9895.1708.17141. (in Chinese)

Wang, L., X. S. Shen, J. J. Liu, et al., 2020: Model uncertainty representation for a convection-allowing ensemble prediction system based on CNOP-P. *Adv. Atmos. Sci.*, **37**, 817–831, https://doi.org/10.1007/s00376-020-9262-z.

Wang, Q. P., X. Pan, B. Y. Zhou, et al., 2023: Cosine analysis constraint scheme based on ETKF initial perturbations in the GRAPES regional ensemble prediction system. *Chinese J. Atmos. Sci.*, **47**, 1731–1745. Available online at http://www.iap-journals.ac.cn/dqkx/en/article/doi/10.3878/j.issn.1006-9895.2210.22062. Accessed on 7 May 2025. (in Chinese)

Wang, X. G., and C. H. Bishop, 2003: A comparison of breeding and ensemble transform Kalman filter ensemble forecast schemes. *J. Atmos. Sci.*, **60**, 1140–1158, https://doi.org/10.1175/1520-0469(2003)060<1140:ACOBAE>2.0.CO;2.

Wang, Y., M. Bellus, J. F. Geleyn, et al., 2014: A new method for generating initial condition perturbations in a regional ensemble prediction system: Blending. *Mon. Wea. Rev.*, **142**, 2043–2059, https://doi.org/10.1175/MWR-D-12-00354.1.

Wei, M. Z., Z. Toth, R. Wobus, et al., 2006: Ensemble transform Kalman filter-based ensemble perturbations in an operational global prediction system at NCEP. *Tellus A*, **58**, 28–44, https://doi.org/10.1111/j.1600-0870.2006.00159.x.

Wei, M. Z., Z. Toth, R. Wobus, et al., 2008: Initial perturbations based on the ensemble transform (ET) technique in the NCEP global operational forecast system. *Tellus A*, **60**, 62–79, https://doi.org/10.1111/j.1600-0870.2007.00273.x

Whitaker, J. S., and T. M. Hamill, 2002: Ensemble data assimilation without perturbed observations. *Mon. Wea. Rev.*, **130**, 1913–1924, https://doi.org/10.1175/1520-0493(2002)130<1913:EDAWPO>2.0.CO;2.

Wilks, D. S., 2011: Chapter 8: Forecast verification. *Int. J. Geophys.*, **100**, 301–394, https://doi.org/10.1016/B978-0-12-385022-5.00008-7.

Williams, R. M., C. A. T. Ferro, and F. Kwasniok, 2014: A comparison of ensemble post-processing methods for extreme events. *Quart. J. Roy. Meteor. Soc.*, **140**, 1112–1120, https://doi.org/10.1002/qj.2198.

Wu, Z. Q., J. Zhang, J. Chen, et al., 2020: The study on the method of conditional typhoon vortex relocation for GRAPES regional ensemble prediction. *Acta Meteor. Sinica*, **78**, 163–176, https://doi.org/10.11676/qxxb2020.027. (in Chinese)

Xia, F., and J. Chen, 2012: The research of extreme forecast index based on the T213 ensemble forecast and the experiment in predicting temperature. *Meteor. Mon.*, **38**, 1492–1501. Available online at http://qxqk.nmc.cn/qxen/article/abstract/20121206. Accessed on 7 May 2025. (in Chinese)

Xia, Y., J. Chen, J. Du, et al., 2019: A unified scheme of stochastic physics and bias correction in an ensemble model to reduce both random and systematic errors. *Wea. Forecasting*, **34**, 1675–1691, https://doi.org/10.1175/WAF-D-19-0032.1.

Xu, Z. Z., J. Chen, Y. Wang, et al., 2019: Sensitivity experiments of a stochastically perturbed parameterizations (SPP) scheme for mesoscale precipitation ensemble prediction. *Acta Meteor. Sinica*, **77**, 849–868, https://doi.org/10.11676/qxxb2019.039. (in Chinese)

Xu, Z. Z., J. Chen, M. Mu, et al., 2022a: A nonlinear representation of model uncertainty in a convective-scale ensemble prediction system. *Adv. Atmos. Sci.*, **39**, 1432–1450, https://doi.org/10.1007/s00376-022-1341-x.

Xu, Z. Z., J. Chen, M. Mu, et al., 2022b: A stochastic and non-linear representation of model uncertainty in a convective-scale ensemble prediction system. *Quart. J. Roy. Meteor. Soc.*, **148**, 2507–2531, https://doi.org/10.1002/qj.4322.

Yang, M., P. L. Yu, L. F. Zhang, et al., 2024: Predictability of the 7·20 extreme rainstorm in Zhengzhou in stochastic kinetic-energy backscatter ensembles. *Sci. China Earth Sci.*, **67**, 2226–2241, https://doi.org/10.1007/s11430-023-1357-1.

Yang, X., K. Dai, and Y. J. Zhu, 2022: Progress and challenges of deep learning techniques in intelligent grid weather forecasting. *Acta Meteor. Sinica*, **80**, 649–667, https://doi.org/10.11676/qxxb2022.051. (in Chinese)

Yang, X. S., D. H. Chen, T. B. Leng, et al., 2002: The comparison experiments of SV and LAF initial perturbation techniques used at the NMC ensemble prediction system. *J. Appl. Meteor. Sci.*, **13**, 62–66, https://doi.org/10.3969/j.issn.1001-7313.2002.01.007. (in Chinese)

Yano, J.-I., M. Z. Ziemiański, M. Cullen, et al., 2018: Scientific challenges of convective-scale numerical weather prediction. *Bull. Amer. Meteor. Soc.*, **99**, 699–710, https://doi.org/10.1175/BAMS-D-17-0125.1.

Ye, L., Y. Z. Liu, J. Chen, et al., 2020: A study on multi-scale singular vector initial perturbation method for ensemble prediction. *Acta Meteor. Sinica*, **78**, 648–664, https://doi.org/10.11676/qxxb2020.042. (in Chinese)

Yuan, H. L., S. L. Mullen, X. G. Gao, et al., 2005: Verification of probabilistic quantitative precipitation forecasts over the southwest United States during winter 2002/03 by the RSM ensemble system. *Mon. Wea. Rev.*, **133**, 279–294, https://doi.org/10.1175/MWR-2858.1.

Yuan, Y., X. L. Li, J. Chen, et al., 2016: Stochastic parameterization toward model uncertainty for the GRAPES mesoscale ensemble prediction system. *Meteor. Mon.*, **42**, 1161–1175. Available online at http://qxqk.nmc.cn/html/2016/10/20161001.html. Accessed on 7 May 2025. (in Chinese)

Zhang, F. Q., N. F. Bei, R. Rotunno, et al., 2007: Mesoscale predictability of moist baroclinic waves: Convection-permitting experiments and multistage error growth dynamics. *J. Atmos. Sci.*, **64**, 3579–3594, https://doi.org/10.1175/JAS4028.1.

Zhang, H., W. S. Duan, and Y. C. Zhang, 2023: Using the orthogonal conditional nonlinear optimal perturbations approach to address the uncertainties of tropical cyclone track forecasts generated by the WRF model. *Wea. Forecasting*, **38**, 1907–1933, https://doi.org/10.1175/WAF-D-22-0175.1.

Zhang, H. B., J. Chen, X. F. Zhi, et al., 2015: Study on multi-scale blending initial condition perturbations for a regional ensemble prediction system. *Adv. Atmos. Sci.*, **32**, 1143–1155, https://doi.org/10.1007/s00376-015-4232-6.

Zhang, H. B., X. F. Zhi, J. Chen, et al., 2017: Achievement of perturbation methods for regional ensemble forecast. *Trans. Atmos. Sci.*, **40**, 145–157, https://doi.org/10.13878/j.cnki.dqkxxb.20160405001. (in Chinese)

Zhang, X. Y., J. Z. Min, and T. J. Wu, 2020: A study of ensemble-sensitivity-based initial condition perturbation methods for convection-permitting ensemble forecasts. *Atmos. Res.*, **234**, 104741, https://doi.org/10.1016/j.atmosres.2019.104741.

Zhang, Y. C., W. S. Duan, S. Vannitsem, et al., 2023: A new approach to represent model uncertainty in the forecasting of tropical cyclones: The orthogonal nonlinear forcing singular vectors. *Quart. J. Roy. Meteor. Soc.*, **149**, 2206–2232, https://doi.org/10.1002/qj.4502.

Zhao, X. H., and R. D. Torn, 2022: Evaluation of independent stochastically perturbed parameterization tendency (iSPPT) scheme on HWRF-based ensemble tropical cyclone intensity forecasts. *Mon. Wea. Rev.*, **150**, 2659–2674, https://doi.org/10.1175/MWR-D-21-0303.1.

Zhi, X. F., H. X. Qi, Y. Q. Bai, et al., 2012: A comparison of three kinds of multimodel ensemble forecast techniques based on the TIGGE data. *Acta Meteor. Sinica*, **26**, 41–51, https://doi.org/10.1007/S13351-012-0104-5.

Zhi, X. F., X. D. Ji, J. Zhang, et al., 2013: Multimodel ensemble forecasts of surface air temperature and precipitation using TIGGE datasets. *Trans. Atmos. Sci.*, **36**, 257–266, https://doi.org/10.3969/j.issn.1674-7097.2013.03.001. (in Chinese)

Zhi, X. F., T. Wang, and Y. Ji, 2020: Multimodel ensemble forecasts of surface air temperature over China based on deep learning approach. *Trans. Atmos. Sci.*, **43**, 435–446, https://doi.org/10.13878/j.cnki.dqkxxb.20200219003. (in Chinese)

Zhou, X. Q., Y. J. Zhu, D. C. Hou, et al., 2016: A comparison of perturbations from an ensemble transform and an ensemble Kalman filter for the NCEP global ensemble forecast system. *Wea. Forecasting*, **31**, 2057–2074, https://doi.org/10.1175/WAF-D-16-0109.1.

Zhou, X. Q., Y. J. Zhu, D. C. Hou, et al., 2017: Performance of the new NCEP global ensemble forecast system in a parallel experiment. *Wea. Forecasting*, **32**, 1989–2004, https://doi.org/10.1175/WAF-D-17-0023.1.

Zhou, X. Q., Y. J. Zhu, D. C. Hou, et al., 2022: The development of the NCEP global ensemble forecast system version 12. *Wea. Forecasting*, **37**, 1069–1084, https://doi.org/10.1175/WAF-D-21-0112.1.

Zhu, S. P., X. F. Zhi, F. Ge, et al., 2021: Subseasonal forecast of surface air temperature using superensemble approaches: Experiments over Northeast Asia for 2018. *Wea. Forecasting*, **36**, 39–51, https://doi.org/10.1175/WAF-D-20-0096.1.

Zhu, Y. J., Z. Toth, R. Wobus, et al., 2002: The economic value of ensemble-based weather forecasts. *Bull. Amer. Meteor. Soc.*, **83**, 73–84, https://doi.org/10.1175/1520-0477(2002)083<0073:TEVOEB>2.3.CO;2.

Zhuang, X. R., J. Z. Min, T. J. Wu, et al., 2017: Development mechanism of multi-scale perturbation based on different perturbation methods in convection-allowing ensemble prediction. *Plateau Meteor.*, **36**, 811–825. (in Chinese)

Zhuang, X. R., M. Xue, J. Z. Min, et al., 2021: Error growth dynamics within convection-allowing ensemble forecasts over central U.S. regions for days of active convection. *Mon. Wea. Rev.*, **149**, 959–977, https://doi.org/10.1175/MWR-D-20-0329.1.

doi:10.11676/qxxb2025.20240151 气象学报

集合预报进展、挑战及展望*

陈 静[1,2] 朱跃建[1,2] 段晚锁[3] 智协飞[4] 闵锦忠[4] 李晓莉[1,2] 邓 国[1,2]
袁慧玲[5] 冯 杰[6] 杜 钧[7] 李巧萍[1,2] 龚建东[1,2] 沈学顺[1,2] 穆 穆[6]
CHEN Jing[1,2] ZHU Yuejian[1,2] DUAN Wansuo[3] ZHI Xiefei[4] MIN Jinzhong[4] LI Xiaoli[1,2] DENG Guo[1,2]
YUAN Huiling[5] FENG Jie[6] DU Jun[7] LI Qiaoping[1,2] GONG Jiandong[1,2] SHEN Xueshun[1,2] MU Mu[6]

1. 中国气象局地球系统数值预报中心, 北京, 100081
2. 灾害天气科学与技术全国重点实验室, 中国气象局地球系统数值预报中心, 北京, 100081
3. 中国科学院大气物理研究所, 北京, 100029
4. 南京信息工程大学, 南京, 210044
5. 南京大学, 南京, 210008
6. 复旦大学, 上海, 200433
7. 美国国家海洋大气局国家环境预报中心, 马里兰, 20740

1. *CMA Earth System Modeling and Prediction Centre*，*Beijing* 100081，*China*
2. *State Key Laboratory of Severe Weather Meteorological Science and Technology*，*CEMC*，*Beijing* 100081，*China*
3. *Institute of Atmospheric Physics*，*Chinese Academy of Sciences*，*Beijing* 100029，*China*
4. *Nanjing University of Information Science and Technology*，*Nanjing* 210044，*China*
5. *Nanjing University*，*Nanjing* 210008，*China*
6. *Fudan University*，*Shanghai* 200433，*China*
7. *National Centers for Environmental Predictions*，*National Oceanic and Atmospheric Administration*，*Maryland* 20740，*USA*

2024-09-11 收稿, 2025-02-12 改回.

陈静, 朱跃建, 段晚锁, 智协飞, 闵锦忠, 李晓莉, 邓国, 袁慧玲, 冯杰, 杜钧, 李巧萍, 龚建东, 沈学顺, 穆穆. 2025. 集合预报进展、挑战及展望. 气象学报, 83(3): 480-502

Chen Jing, Zhu Yuejian, Duan Wansuo, Zhi Xiefei, Min Jinzhong, Li Xiaoli, Deng Guo, Yuan Huiling, Feng Jie, Du Jun, Li Qiaoping, Gong Jiandong, Shen Xueshun, Mu Mu. 2025. A review on development, challenges, and future perspectives of ensemble forecast. *Acta Meteorologica Sinica*, 83(3):480-502

Abstract This paper reviews the development of ensemble weather forecast and the primary techniques employed in themain ensemble prediction systems (EPSs) designed by China and other countries. Here, the emphasis is placed on theadvancements in the China Meteorological Administration (CMA) global and regional ensemble prediction systems (i.e., CMA-GEPS and CMA-REPS), with particular attention to operational technologies such as initial and modelperturbation methods and the applications of ensemble forecast. Through comparative verification with EPSs fromother leading international numerical weather prediction (NWP) centers, CMA's EPSs demonstrate forecast skillscomparable to its global counterparts. As EPSs progress to convective scales and coupled systems between sea, land,air, and ice, the paper addresses some key challenges in ensemble forecast technologies across the aspects of opera-tion, science, integration of artificial intelligence (AI), merging of weather and climate models, and challenging

* 资助课题: 国家自然科学基金项目(U2242213、42341209)。
作者简介: 陈静, 主要从事数值预报及集合预报科学研究、技术研发和业务发展。E-mail: chenj@cma.gov.cn

userrequirements. Finally, a summary of conclusions and future perspectives on ensemble forecast are provided.

Key words　Ensemble forecast，Method，CMA ensemble forecast，Review

摘　要　系统概述了集合预报的发展历程和中外主要的集合预报方法，重点回顾了中国全球/区域集合预报系统的发展历程、集合预报系统业务技术、初值扰动技术、模式扰动技术和集合预报应用的进步，以及与当前国际主要数值预报中心集合预报水平的对比。针对集合预报系统逐步走向对流尺度、人工智能模型的趋势，从业务、科研、人工智能与集合预报、天气与气候一体化以及用户需求等方面分析了集合预报技术发展面临的主要挑战，并对未来发展做了展望。

关键词　集合预报，方法，中国集合预报，回顾

中图法分类号　P456

1　引　言

数值预报是20世纪最伟大的科技发展之一，被称之为静悄悄的革命（Bauer, et al, 2015; 沈学顺等, 2020），其中四维变分资料同化和集合预报是公认的两项重要成就。集合预报的理论基础是Lorenz（1963）提出的大气运动可预报性理论。大气系统本质上是非线性动力系统，具有对初始小扰动敏感的混沌特性，即使在数值模式完美的情况下，由观测和同化系统等带来的初始状态不确定也会随预报时效的延长导致明显的预报误差（Lorenz, 1963; Chou, 1986; Mu, et al, 2003），加之数值模式采用了离散化求解、次网格参数化等方案对实际大气的动力和物理近似，这意味着单一确定性数值预报模式本质上就存在不确定性（Li, et al, 2000; Arakawa, 2004; Chen, et al, 2004），估计数值预报的不确定程度是数值预报的重点任务之一。人们提出了随机动力概率预报的理论，利用蒙特卡罗法（Monte Carlo）建立现代集合预报的理论框架，将单一确定数值预报转变为概率密度函数（Probability Density Function, PDF）分布并估计确定性数值预报的不确定程度（Epstein, 1969; Leith, 1974）。

理论上，概率密度函数（PDF）随时间的变化问题采用刘维尔公式表述，但实际求解该方程非常困难，即使在只有几个自由度的非线性系统中也是不可能的。因此，人们寻找了一种可以在实际应用中变通解决这个问题的方法，即集合预报（Molteni, et al, 1996）。集合预报的具体方法是通过一定的数学方法，获得在初始误差分布范围内的一组初值集合，每个初值都可能代表大气的真实状况，再用数值模式对每个初值积分，从而可以产生一组预报结果的集合，进而推演未来天气要素的PDF分布。如果初值集合能正确估计分析初值误差概率分布且大气模式相当精确，则集合预报将能够大致估计出大气状态概率密度函数分布。

集合预报的核心问题是如何合理表征数值预报误差来源，合理估计数值预报的不确定程度。众所周知，数值预报误差主要来源于同化初值误差和模式自身的误差，相应的集合预报方法源自第一类可预报性和第二类可预报性理论，各种扰动方法主要代表模式的初值误差和模式自身的各种随机误差特征，并发展了相应的集合预报初值扰动技术和模式扰动技术（陈静等, 2002）。在初值扰动技术方面，发展了如奇异向量扰动法（Singular Vector, SV; Buizza, 1997）、增长模繁殖法（Breeding of Growing Mode, BGM; Toth, et al, 1993）、观测扰动法（Houtekamer, et al, 1995）、集合变换卡尔曼滤波法（Ensemble Transform Kalman Filter, ETKF; Wang, et al, 2003; Wei, et al, 2006）、集合变换重尺度化法（Ensemble Transform with Rescaling, ETR; Wei, et al, 2008）、集合平方根滤波（Ensemble Square Root Filter, EnSRF; Whitaker, et al, 2002; Zhou, et al, 2022）、SV扰动与集合资料同化（Ensemble Data Assimilation, EDA）混合扰动（Isaksen, et al, 2010）等。在模式扰动方面，发展了多物理过程组合法（陈静等, 2003）、随机扰动物理过程倾向项方案（Stochastically Perturbed Parameterization Tendencies, SPPT; Buizza, et al, 1999; 谭宁等, 2013）、随机动能补偿方案（Stochastic Kinetic-Energy Backscatterscheme, SKEB; Shutts, 2005; 彭飞等, 2019）、物理过程关键参数随机扰动法（Stochastically Perturbed Parameterization, SPP; Jankov, et al, 2019; 徐致真等, 2019）等。这些研究促进了业务集合预报系统的不断进步，改进了业务集合预报效果。

20世纪90年代以来，随着集合预报理论和技

术发展,集合预报业务获得了巨大进步。1992年,欧洲中期天气预报中心(European Centre for Medium-Range Weather Forecasts, ECMWF)和美国环境预报中心(National Centers for Environmental Prediction, NCEP)首次建立了全球中期集合预报系统,集合预报业务实现了飞跃(Toth, et al, 1993; Molteni, et al, 1996; Buizza, 1997)。伴随模式技术和高性能计算能力显著提升,2023年6月,ECMWF率先将传统高分辨率确定性模式与低分辨率集合预报模式组合的数值天气预报业务系统进行了改进,使确定性模式与集合预报模式均采用高分辨率模式,更好地描述高分辨率模式下的预报不确定性。世界气象组织(World Meteorological Organization, WMO)2006年推动了全球观测系统研究和可预报性试验科学计划(The Observing system Research and Predictability Experiment, THORPEX)中的全球交互式大集合预报应用(the THORPEX Interactive Grand Global Ensemble, TIGGE; Jiao, 2010)。近年来,集合预报思想拓展到资料同化、物理过程参数化方案、洪水预报、强天气预报、台风路径预报等领域,集合预报思想贯穿了数值预报业务的全流程。

中国科学家较早开展了集合预报研究和业务化工作(李小泉等, 1997; 陈静等, 2002; 李泽椿等, 2002)。初值扰动方面,相继提出条件非线性最优扰动(Conditional Nonlinear Optimal Perturbation, CNOP; Mu, et al, 2003; Duan, et al, 2016)、异物理模态法(陈静等, 2005)、非线性局部Lyapunov向量(Nonlinear Local Lyapunov Vector, NLLV; Feng, et al, 2014)、多尺度混合初值扰动(Zhang, et al, 2015)、多尺度奇异向量法(叶璐等, 2020)等。模式扰动方面,相继研究了多物理过程组合法(陈静等, 2003)、物理过程随机扰动法(谭宁等, 2013)、非线性强迫奇异向量(Nonlinear Forcing Singular Vector, NFSV; 段晚锁等, 2013)、物理过程关键参数扰动法(徐致真等, 2019)、系统偏差和随机误差结合的模式倾向扰动方法(韩雨盟等, 2023)等。同时中国集合预报业务从最初以引进集成为主的谱模式集合预报发展到自主可控的全球/区域同化预报(Global/Regional Assimilation and Prediction System, GRAPES)的集合预报系统(陈静等, 2020),初值扰动方法从ETKF(马旭林等, 2008; 龙柯吉等, 2011; 张涵斌等, 2017)到多尺度SV初值扰动方法(刘永柱等, 2011; 叶璐等, 2020)的升级,同时采用SPPT和SKEB结合的方法产生模式扰动,实现中国集合预报里程碑式的进步(陈静等, 2020; 沈学顺等, 2020)。

文中系统介绍中外集合天气预报方法,重点回顾中国全球/区域集合预报系统发展历程、集合预报系统业务技术、初值扰动技术、模式扰动技术和集合预报应用方面的进步,以及与当前国际主要数值预报中心的集合预报参数及预报技巧对比。从业务、科学研究、人工智能与集合预报、天气-气候一体化以及用户需求等方面,分析集合预报技术发展面临的主要挑战以及对未来的展望。

2 集合预报方法回顾

2.1 初始误差源及初值扰动方法发展

初始误差源是数值模拟中的一个重要概念,主要源于观测资料的不准确、资料分析和同化处理中导入的误差。表征初始误差源的初值扰动方法是在全球中期集合预报系统中发展起来的。初值扰动方法的发展经历了从最初的人为随机扰动到基于统计方法的扰动技术(比如Monte Carlo、BGM、SV、ETKF、CNOP方法)等多个阶段。这些方法在不同的集合预报系统建设中得到了广泛应用,为改善预报的不确定性提供了有效手段。

2.1.1 估计同化分析误差的初始扰动

这一类方法的主要特点是估计同化分析初值的误差概率分布。如将随机噪声作为扰动场叠加在初值的蒙特卡罗随机扰动方法(Hollingsworth, 1979)和将过去间隔一定时间的模式分析场作为扰动初始场的滞后平均法(Hoffman, et al, 1983),加拿大气象局第一代全球集合预报系统即采用对观测资料进行蒙特卡罗随机扰动产生(Houtekamer, et al, 1996);随着同化系统与集合预报系统的融合发展,加拿大(Houtekamer, et al, 2005)和NCEP(Zhou, et al, 2016)采用对观测资料进行随机扰动的集合卡尔曼滤波(Ensemble Kalman Filter, EnKF)初值扰动方法。这类扰动的优点是能较好地代表分析初值误差的不确定性,产生大量的集合成员,缺点是初始扰动能量难以增长,集合预报离散度不足,难以描述预报的不确定性。潘贤等(2021)和王秋萍等(2023)提出的分析约束方案,有效吸收同化分析增量特征,改善集合初始扰动质量,提高了集

合离散度与预报误差的一致性。

2.1.2　估计误差增长最快的初始扰动

这类初始扰动是建立在大气可预报性研究成果基础上的，通过分析数值预报误差在相空间中的增长方向和速度，沿最不稳定的方向来扰动初始场，代表性方法是基于非线性动力学有限时间不稳定理论发展的奇异向量法（SV；Molteni, et al, 1996；杨学胜等，2002；刘永柱等，2011）和NCEP将初始随机扰动场通过非线性模式循环和尺度化方法最终产生初始扰动场的增长模繁殖法（BGM；Toth, et al, 1993）；SV和BGM方法都试图通过捕捉大气斜压不稳定区初值误差，代表大尺度不稳定波动的预报不确定性，SV方法通常与四维变分系统协同发展，物理意义清晰，可以获得较好的集合预报效果，被ECMWF、日本、中国等应用于中期天气集合预报中，取得了巨大成功。Zhang等（2020）为了代表初始分析误差特点，提出了一种结合ESA（Ensemble Sensitivity Analysis，集合敏感性分析）和BGM的初值扰动方法，其扰动的分布是来自敏感模态和由BGM计算的快速增长扰动，可适应天气状况的变化并提供对流系统的位置和强度的精确模拟。BGM方法凭借其有效、简单和较小的计算成本，在业务预报中心受到欢迎。此外，NCEP还发展了集合变换重尺度化（Wei, et al, 2008），其与BGM方法类似，但扰动结构接近正交，可以减小集合成员之间的相关。

SV在业务集合预报中取得了巨大成功，但SV方法对非线性模式采取了线性近似，不能充分反映非线性物理过程的影响，抑制了集合预报技巧的进一步提高，Mu等（2003）提出的CNOP方法全面考虑了非线性过程的影响，能够揭示非线性模式中发展最快的初始扰动，克服SV的局限。Duan等（2016）将CNOP拓展到不同扰动相空间，发展了正交CNOP集合预报初始扰动方法，且在台风路径的集合预报研究中获得了成功应用，揭示了正交CNOP较SV和BGM方法产生的初始扰动能够更加显著地提高台风路径预报技巧，尤其是台风异常路径的集合预报技巧（Zhang H, et al, 2023）。

针对对流不稳定导致的中、小尺度误差快速增长的影响，陈静等（2005）提出了一种针对对流不稳定构造具有中尺度运动特征的集合预报扰动初始新方法——异物理模态法。通过不同积云对流参数化方案的预报离差，寻找对流敏感区域，提取扰动变量、扰动结构、扰动幅度，从而构造初始扰动。这种方法与以往的初值扰动方法如BGM或SV的不同之处在于，它扰动对流不稳定区的初值，从而促使与对流运动有关的不稳定扰动快速增长。

2.1.3　估计多尺度系统误差的初始扰动

随着数值预报模式的分辨率不断提升，多尺度初值误差快速增长的现象对模式预报技巧的影响十分显著。针对有限区域模式缺乏大尺度初始扰动误差信息，而动力降尺度方法得到的初始扰动场难以描述局地小尺度误差信息，一些中国科技工作者提出了一种形成初始扰动的新方法——混合扰动方法（Wang, et al, 2014；Zhang, et al, 2015；庄潇然等，2017；马旭林等，2018），该方法采用滤波和谱分析方法从区域集合预报中提取小尺度扰动，从全球集合预报中提取大尺度扰动，将两者混合获得扰动场。混合产生的初始扰动可以很好地代表分析中的大尺度和小尺度的不确定性，并且更符合全球集合预报系统提供的侧边界扰动，从而大幅度提高区域集合预报系统的预报技巧。此外，中国气象局（叶璐等，2020；Liu, et al, 2024）和日本气象厅（Ono, et al, 2021）基于区域和全球集合预报模式开展了多尺度奇异向量初值扰动方法研究，得到了包含更多尺度不确定性信息的增长型初始扰动，进而更有效地反映初始误差的多尺度变化特征，提高了区域和全球集合预报效果。

总体而言，估计同化分析误差的初始扰动形成的集合预报精度略高但离散度偏小，而基于大气不稳定增长理论估计初始扰动的集合预报离散度略大但预报精度略低（Pauluis, et al, 2013）。

2.2　模式误差源及模式扰动方法发展

早期的集合预报研究主要集中在初始扰动，然而随着研究的不断深入，学者们逐渐意识到仅考虑初始不确定性可能会存在离散度不足等问题，使得预报结果发生显著偏差（Palmer, et al, 2009）。因此，有必要在集合预报中考虑模式误差或模式本身缺陷造成的不确定性。模式误差主要来源于模式对物理过程和动力过程描述不准确产生的误差（穆穆等，2011）。目前，集合预报系统考虑的模式误差大部分来源于对次网格参数化过程的不准确描述。

2.2.1　估计模式的不确定程度

在单一模式框架内通过不同物理参数化方案

组合来描述模式物理过程的不确定性(Houtekamer, et al, 1996),被称为多物理组合方案。该方案早期应用于加拿大环境局的全球集合预报系统中和各国区域集合预报(Stensrud, et al, 2000; 陈静等, 2003; 智协飞等, 2013),以提高集合预报技巧评分。另一个模式扰动方法是多模式组合(Krishnamurti, et al, 1999)。多模式方法能抓住不同模式预报的系统偏差,使集合成员产生较大的离散度,提高了中期预报和有限区域的中、小尺度集合预报的准确度(张涵斌等, 2017)。但是,由于多模式方案或多物理方案的集合成员采用不同的模式或者物理过程,失去物理上的一致,难以满足"成员等同性"要求,还增加了概率计算中处理集合预报成员权重的复杂程度(Berner, et al, 2015)。因此,近年来估计模式物理过程参数化方案不确定程度的模式扰动方法获得了更多的发展。

2.2.2 估计物理过程参数化方案的不确定程度

随机物理扰动方法是当前估计模式物理过程参数化方案不确定程度的主流方案。其理论基础是在模式某些参数值或相关项上(倾向项、扩散项)引入一个随机过程或因子对其进行扰动,从而表征模式的不确定程度。该类型扰动方案主要有随机扰动物理过程倾向项方法(SPPT; Buizza, et al, 1999; 袁月等, 2016)、随机动能补偿方法(SKEB; Shutts, 2005)和随机参数扰动方法(Random Parameters, RP; Stochastic Perturbed Parameterization, SPP; 陈静等, 2003; Bowler, et al, 2008; 谭宁等, 2013; Jankov, et al, 2017)等。

SPPT方案是应用最广泛的随机物理扰动方法,利用时、空上片段连续并满足均匀分布的随机数乘以次网格物理过程的参数化倾向,并对不同的倾向项使用不同的扰动值,提高了集合预报的离散度和概率预报效果(Li, et al, 2008)。目前SPPT方案是国际数值预报中心应用最多的集合预报模式扰动方法(Charron, et al, 2010; Sanchez, et al, 2016; 彭飞等, 2020)。但SPPT方案也存在一些缺点,如扰动幅度可能造成模式层顶和近地表通量不连续和能量不守恒,长期积分将产生系统偏差(Leutbecher, et al, 2017)。袁月等(2016)在中国气象局(China Meteorological Administration, CMA)区域集合预报系统中引入SPPT技术,显著改进了大雨级别预报后期的效果。Qiao等(2017)提出了一种基于模式耗散项不确定性的随机扰动耗散参数化倾向方法,该方案遵循SPPT方法相同的原理,但使用递归滤波器来生成平滑扰动,并采用水平和垂直局部化,以保持在强切变区域扰动的影响,有效改进了涡旋强度系统性偏弱的情况。类似的结果在微物理过程的扰动研究中也有表现(Qiao, et al, 2018)。

SKEB方案是针对数值模式动力框架在截断尺度存在的动量过度耗散误差,通过随机扰动弥补耗散能量对可分辨尺度的影响。SKEB方案在全球中期集合预报中得到应用(Berner, et al, 2009; Zhou, et al, 2017),也逐渐应用于区域对流尺度集合预报(蔡沅辰等, 2017; Yang, et al, 2024)。彭飞等(2020)发现,在GRAPES全球集合预报中联合应用SKEB方案和SPPT方案可有效提高热带地区的离散度。SKEB方案能激发出大气运动中可能存在的不稳定(Berner, et al, 2015),从而引起更大的集合离散度并捕捉到低概率事件,但由于SKEB方案的计算代价比SPPT方案大,且在平衡离散度和均方根误差方面并不理想,SKEB方案的价值逐渐降低,目前ECWMF已经停止使用该方案(陈超辉等, 2021)。

RP/SPP方法是对物理过程参数化方案中具有主观性的经验或半经验参数进行随机扰动来表征模式的不确定性(Bowler, et al, 2008),代表了小尺度系统变化的预报不确定性。该方法虽然提高了集合预报技巧,但存在一定的不合理性,如参数值会在某一时刻突然有较大变化(Jankov, et al, 2019)。此外,研究发现SPP方法扰动积云对流方案和行星边界层方案中的参数影响更显著(徐致真等, 2019),但中、长期预报的离散度不足(Leutbecher, et al, 2017)。

除了这3种常见的模式随机物理扰动方案,不少学者针对模式其他方面的不确定性来源设计了不同的解决方案,如对流的随机触发(Stochastic Trigger of Convection, STC; 李俊等, 2015)、边界层湿度随机扰动方案(Stochastic Boundary-layer Humidity, SHUM; Tompkins, et al, 2008)、涡度约束方案(Vorticity Confinement, VC; Steinhoff, et al, 1994)、中小尺度地形扰动方案(李俊等, 2017)、结合模式系统偏差和随机误差的模式倾向扰动方法(韩雨盟等, 2023)等。Zhao等(2022)将独立随机扰动参数化方案应用于单个参数化扰动,个例结

果表明，湍流混合随机扰动可增加台风强度的集合标准偏差，而对微物理、辐射和积云倾向的随机扰动的影响可以忽略不计。SHUM方案提高了热带地区离散度与预报误差的一致性，同时减小了集合平均预报误差，被应用于NCEP全球预报系统EnKF-3DVAR的混合资料同化模块中。VC方法应用于NCEP全球集合预报系统，增大了亚热带集合离散度。结合模式系统偏差和随机误差的模式倾向扰动方法减小了模式的系统偏差，被应用于CMA全球中期集合预报系统中。

2.2.3　估计模式误差增长的非线性特征

如何准确描述模式误差增长的非线性特征是当代高分辨率集合预报面临的重要挑战。Wang等(2020)将条件非线性最优参数扰动(CNOP related to Parameters, CNOP-P)方法应用于GRAPES，开展对流尺度集合预报试验，对对流层的湿度和温度的预报产生了更大的离散度，并且在近地面变量和降水预报方面有更加可靠的预报技巧。Xu等(2022a)采用非线性强迫奇异向量方法(NFSV，亦即CNOP-Forcing, CNOP-F; Duan, et al, 2013)描述不同来源模式误差的综合影响，在SPPT扰动上叠加具有特定结构的NFSV扰动，更好地表征了模式不确定对对流尺度集合预报的影响(Xu, et al, 2022b)。另外，Zhang Y C等(2023)进一步将NFSV拓展到倾向扰动正交子空间，发展了正交NFSV集合预报模式扰动方法，应用于台风强度的集合预报，获得了较SPPT和SKEB明显更高的预报技巧，尤其是为台风快速增强过程的预报提供了更多预警信息。

综上所述，多模式和多物理过程存在成员平均误差、天气学意义的不等同性以及后期概率计算的复杂性而逐渐被淘汰，随机物理扰动方法受到越来越多的重视，但合理的随机函数及随机噪声的时、空相关尺度对物理过程不确定性的代表性及环流依赖性仍然需要深入研究。

2.3　集合预报不确定信息后处理及检验评估

集合预报系统生成了大量数据产品。与单一确定性预报相比，集合预报能够提供未来大气可能状态的概率分布及预报不确定特征，在极端天气预报、预警中更具优势(杜钧等, 2010; 高丽等, 2019)。如何设计合理的后处理技术，对集合预报产品分布做出有气象意义的解释，并提取集合预报成员间的相似关系、差异和极端信息是集合预报后处理面临的重要任务(Williams, et al, 2014)。当前集合预报后处理技术主要包括如何获得描述预报不确定的概率预报信息、如何订正模式系统误差、如何从集合预报概率尾端获得极端天气预报信息等。

2.3.1　基于集合预报的概率预报信息

集合平均(ensemble mean)和集合预报离散度(ensemble spread)是基本的集合预报产品。集合平均代表集合预报产品的第一级信息，集合平均可以过滤掉集合成员的不可预报因素，给出总体的预报趋势，但由于其平滑作用，集合平均不能预报极端天气；集合预报离散度是集合预报不确定性或者集合成员相对于集合平均的波动振幅的量度指标。它可以用集合成员与对照预报场的均方差(Root Mean Square, RMS)量度，也可用各成员同总体平均场的距平相关系数(Anomaly Correlation Coefficient, ACC)平均值量度。离散度在一定程度上可代表集合预报技巧，一般说来，离散度小，预报技巧较高，预报可信度高；但是离散度大，预报技巧不一定低，预报可信度也不一定很低。

天气要素概率预报是重要的集合预报产品，通过对降水、气温、风等天气要素计算不同量级预报概率，代表某类天气要素的可能性。如降水可分为＞1 mm/d、＞5 mm/d、＞10 mm/d、＞20 mm/d，或给出某些站点的天气要素的预报概率。面条图是另一类概率预报产品，通过选取某一条特征等值线，把所有成员中预报的该等值线绘制在同一张图上。一般来说，等值线的发散程度大致反映预报的可信度，越是集中可信度越高。

集合预报分簇产品是用聚类分析(clustering)集合成员预报进行聚类分型，可以提供不同类型产品，聚类分析算法包括系统聚类法、非系统聚类法、管态聚类法(tubing)。通过聚类分型，可比较每类的成员数，获得最有可能发生的天气概率。此外，还有烟羽图(plumes charts)、面条图(spaghetti chart)，用聚类分析原理对500 hPa环流聚类分型，给用户提供有利用价值的信息。

2.3.2　集合预报系统误差订正后处理方法

常见的集合预报系统误差后处理方法主要可以分为参数化和非参数化两类(Mylne, et al, 2022)。参数化后处理方法通常假定目标变量服从特定的概率分布并对其参数进行分布回归，如集合模式输

出统计(Ensemble Model Output Statistics, EMOS)、贝叶斯模式平均(Bayesian Model Averaging, BMA)、贝叶斯联合概率(Bayesian Joint Probability, BJP)等。还有针对不同物理量发展了基于不同概率分布的订正方法,如针对气温和气压的高斯分布、针对风的截断正态分布和对数正态分布、针对降水的Γ分布和截断Γ分布;基于雨量分级的集合预报订正也被提出并用于提高各量级降水尤其是极端降水的预报技巧(Ji, et al, 2023)。

非参数化后处理方法无须预设目标变量的概率分布,相对比较灵活。常见的非参数化方法主要包括分位数映射法(Quantile Mapping, QM)、频率匹配法(Frequency Matching, FM)、概率匹配法(Probability Matching, PM)、逐成员订正法(Member by Member, MBM)、最优百分位法、等效分布回归法(Isotonic Distributional Regression, IDR)等。

同时,通过组合多个模式的有效预报信息进行多模式集合预报,发展了基于误差分析的超级集合、卡尔曼滤波等非等权集合方法(智协飞等, 2013; Zhu, et al, 2021)。引入滑动训练期的思想(Zhi, et al, 2012),已被广泛应用于热带气旋、气温、降水、风等预报订正中。为了降低目标系统预报的位置和结构偏差,提出了多种基于空间特征的集合预报后处理方法,如邻域法、模态投影法、基于目标对象的订正方法(Ji, et al, 2020)等。

近年来,机器学习技术以其高度非线性和强鲁棒性被广泛使用。随机森林、支持向量机、卷积神经网络、长短期记忆神经网络、U-Net神经网络等深度学习算法近年来也被广泛应用于集合预报的后处理过程中,取得了显著的效果(智协飞等, 2020; 杨绚等, 2022; Lyu, et al, 2023)。与此同时,将机器学习算法与传统的统计方法相结合,设计混合机器学习-统计方法,以进一步提高集合预报的可靠性,上述系统误差后处理方法的详细介绍可参考世界气象组织出版的集合预报指导手册(Mylne, et al, 2022)。

2.3.3 基于集合的极端预报信息提取

为了从集合预报中提取极端天气的早期预警信息,利用ECMWF集合预报结果建立了极端预报指数(Extreme Forecast Index, EFI; Lalaurette, 2003)。该指数表征集合预报结果的累积概率分布与模式气候累积概率分布的连续差异,其数值越大,说明预报偏离模式气候态越远,预报极端天气出现的可能性越高,并据此认定实际出现极端天气的概率越大。NCEP也进行了基于EFI的极端天气预报研究,Guan等(2017)指出,基于NCEP全球集合预报的EFI指数对美国2013/2014年冬季出现的极端降水和极端低温天气具有一定的中期预报能力。除了温度、降水、10 m风等常规天气要素外,EFI指数还可应用于对流参数(如对流有效位能)、整层水汽通量等诊断量(Tsonevsky, et al, 2018)。EFI指数的应用范围由最初的大尺度中期集合预报不断扩展至对流尺度以及次季节-季节尺度集合预报(Dutra, et al, 2013; Raynaud, et al, 2018)。中国已有不少学者研究了EFI指数(夏凡等, 2012; 刘琳等, 2018; 彭飞等, 2024)。利用中国气象局全球集合预报开展基于EFI的极端天气预报方法研究表明,EFI对中国极端低温与极端强降水均具有一定的识别能力,存在较高的中期预报技巧。

2.3.4 检验评估方法

集合预报的准确度与可靠性在气象预报中至关重要,这推动了集合预报检验与评估方法的持续发展和完善。Wilks(2011)及Jolliffe等(2012)的著作分别全面总结了气象预报的检验方法,涵盖了确定性预报、概率预报和定性预报的分类及应用实例。对于集合平均或单个集合成员的确定性预报,常用的检验指标包括均方根误差(Root Mean Square Error, RMSE)和空间相关系数等。在概率预报的检验方面,主要的评估方法包括Brier技巧评分(Brier Skill Score, BSS)、连续秩概率技巧评分(Continuous Ranked Probability Skill Score, CRPSS; Hersbach, et al, 2000)、可靠性曲线、相对作用特征(Relative Operating Characteristics, ROC)曲线以及潜在经济价值(Zhu, et al, 2002)。

在量化不确定性方面,集合离散度和Talagrand分布是衡量预报系统不确定性的关键指标。通常使用“离散度-误差”(ensemble spread-error)相关关系来评估集合预报系统的可预报性(或称spread-skill relationship),但实际系统通常表现为欠离散,尤其是在定量降水预报中(李翀, 2001; 李俊等, 2009; Su, et al, 2014)。量化不确定性时,通常采用bootstrapping方法(Hamill, 1999),并用误差区间表示评分的置信区间。此外,Torn等(2008)提出了

集合敏感性分析（Ensemble Sensitivity Analysis, ESA）方法，以评估预报结果对初始条件或其他输入参数微小变化的敏感性。

Su等（2014）提出了面积加权检验方法，对降水概率预报评分进行了空间加权。在降水预报领域，一些学者将这些空间检验方法融入集合预报的评估中。例如，Ji等（2020）研究了将Method for Object-Based Diagnostic Evaluation（MODE）与集合预报技术结合的方法，发现其在评估和改进降水预报的空间结构特征方面具有显著优势。Chen等（2018）通过“降水一致性尺度”方法，研究了江淮梅雨降水预报的集合离散度与预报误差的空间关系，揭示了不同降水阈值下位置误差对预报技巧的影响。此外，杜钧等（2020）提出了新的预报评价指标——预报挑战度（Measure of Forecast Challenge, MFC）和可预报性演变指数（Predictability Horizon Diagram Index, PHDX）。MFC综合考虑了预报误差和不确定性，是衡量预报难度的新指标；PHDX则进一步考察了过去预报的时间演变对决策过程的影响，旨在更全面地反映预报信息的演变特征。

需要注意的是，集合预报检验中评分的准确性可能受到参考值的影响。例如，在计算BSS时，如果使用的格点气候样本频率较高，评分可能会被低估（Hamill, et al, 2006）。此外，检验数据的不确定性和质量也会显著影响评估结果，特别是在降水预报的检验中（Yuan, et al, 2005）。随着高分辨率集合预报和观测数据的不断发展，集合预报的检验方法将在未来进一步精细化和科学化。

3　中国集合预报业务系统及应用

3.1　全球/区域集合预报系统发展历程

3.1.1　全球谱模式集合预报系统

20世纪90年代，国家气象中心开始发展全球集合预报系统（李小泉等，1997），于1996年采用时间滞后方法建立了T63L16全球集合预报系统，集合预报成员12个，预报时长10 d。1999年发展了基于奇异向量方法的T106L19全球集合预报系统（李泽椿等，2002），集合预报成员32个，预报时效10 d。2007年建立了基于增长模繁殖法的T213全球集合预报系统（田华等，2007），集合预报成员15个，预报时效10 d。2014年在T213模式基础上升级为T639集合预报系统，首次在中国集合预报业务系统中采用了随机物理过程倾向项扰动方案加入模式扰动（谭宁等，2013）。

3.1.2　区域集合预报系统

中国区域集合预报系统的探索始于21世纪初，2005年基于MM5模式开展区域集合预报研究，提出新的异物理模态法构造初始扰动（陈静等，2005），并开展多物理过程、随机物理参数扰动等试验（陈静等，2003；冯汉中等，2006；王晨稀等，2007）。2006年国家气象中心基于WRF模式、增长模繁殖方法和多物理过程组合方案（邓国等，2010），建立了中国区域中尺度集合预报系统（马清等，2008），2010年11月15日实现业务化运行，系统水平分辨率15 km，15个集合预报样本，每天运行4次。

3.1.3　GRAPES区域/全球集合预报系统

GRAPES模式是中国气象局自主研发的新一代数值天气预报模式（陈德辉等，2008），自2005年起开启GRAPES集合预报技术的研发。中国气象科学研究院相继应用增长模繁殖法、集合变换卡尔曼滤波法开展了GRAPES区域集合预报技术和系统研究（谭燕等，2007；田伟红等，2008；纪永明等，2011），建立了GRAPES区域集合预报系统（GRAPES Regional Ensemble Prediction System, GRAPES-REPS）。2014年采用集合变换卡尔曼滤波初值扰动技术的中国区域集合预报系统GRAPES-REPS 1.0版实现业务化运行，替代了WRF区域集合预报系统，成为国家气象中心业务化区域集合预报系统，该系统水平分辨率15 km，集合预报成员15个；2015年该系统的初值扰动方案更换为多尺度混合初值扰动方法（Zhang, et al, 2015），其中大尺度初值扰动信息由T639全球集合预报系统通过增长模繁殖法获得，中尺度初值扰动信息由GRAPES区域集合预报系统通过集合变换卡尔曼滤波方法得到，GRAPES区域集合预报系统更新为2.0版；2019年9月，随着基于奇异向量初值扰动方法（刘永柱等，2011）的GRAPES全球中期集合预报系统业务化运行，GRAPES区域集合预报系统的侧边界扰动来源由GRAPES全球集合预报系统替换了原有的T639全球集合预报，同时初值扰动技术和模式扰动技术均实现业务更新，业务系统升级为3.0版（陈静等，2020）。

GRAPES全球集合预报的发展始于2008年，

首先开展了全球集合变换卡尔曼滤波方法(马旭林等, 2008)研究。随着GRAPES全球四维变分同化技术的发展,研发了GRAPES奇异向量初值扰动技术(李晓莉等, 2019),2018年12月基于奇异向量初值扰动法的GRAPES全球中期集合预报系统实现业务运行,替代T639全球集合预报系统,标志着中国首次实现了技术自主可控的全球和区域集合预报业务系统(陈静等, 2020)。

在表征GRAPES模式不确定程度方面,研究人员在国家气象中心T213和T639全球中期集合预报模式不确定性扰动研究基础上,基于GRAPES区域集合预报系统和全球集合预报系统进行了多种模式扰动方法的探索,如多物理过程组合方法(Multi-Physics, MP; 冯汉中等, 2006)、随机物理过程倾向扰动方法(SPPT, 袁月等, 2016)、随机动能补偿方法(SKEB, 彭飞等, 2019)和随机参数扰动方法(SPP, 徐致真等, 2019)。2015年, SPPT方案在GRAPES区域集合预报系统中获得业务应用;2018年, SPPT和SKEB方案在GRAPES全球集合预报系统中实现业务应用(陈静等, 2020)。

2018年以来,持续改进了热带气旋奇异向量法、SV-EDA混合扰动、海温扰动方案(霍振华等, 2020; 齐倩倩等, 2022);基于GRAPES-REPS,研究人员针对初值扰动和模式扰动开展了随机参数扰动(徐致真等, 2019)、条件台风涡旋重定位(吴政秋等, 2020)、雷达反射率因子算法(Chen, et al, 2021)、结合模式系统偏差和随机误差的模式倾向扰动(韩雨盟等, 2023)等改进工作。

2020年以来,开展了对流尺度集合预报研究。研究人员基于GRAPES-Meso 3 km对流尺度模式开展了多种模式扰动和初值扰动试验,如多尺度初值扰动试验(马雅楠等, 2023)、条件非线性最优扰动结合随机物理扰动构造模式扰动(Xu, et al, 2022a, 2022b)。建立的3 km区域集合预报试验系统,在北京冬季奥林匹克运动会、杭州亚运会等重大活动中得到应用。借助“WMO研究示范项目——杭州亚运会对流尺度集合预报及应用研发项目”,在杭州建立了全流程自主可控3 km泛华东对流尺度集合预报系统。该系统于2023年5月21日正式投入业务运行,为预报员的最终决策提供了充分的概率信息和多角度支持。

3.2 中国集合预报系统技术

3.2.1 全球/区域一体化多尺度奇异向量初值扰动技术

奇异向量(SV)初值扰动可有效体现分析误差在基本气流中不断增长和加强的主要误差信息和敏感特征。CMA全球四维变分系统发展的切线性(Tangent Linear Model, TLM)和伴随模式(Adjoint model, ADM)为CMA全球集合预报SV扰动技术的研究和发展提供了条件(刘永柱等, 2017)。CMA全球集合预报大尺度系统SV初值扰动计算方案是由全球热带外地区和热带气旋奇异向量计算两部分组成,具体的数学处理方案简述如下。

(1)热带外地区奇异向量计算方案

CMA全球奇异向量求解可归结为演化扰动向量模与初始扰动向量模比值的最大化问题,如式(1)所示

$$(E^{-1/2}L^{\mathrm{T}}P^{\mathrm{T}}EPLE^{-1/2})x(t_0)=\lambda^2 x(t_0) \tag{1}$$

式中,$\boldsymbol{L}$是CMA全球四维变分同化系统中的切线性模式,$\boldsymbol{L}^{\mathrm{T}}$是对应的伴随模式,$\boldsymbol{E}$是衡量扰动大小权重模,$x$表示奇异向量,$\lambda$为对应的奇异值。$\boldsymbol{P}$是投影算子,其作用是将目标区之外的奇异向量扰动设置为0。由式(1)可见,影响奇异向量结构的因素有3点:(1)奇异向量扰动大小权重模($\boldsymbol{E}$)的定义;(2)切线性模式($\boldsymbol{L}$)及伴随模式($\boldsymbol{L}^{\mathrm{T}}$)的特点,主要为线性化物理过程参数化方案使用;(3)切线性模式($\boldsymbol{L}$)向前及伴随模式($\boldsymbol{L}^{\mathrm{T}}$)向后的积分时间长度(最优化时间间隔)。

CMA全球奇异向量采用干空气总能量定义权重模(刘永柱等, 2013),设CMA全球TLM和ADM的预报量——水平风分量(u, v)、扰动位温(θ')、扰动无量纲气压(Π')对应的扰动量(可表示为:u'、v'、$(\theta')'$、$(\Pi')'$),总能量模($\boldsymbol{E}$)的计算公式为

$$\boldsymbol{E}=\iiint_V\left(\frac{\rho_{\mathrm{r}}\cos\varphi}{2}(u')^2+\frac{\rho_{\mathrm{r}}\cos\varphi}{2}(v')^2+\frac{\rho_{\mathrm{r}}\cos\varphi c_p T_{\mathrm{r}}}{\theta_{\mathrm{r}}^2}((\theta')')^2+\frac{\rho_{\mathrm{r}}\cos\varphi c_p T_{\mathrm{r}}}{\Pi_{\mathrm{r}}^2}((\Pi')')^2\right)\mathrm{d}V \tag{2}$$

式中,等号右边前面两项之和为扰动动能(Kinetic Energy, KE)模,后两项之和表示扰动位能(Potential Energy, PE)模,其中第3项和第4项分别表示扰动位能中扰动位温和扰动无量纲气压的贡献;$\mathrm{d}V=\mathrm{d}\lambda\mathrm{d}\phi\mathrm{d}\hat{z}$, $\hat{z}$为地形追随坐标,λ和φ分别代表模式

球面坐标系中的经度和纬度，c_p为干空气的定压比热。T_r、θ_r、Π_r和ρ_r分别表示参考温度、参考位温、参考无量纲气压和参考密度。

基于上述CMA全球SV计算技术，采用不同分辨率和不同最优时间间隔定义了3种不同尺度的SV。首先是大尺度奇异向量（Large-scale SV, LSV），其水平分辨率为2.5°，最优时间间隔为48 h，采用干空气线性化物理过程进行计算，LSV主要用于捕捉天气尺度的不确定性信息。其次是中尺度奇异向量（Meso-scale SV, MSV），其水平分辨率为1.5°，最优时间间隔为24 h，采用干空气线性化物理过程进行计算，MSV主要用于捕捉α中尺度的不确定信息。最后是小尺度奇异向量（Small-scale SV, SSV），其水平分辨率为0.5°，最优时间间隔为6 h，与前两种奇异向量不同，SSV的计算过程中引入了湿空气线性化物理过程，主要用于捕捉β中尺度的不确定信息。CMA全球/区域一体化多尺度奇异向量的具体设置如表1所示。

（2）热带气旋奇异向量计算方案

考虑热带气旋的特殊性，在CMA全球集合预报中发展了热带气旋SV计算方案（霍振华等，2020），即如果有热带气旋生成，则以热带气旋为中心10个经纬度区域为目标区计算奇异向量，最多可以同时计算6个热带气旋奇异向量。

因此，CMA全球集合预报奇异向量的计算目标区域有3个，包括热带外南、北半球区域和热带气旋区域。不仅体现了南、北半球中、高纬度大气的斜压不稳定扰动发展，还在有热带气旋时考虑了热带气旋的发展。

基于上述计算产生的北半球初始SV、南半球初始SV和热带气旋初始SV，采用高斯取样技术构造CMA全球集合预报初值扰动场。还利用尺度化放大因子对所有的初值扰动幅值进行尺度化，使得初值扰动的振幅大小与实际分析误差量级相当。最后，在同化分析初值的基础上做成对加减计算处理，由此构造出CMA全球集合预报扰动初值。

3.2.2　区域短期多尺度混合初值扰动技术

受全球集合预报分辨率限制，动力降尺度方法缺乏区域模式能分辨的更小尺度的不确定性信息，而中小尺度初值扰动对局地强天气不确定性的捕捉十分重要，CMA区域集合预报发展了一套基于ETKF方法的区域多尺度混合初值扰动技术。

3.2.2.1　集合变换卡尔曼滤波初值扰动方法

ETKF方法是基于卡尔曼滤波理论发展的一种初值扰动方案，其原理是由集合预报扰动方差和观测误差方差快速估计分析误差（龙柯吉等，2011），有利于捕捉中、小尺度系统初值不确定信息。

在CMA区域集合预报系统中，将预报扰动向量（$\boldsymbol{X}^{\mathrm{f}}$）更新为分析扰动（$\boldsymbol{X}^{\mathrm{a}}$），利用变换矩阵（$\boldsymbol{T}$）来建立预报扰动和分析扰动的关系，如式（3）所示，即通过变换矩阵（$\boldsymbol{T}$）对当前时刻预报扰动向量进行线性组合，构造当前时刻的分析扰动

$$\boldsymbol{X}^{\mathrm{a}} = \boldsymbol{X}^{\mathrm{f}}\boldsymbol{T} \tag{3}$$

ETKF初值扰动方法的核心是如何获得变换矩阵（$\boldsymbol{T}$），在CMA区域集合预报ETKF方案中，采用Wang等（2003）的方法定义变换矩阵，为了使集合扰动成员相对于集合平均中心化，采用球面单形中心化方案。在CMA区域集合预报业务系统版本中，模拟观测资料由全球背景分析场插值到观测空间得到（王婧卓等，2018）；变换矩阵（$\boldsymbol{T}$）的计算变量为经向风（v）和纬向风（u），放大因子计算变量为风（u、v）和比湿（q）；采用6 h循环扰动计算方案，每天运行4次，分别为00、06、12和18时（世界时，下同），其中00与12时做84 h预报，06与18时只做6 h预报，为ETKF循环提供6 h预报扰动场。

表1　多尺度奇异向量计算设置

Table 1　The settings of calculation for multi-scale singular vectors

	LSV	MSV	SSV
目标区域	30°—80°N 30°—80°S	30°—80°N 30°—80°S	105°—125°E 20°—50°N
切线性模式分辨率/优化时间	2.5°/48 h	1.5°/24 h	0.5°/6 h
能量模	干能量	干能量	干能量
线性化物理过程	次网格地形拖曳， 垂直扩散	次网格地形拖曳， 垂直扩散	次网格地形拖曳， 垂直扩散，大尺度凝结
SV个数	10	10	10

3.2.2.2 多尺度混合初值扰动方法

实践表明,全球集合预报动力降尺度得到的区域集合预报初值扰动场包含更多的大尺度扰动信息。自2016年起,CMA区域集合预报采用了多尺度混合初值扰动技术(Multi-Scale Blending, MSB; Zhang, et al, 2015; Xia, et al, 2019)。该方法利用二维离散余弦变换(2-Dimensional Discrete Cosine Transform, 2D-DCT; Denis, et al, 2002)对区域集合预报ETKF生成的初值扰动和T639全球集合预报扰动场降尺度初值扰动进行滤波,再通过2D-DCT逆变换对来自全球集合预报的大尺度扰动和区域集合预报的中、小尺度扰动进行重构得到包含更多尺度初值不确定信息的初值扰动场。

3.2.2.3 集合预报条件性台风涡旋重定位技术

为了在集合预报中更合理地描述台风涡旋中心定位的不确定信息,吴政秋等(2020)采用2009—2018年中国气象局和日本气象厅台风最佳路径数据,分析了台风最佳路径涡旋中心定位的不确定性特征,设计了台风涡旋条件重定位方法(Conditional Typhoon Vortex Relocation, CTVR),构建了集合成员台风涡旋中心重定位阈值判别、台风涡旋分离数学处理及涡旋重定位数学处理过程。

通过分析2009—2018年中国气象局和日本气象厅最佳台风涡旋中心定位差异,发现10 a中定位误差年平均值最大为17.18 km(2009年),最小为11.98 km(2015年),结合CMA-REPS的水平分辨率(10 km),以15 km为临界阈值,判别是否对集合预报成员进行台风涡旋重定位处理,即如果集合成员初值场中台风涡旋中心与最佳路径距离差值大于15 km,则判断该集合成员初始场中台风涡旋中心定位超出分析的不确定范围,需要对该成员进行条件性台风涡旋重定位处理,否则认为该集合成员台风涡旋中心定位误差在分析不确定范围内,不进行条件性台风涡旋重定位处理。重定位方法采用美国地球流体动力实验室发展的台风涡旋分离技术,对需要进行重定位的台风集合预报成员进行台风初始场与台风涡旋的分离,将分离出的台风部分通过插值平移至观测位置,该方案于2019年应用于CMA区域集合预报业务系统3.0版。

3.2.3 次网格物理过程随机误差模式扰动技术

仅使用初值扰动的集合预报系统存在集合成员不够发散、集合预报系统可靠性不足的缺陷。在一个完整的集合预报系统中,考虑模式误差的影响,引入能够合理表征模式不确定信息的模式扰动技术也是至关重要的环节之一(Palmer, et al, 2009)。因此,有必要在CMA全球/区域集合预报系统中引入模式扰动技术,以表征由于模式误差或模式本身缺陷而造成的不确定性。当前在CMA全球/区域集合预报系统中主要使用了SPPT和SKEB两种模式扰动技术,下面分别对其做简要介绍。

3.2.3.1 随机物理过程倾向项扰动方案(SPPT)

CMA全球/区域集合预报系统中的SPPT方案的主要设计思路与ECMWF相同(Buizza, et al, 1999)。即在数值积分过程中,模式积分倾向项可分解为非参数化过程(动力过程)积分倾向项和参数化物理过程积分倾向项,SPPT方案扰动后的模式积分倾向项可表示为

$$e_j(t_e)=\int_0^{t_e}\{A(e_j,t)+\Psi(\lambda,\phi,t)P(e_j,t)\}\mathrm{d}t \tag{4}$$

式中,$A(e_j,t)$为动力倾向项,$P(e_j,t)$为物理倾向项,$\Psi(\lambda,\phi,t)$是具有时、空相关特征的三维随机场,其中引入了拉伸函数来实现自定义扰动量的范围(Li, et al, 2008),其定义为

$$\Psi(\lambda,\phi,t)=\mu+\left\{2-\frac{1-\exp\left[\beta\left(\frac{\psi-\mu}{\Psi_{\max-\mu}}\right)\right]^2}{1-\exp\beta}\right\}(\psi-\mu) \tag{5}$$

式中,β是常数,其值为−1.27,$\mu=(\Psi_{\max}+\Psi_{\min})/2$,其中$\Psi_{\max}$和$\Psi_{\min}$分别代表随机场$\Psi(\lambda,\phi,t)$的上、下边界。式(5)中$\psi$是具有时、空相关特征的三维随机场,定义为

$$\psi(\lambda,\phi,t)=\mu+\sum_{l=1}^{L}\sum_{m=-l}^{l}\alpha_{l,m}(t)Y_{l,m}(\lambda,\phi) \tag{6}$$

式中,λ、ϕ、t分别表示模式格点经度、纬度和时间,$Y_{l,m}$为球谐函数,L为随机场的水平截断尺度,l、m分别为水平方向总波数、纬向波数,$\alpha_{l,m}(t)$为随机场谱系数。随机场谱系数$\alpha_{l,m}(t)$在时间维的相关变化特征是通过一阶马尔克夫链随机过程(也称一阶自回归随机过程)来实现,如下式所示

$$\alpha_{l,m}(t+\Delta t)=\mathrm{e}^{-\Delta t/\tau}\alpha_{l,m}(t)+\sqrt{\frac{4\pi\sigma^2(1-\mathrm{e}^{-2\Delta t/\tau})}{L(L+2)}}R_{l,m}(t) \tag{7}$$

式中，Δt是特定的时间间隔（在CMA集合预报系统中，可以对应模式的积分步长），τ是随机场失相关的时间尺度。$R_{l,m}(t)$为服从方差为1、均值为0的高斯分布随机过程。通过上述公式构造出的随机型函数具有时间尺度和空间尺度的相关关系以及扰动量可控制等特点。在CMA全球/区域集合预报系统中，均只对位温、水平风分量和湿度预报变量的净倾向项进行扰动。

考虑到全球模式和区域模式积分时间、预报对象不同，SPPT方案在CMA全球集合预报和区域集合预报业务系统的参数设置存在差异。在CMA区域集合预报系统中，SPPT扰动幅度取值为[0.2, 1.8]，扰动场均值为1，失相关时间尺度为6 h，最大波数24，标准差（σ）为0.27。在CMA全球集合预报系统中，为了运行稳定，将随机型函数的扰动幅度取值范围设置为[0.5, 1.5]，在近地面层和大气层顶处引入倾向扰动垂直廓线，对近地面层和大气层顶附近的物理倾向不进行扰动或者进行较小幅度的扰动。SPPT方案能够显著改进温度和风速预报的集合离散度和漏报率，提高强降水的概率预报技巧，显著增大热带地区各要素（高度场、温度场和风速）预报的集合离散度，弥补了SV初值扰动技术在热带地区扰动不足的问题（彭飞等，2020）。

3.2.3.2　随机动能补偿扰动方案（SKEB）

SKEB方案的主要目的是代表模式中次网格尺度能量升尺度转换的随机过程和不确定性（Shutts, 2005）。CMA全球集合预报系统中的SKEB方案是通过一定时、空相关关系的随机型以及局地动能耗散率来构造随机流函数强迫的方式对上述过度耗散的能量进行补偿（彭飞等，2019）。随机流函数强迫（F_ψ）定义为

$$F_\psi = \frac{\alpha \Delta x}{\Delta t} \Psi(\lambda,\varphi,t) \sqrt{\Delta t D(\lambda,\varphi,\eta,t)} \qquad (8)$$

式中，$\Psi(\lambda, \varphi, t)$为随机型，其产生方法与SPPT的随机型定义相同，具体参见式（5）；$D(\lambda, \varphi, \eta, t)$为局地动能耗散率。目前，CMA全球集合预报系统中SKEB方案基于显式水平方案来构造局地动能耗散率

$$D(\lambda,\varphi,\eta,t) = -k \times u \times u' \qquad (9)$$

式中，k是大于1的常数因子，u为水平风速，u'为水平扩散方案应用前、后水平风速的变化。基于流函数与水平风场的旋转分量的关系构建CMA全球集合预报系统的水平风场扰动强迫项（S_u、S_v），即在模式水平风场倾向项中加入以S_u、S_v表示的倾向项随机强迫。

$$S_u = -\frac{1}{\alpha} \frac{\partial F_\psi}{\partial \phi} \qquad (10)$$

$$S_v = \frac{1}{\alpha \cos\phi} \frac{\partial F_\psi}{\partial \lambda} \qquad (11)$$

在CMA全球集合预报系统中，SKEB方案随机型函数最小截断波数$L_{\min}$为10、最大截断波数$L_{\max}$为80、失相关时间尺度（τ）为6 h、均值（μ）为0，标准差（σ）为0.27、最大值（$\Psi_{\max}$）为0.8、最小值（$\Psi_{\min}$）为−0.8。SKEB方案的应用能够改善CMA全球集合预报系统对大气动能谱的模拟能力，显著改进热带地区风场预报的集合平均误差与集合离散度的关系。

3.2.4　系统偏差、极端信息提取

除了上述初值扰动技术和模式扰动技术之外，在CMA全球/区域集合预报系统中还创新性地发展了一系列的集合预报后处理及极端天气预报应用技术，如扣除系统偏差的集合预报动力订正模型（Chen, et al, 2020）、次网格尺度降水雷达反射率因子（Chen, et al, 2021）、极端天气预报指数模型等。这一系列技术解决了概率预报分布尾部极端预报信息获取和模式系统性偏差问题，显著改善了CMA全球/区域集合预报概率密度分布和极端天气预报能力。下面对其做简要介绍。

3.2.4.1　扣除模式系统偏差集合预报动力订正方法

当前集合预报技术主要是处理模式的随机误差，但在模式系统偏差较大的情况下，仅采用初值扰动或者模式扰动方法较难改善集合预报误差与离散度的关系。在研究了CMA全球/区域模式系统偏差对集合预报的概率密度分布影响后，提出了一种扣除系统偏差的集合预报动力订正方法，在模式积分公式的动力和物理倾向项上扣除偏差倾向项，如式（12）（Chen, et al, 2020; 韩雨盟等，2023）。

$$e_j(t_e) = \int_0^{t_e} \left\{ A(e_j, t) + P(e_j, t) - \hat{B}_l(e_0) \right\} \mathrm{d}t \qquad (12)$$

式中，$e_j(t_e)$为倾向项，$A(e_j, t)$为动力倾向项，$P(e_j, t)$为物理倾向项，$\hat{B}_l(e_0)$为偏差扣除项。通过线性回归计算出线性偏差率，进而在每一步积分倾向项计

算过程中扣除线性偏差部分。该方法显著改善了集合预报概率密度分布的一阶矩(集合预报平均)和二阶矩(集合预报离散度),提高了地面要素概率预报的技巧。

3.2.4.2 次网格尺度降水雷达反射率因子计算新方法

雷达回波强度可以较好地反映强对流天气过程发生、发展特征,故雷达回波的模式预报不确定性受到了预报员的高度重视。为了更好地提供雷达回波的预报不确定信息,针对CMA区域模式中模拟雷达回波不能反映次网格物理过程(Kain-Fritsch方案)中次网格降水信息的问题,发展了一种次网格降水的雷达回波计算新方法(Chen, et al, 2021),并应用于CMA区域集合预报系统中。方法的基本公式如式(13)所示

$$Z_{\text{total}} = Z_{\text{micro}} + AR_{\text{cu}}^{b} \tag{13}$$

式中,Z_{total}是新的总模拟雷达反射率因子,Z_{micro}是云微物理方案中得到的雷达反射率因子,R_{cu}是计算出的次网格降水量,A和b则分别为雷达估测降水Z-R公式中的经验参数。其原理是将次网格降水率减去下沉气流蒸发率,再根据雷达估测降水Z-R关系,估计每一层上的雷达回波强度,并与微物理过程模拟的雷达回波强度结合,形成新的三维雷达回波模拟结果。新的雷达回波对于模式中由积云对流方案产生的降水有明显指示作用,尤其对于次网格降水过程较多的情况下,能更好地模拟出单个集合预报成员与次网格降水相关的雷达回波,进而改进了CMA区域集合预报系统的雷达反射率因子概率预报技巧。

3.2.4.3 极端天气预报产品

基于CMA全球集合预报系统31个集合成员的预报数据、模式气候数据和历史气候数据等,开发了极端天气预报产品,包括地面要素极端预报指数(EFI)、2 m气温异常概率预报产品及基于卡尔曼滤波偏差订正技术的中期距平概率预报产品等。

(1)基于CMA全球模式气候概率的地面要素EFI产品

伴随着各预报要素(降水、风、温度和云量)的确定性预报和集合预报的发展,预报员希望能利用集合预报系统对极端事件发出早期的预警信号。然而直接比较观测的气象要素和模式输出的预报之间的差别是很难的,因此基于CMA全球集合预报系统,研发了CMA集合预报极端天气预报方法——极端预报指数EFI。其原理是计算累积的模式气候概率分布和集合预报概率分布之差。极端预报指数的计算中至关重要的环节在于模式气候百分位的计算,但CMA全球集合预报系统历史资料较少,在历史预报数据有限的情形下,计算模式预报气候百分位时,选取当前计算日期及前后7 d为滑动时间窗(15 d)、计算格点及附近9个格点为空间窗的预报场作为逐日模式气候序列进行升序排序,然后分别将每个百分位(1, 2, 3, …, 99, 100)上的预报值取出,形成模式预报的气候百分位分布(汪娇阳等, 2014; 彭飞等, 2024)。

(2)基于卡尔曼滤波偏差订正技术的中期距平概率预报产品

发展了基于卡尔曼滤波偏差订正技术的中期距平概率预报产品,主要包括500 hPa高度场、850 hPa温度场和850 hPa风场的大气环流距平异常概率产品等。这些产品有助于更好地抓住极端天气的特征,提高极端天气的概率预报技巧。

3.3 中国全球/区域集合预报系统及国际对比

3.3.1 中国全球/区域集合预报系统参数

针对CMA全球及区域模式初值误差和模式误差特点,中国技术人员自主创新发展了集合预报关键技术,突破初值扰动技术、模式扰动技术和集合预报应用技术瓶颈,从无到有,建成了自主可控的0—15 d全球50 km分辨率全球集合预报业务系统、0—3 d中国区域10 km分辨率区域集合预报和0—3 d的3 km对流尺度分辨率集合预报业务系统,在中国首次以自主研发技术提供了0—15 d集合概率预报业务的科技支撑,促进中国数值预报业务取得显著进步,总体技术指标达到国际先进水平。CMA全球/区域集合预报系统的业务化,标志着中国首次建成了一套完整的数值预报业务体系,促进了业务数值预报取得了里程碑式的进步。同时,CMA全球/区域集合预报系统除了提供中国区域日常预报服务和重大气象服务保障外,CMA全球集合预报产品持续向TIGGE中心提供多种预报数据,还为世界气象中心(北京)和WMO SWFDPSeA网页产品提供了核心支持,进一步提升了中国气象的国际地位。表2是CMA全球/区域业务集合预报系统参数设置。

表 2　CMA 全球/区域业务集合预报系统参数设置

Table 2　Parameter configurations of CMA global and regional operational ensemble prediction system

	全球集合预报系统	区域集合预报系统	3 km对流尺度分辨率集合预报系统
模式版本	CMA-GFS V3.1	CMA-MESO V4.3	CMA-MESO V5.1
水平分辨率/垂直层次/预报区域	0.5°/87层(全球)	0.1°/50层（10°—60°N, 70°—145°E）	0.03°/50层（10°—60°N, 70°—145°E）
对照预报初值生成	由CMA-GFS 4DVAR高分辨率同化分析场经过动力升尺度技术生成	全球模式动力降尺度生成	由三维变分同化系统生成
初值扰动技术	奇异向量初值扰动	ETKF初值扰动技术	多尺度奇异向量混合初值扰动
模式扰动技术	SPPT, SKEB	SPPT	SPPT
侧边界	/	CMA-GEPS全球集合预报	混合侧边界动态扰动
集合成员数	31(1个对照预报+30个扰动成员)	15(1个对照预报+14个扰动成员)	15(1个对照预报+14个扰动成员)
预报时效	15 d(00、12时)	84 h(00、12时) 6 h(06、18时)	72 h(00、12时)
集合产品输出频率	0—84 h预报/3 h; 84—360 h/6 h	1 h	1 h
集合预报后处理产品	GRIB2数据、常规集合预报产品和极端天气集合预报产品、台风集合预报产品	GRIB2数据、常规天气预报产品、应急服务产品、台风集合预报产品	GRIB2数据、常规天气预报、特殊服务集合预报产品、台风集合预报产品

CMA-GEPS 全球集合预报系统集成了奇异向量初值扰动技术、模式随机物理扰动技术和极端中期概率预报产品生成技术，模式水平分辨率 0.5°，预报时效 0—15 d，集合预报成员 31 个。基于 ECFLOW 技术，构建了 CMA-GEPS 业务系统运行流程，实现每日 00 和 12 时运行，提供 0—15 d 的常规集合产品、极端天气概率产品等 29 种产品。

CMA 区域集合预报系统 3.0 版集成了集合变换卡尔曼滤波初值扰动方法(ETKF)、多尺度混合初值扰动技术、随机物理过程倾向扰动方法(SPPT)、混合侧边界动态扰动、集合成员条件性台风涡旋重定位方法(CTVR)和次网格尺度降水雷达反射率因子新算法等关键技术研究成果，集合成员为 15 个，每日 00、06、12 和 18 时运行 4 次，00 和 12 时的预报时效 84 h，06 和 18 时的预报时效是 6 h，主要提供 ETKF 预报循环，为 ETKF 计算预报扰动准备资料，提供局地强天气、台风等概率预报产品为主的 49 种集合预报产品。

3.3.2　国际主要数值预报中心的对比分析

3.3.2.1　集合预报关键技术及系统比较

表 3 是国际主要业务集合预报系统技术综合比较。从表可见中国气象局集合预报的主要技术特点：

(1)CMA 全球集合预报奇异向量初值扰动技术创新设计了扰动能量模、并行计算、尺度化及高斯分布线性取样初始扰动三维结构算法，较好地捕捉到大尺度斜压不稳定扰动能量增长，是 CMA 全球集合预报的核心技术。奇异向量初值扰动技术难度大，国际上仅有 ECMWF、法国气象局和日本气象厅全球集合预报系统采用了该方法。该项成果技术水平与国际先进数值预报中心相当，跻身国际先进行列。

(2)CMA 区域集合预报集成了区域集合变换卡曼滤波初值扰动(ETKF)、多尺度混合初值扰动技术(MSB)和集合成员条件性台风涡旋重定位技术(CTVR)，提高了中国区域降水概率预报水平。ETKF 初值扰动方法与加拿大气象局和日本气象厅业务应用的局地集合变换卡尔曼滤波(LETKF)初值扰动方法原理和构建方案相同。MSB 和 CTVR 方法属自主研发。

(3)随机物理过程倾向扰动(SPPT)、随机动能补偿扰动(SKEB)等模式扰动方法，采用一阶自回归随机过程和球谐函数展开，获得时、空相关和正态分布的随机函数和关键参数，实现了对物理过程倾向和小尺度动能耗散的随机扰动，合理地描述了模式次网格物理过程参数化方案的随机误差增长特征，与 ECMWF、美国、加拿大和英国等欧、美发达国家模式随机扰动技术方案相同。

(4)面向集合预报应用，设计了极端信息提取技术、系统偏差动力订正、考虑模式对流性降水的雷达回波强度等算法，极端天气预报指数等概率预报产品生成技术，为预报员提供了极端天气预报参考信息。

(5)建立了有自主知识产权的中国集合预报系

表3 国际主要业务集合预报系统技术现状

Table 3 Technical status of major international operational ensemble prediction systems

国家和组织	全球集合预报模式/分辨率(成员数)/集合预报技术	区域集合预报模式/分辨率(成员数)/集合预报技术
美国	谱模式/25 km(31)/集合卡尔曼滤波+随机物理倾向扰动+随机动能补偿	WRF和NMMB模式/16 km(26, 北美)、3 km(11, 重点区域)/集合卡尔曼滤波与BGM混合+动力降尺度, 多物理
英国	格点模式MOGREPS-G/20 km(18)/集合同化+随机物理倾向扰动+随机动能补偿	格点模式MOGREPS-UK/2.2 km(3个扰动+18个滞后集合成员)/动力降尺度
法国	谱模式/7.5—37 km(35)/奇异向量+集合变分同化+多物理	谱模式AROME-EPS/2.5 km(16)/集合变分同化+随机物理倾向扰动
德国	格点模式GEPS/40 km(40)/局地集合变换卡尔曼滤波+随机参数扰动	格点模式COSMO-DE/2.2 km(20)/局地集合变换卡尔曼滤波+随机参数扰动
加拿大	格点模式/39 km(21)/局地集合变换卡尔曼滤波+随机参数扰动+随机动能补偿	有限区域HREPS/15 km(21)/动力降尺度+物理倾向扰动
日本	谱模式/27—40 km(27)/奇异向量+局地集合变换卡尔曼滤波+随机物理倾向扰动	格点模式/5 km(21)/多尺度奇异向量
欧盟	谱模式/9 km(51)/奇异向量+集合同化+随机物理倾向扰动	
中国	格点模式GRAPES/50 km(31)/奇异向量+随机物理倾向扰动+随机动能补偿	格点模式GRAPES/10 km(15, 中国区域)、3 km(15, 中国区域)/集合变换卡尔曼滤波+混合多尺度初值扰动+随机物理倾向扰动

统业务体系,包括全球0—15 d中期,中国区域0—72 h短期和对流尺度集合预报系统,促进中国数值天气预报业务取得显著进步。对比多个数值天气预报中心集合预报技术和系统参数可见,国际各主要数值预报中心的全球集合预报分辨率为9—50 km,集合预报成员18—51个,中国的全球集合天气预报系统与国际上大部分集合天气预报系统接近,水平分辨率为50 km,集合预报成员数31个。对比区域集合天气预报系统参数,国土面积较小的国家(如英国、法国、德国),区域集合预报业务系统水平分辨率达到2.5 km左右,集合预报成员数10—20个;而国土面积较大的国家(如加拿大、美国、中国),大都建立了区域中尺度集合预报和对流尺度集合预报两套系统。中国的区域集合预报水平分辨率为10 km,还建立了3 km水平分辨率的对流尺度集合预报系统。

综上所述,中国在全球/区域集合天气预报系统系统参数、构造方案方面形成了具有自主知识产权、独具特色的技术方法和产品。

3.3.2.2 CMA全球/区域集合预报系统预报能力与国际先进中心的对比

图1根据国际全球集合预报检验中心日本气象厅提供的资料,给出了2012—2024年多个数值天气预报中心全球集合预报500 hPa高度场第6天集合预报的CRPS和第10天集合预报平均均方根误差(RMSE)对比。检验资料主要包括了欧盟(ECMWF)、美国(NCEP)、英国(UKMO)、加拿大(CMC)、澳大利亚(BOM)、日本(JMA)、韩国(KMA)、中国(CMA)等多个数值预报中心的全球集合预报系统的预报效果。由图可见,自2018年12月起CMA全球集合预报系统实现业务化后,其在中期预报时效的预报技巧与欧、美等全球集合预报系统相近。

4 集合预报发展面临的挑战与展望

4.1 科学挑战:对流尺度模式可预报性时、空尺度的多变性

对流尺度模式的可预报性具有时、空尺度多变性,一是对流尺度模式可预报性受不同时、空尺度环流相互作用的影响,即使初始误差量级足够小,也会快速饱和并升尺度增长,进而影响到大尺度天气系统的可预报性(Zhang, et al, 2007)。对流尺度模式初值误差具有增长强非线性特征,初值误差增长速度约为天气尺度模式的10倍(Hohenegger, et al, 2007)。二是对流尺度模式通常应用更精细复杂的云微物理、湍流扩散等参数化方案,但这些方案存在诸多假设条件和经验参数影响,加之差分方法、计算截断等误差的影响造成对流尺度模式初值误差增长表现出强非线性特征(穆穆等, 2011; Yano, et al, 2018)。三是不同尺度初值误差增长及对降水的影响与环境强迫条件有关(Johnson, 2014; Zhuang, et al, 2021),不同尺度初值误差的相对重要性取决于湿对流数量和类型,湿对流越多,小尺度误差扰动能量增长越快(Nielsen, 2016)。因

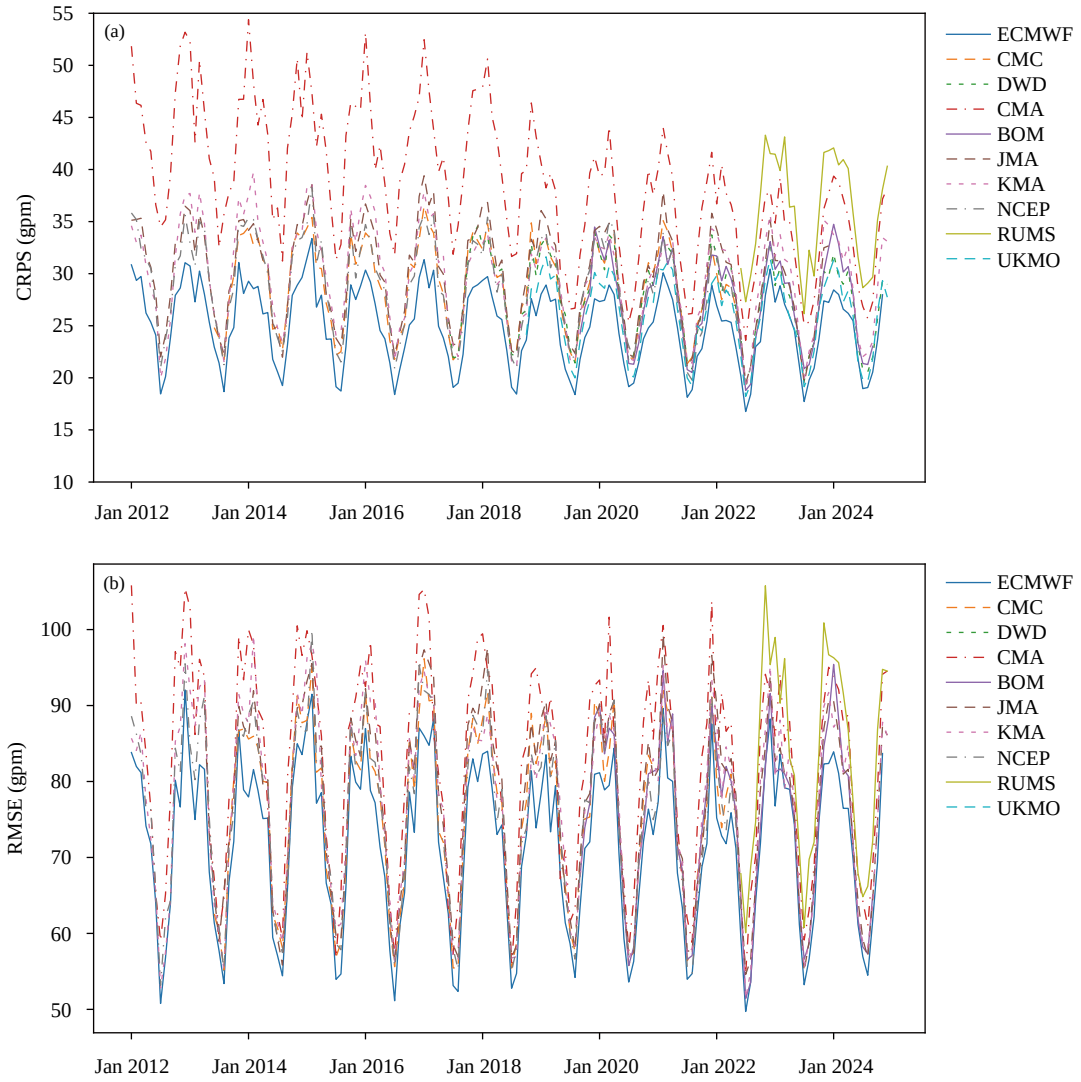

图 1　2012 年 1 月至 2024 年 12 月国际多个全球集合预报业务系统第 6 天和第 10 天 500 hPa 高度场预报的集合预报平均连续秩概率评分（CRPS）（a）和均方根误差（RMSE）（b）对比（月平均值）（图例代表不同的预报中心）

Fig. 1　Ensemble mean Continuous Ranked Probability Score（CRPS, a）and RMSE（b）of 500 hPa geopotential height forecasts at 144 h（day 6）and 240 h（day 10）from major international global ensemble prediction systems, averaged monthly from January 2012 to December 2024（different colors represent different NWP centers, RUMS refers to the regional unified model system）

此，对流尺度集合预报技术面临极大的挑战。

4.2　集合预报与人工智能技术结合的前沿探索

近年来，人工智能（Artificial Intelligence, AI）方法和技术在气象预报中应用取得了突破性进展，基于深度学习的气象大模型的计算代价仅为传统数值模式的万分之一，这为发展大样本集合预报提供了新的可能途径。但同时面临着新的挑战，一是AI 模型的不确定性来源与传统数值模式有所不同，这些不确定性对 AI 模型的预报技巧和模型性能的影响有待深入研究。二是深度学习模型的不确定性与传统数值预报特征不同，如何合理地描述深度学习模型的不确定性特征亟需解决。三是基于AI 的集合预报模型的物理一致性和可解释性饱受争议，需要在 AI 模型发展的同时开展相应研究和改进。此外，AI 方法和技术的发展给集合预报带来了新的挑战和机遇。未来集合预报框架和概念有可能也需要发生转变。比如：（1）集合预报回到概率预报，或者简单说是得到变量 PDF 为核心目标，即寻找预报误差概率分布的思想重新复活。（2）代表性扰动的作用减弱，当机器学习模型可以快速生

成成千上万个集合预报时,这样可以得到更多的预报可能,得到更好的概率统计特征。(3)部分替代动力模型,大气中较小尺度的结构需要高分辨率动力模型去识别,这里动力模型实际上是一种有效但费时的“随机扰动”生成器。能否利用机器学习模型学习并生成值得研究。

4.3 业务挑战:传统集合预报技术的不适用性

近年来,业务集合预报发展面临下面3个不适用性:一是全球和区域业务集合预报走向对流尺度分辨率,在对流尺度模式框架下,模式初值误差和模式误差多尺度结构、非线性演变过程及相互作用对预报误差增长机制的影响一直是科学上的难点,如何构建集合预报扰动方法是发展对流尺度集合预报的技术瓶颈。二是地球系统模式正走向天气、气候一体化无缝隙集合预报系统,而传统集合预报技术在时间和空间尺度上是分别发展的,不适用于这种时、空尺度一体化无缝隙集合预报需求。三是集合预报正在逐步走向地球系统集合预报,但传统的集合预报技术主要是针对大气运动的动力不稳定系统误差增长获得的预报不确定性,而对耦合分量模式和耦合同化中引入的误差特征认识不足,需要发展满足多分量耦合模式的集合预报技术。

5 总 结

中国集合预报从理论方法到业务应用近年来已经取得了卓越的发展和进步,基本上步入国际主要业务集合预报中心的先进行列,但是和ECMWF等最顶尖的业务中心的集合预报系统的性能相比,仍存在一定的差距。目前,国际上集合预报已经逐渐发展和替代确定性预报,成为业务预报的主要形式和重要趋势。概率预报的概念也逐渐在科研人员、预报员和公众中普及和被接受。下面简要总结和讨论集合预报未来发展面临的挑战,也是中国集合预报科研和业务发展需要重点攻坚和解决的问题。

(1)未来全球集合预报系统的集合成员将向对流尺度分辨率提升。这有助于全球范围内对中尺度到对流尺度精细特征的集合预报采样和不确定性估计。ECMWF正引领这一趋势,2025年将实现5 km分辨率的全球集合预报。更高的分辨率不仅对各大业务中心的高性能计算资源提出了严峻考验,也对如何有效生成多尺度初始集合扰动和模式物理扰动,并保证这些扰动的物理协调性提出了极具挑战性的科学和工程问题。

(2)发展全球中期到次季节-季节(S2S)预测的一体化集合预报系统。由于次季节-季节预测中不确定性来源变得愈发多源和复杂,因此开展S2S的集合预报是国际前沿问题。目前国际主要业务中心的发展趋势是利用一体化海-陆-气耦合模式开展从短期、中期到次季节的集合预报。这方面的主要前沿科学问题是如何构建海-气耦合系统的初始集合扰动,以及如何在集合预报中考虑外强迫不确定性对S2S集合预报的影响。

(3)随着全球集合预报分辨率的提升,需要重新考虑区域集合预报系统的发展定位和关键科学问题。区域集合预报需要实现比全球集合预报更高的分辨率,未来可能将向次千米级分辨率发展。其预报对象可能也会逐渐覆盖更小的城区尺度的气象要素变化。而且,如何更有效地考虑初始、侧边界和模式过程多源扰动的协调性和非线性相互作用,仍然是区域集合预报的关键科学问题。

(4)AI技术的兴起给集合预报带来前所未有的挑战和机遇。集合预报的本质是统计采样问题,而AI工具则擅长构建变量的统计特征和变量间的非线性关系。AI技术如何能有效地应用到集合预报中是一个非常宏大且前沿的科学和工程问题。未来这方面的发展将有希望极大地推动集合预报水平的提升。

参考文献

蔡沅辰, 闵锦忠, 庄潇然. 2017. 不同随机物理扰动方案在一次暴雨集合预报中的对比研究. 高原气象, 36(2): 407-423. Cai Y C, Min J Z, Zhuang X R. 2017. Comparison of different stochastic physics perturbation schemes on a storm-scale ensemble forecast in a heavy rain event. Plateau Meteor, 36(2): 407-423 (in Chinese)

陈超辉, 王勇, 何宏让等. 2021. 随机物理集合预报研究进展. 气象科技进展, 11(3): 48-57. Chen C H, Wang Y, He H R, et al. 2021. Review of the ensemble prediction using stochastic physics. Adv Meteor Sci Technol, 11(3): 48-57 (in Chinese)

陈德辉, 薛纪善, 杨学胜等. 2008. GRAPES新一代全球/区域多尺度统一数值预报模式总体设计研究. 科学通报, 53(20): 2396-2407. Chen D H, Xue J S, Yang X S, et al. 2008. New generation of multi-scale NWP system (GRAPES): General scientific design. Chinese Sci Bull, 53(22): 3433-3445

陈静, 陈德辉, 颜宏. 2002. 集合数值预报发展与研究进展. 应用气象学报, 13(4): 497-507. Chen J, Chen D H, Yan H. 2002. A brief review on the development of ensemble prediction system. J Appl Meteor Sci, 13(4): 497-507 (in Chinese)

陈静, 薛纪善, 颜宏. 2003. 华南中尺度暴雨数值预报的不确定性与集合预报试验. 气象学报, 61(4): 432-446. Chen J, Xue J S, Yan H. 2003. The uncertainty of mesoscale numerical prediction of South China heavy rain and the ensemble simulations. Acta Meteor Sinica, 61(4): 432-446 (in Chinese)

陈静, 薛纪善, 颜宏. 2005. 一种新型的中尺度暴雨集合预报初值扰动方法研究. 大气科学, 29(5): 717-726. Chen J, Xue J S, Yan H. 2005. A new initial perturbation method of ensemble mesoscale heavy rain prediction. Chinese J Atmos Sci, 29(5): 717-726 (in Chinese)

陈静, 李晓莉. 2020. GRAPES 全球/区域集合预报系统 10 年发展回顾及展望. 气象科技进展, 10(2): 9-18, 29. Chen J, Li X L. 2020. The review of 10 years development of the GRAPES global/regional ensemble prediction. Adv Meteor Sci Technol, 10(2): 9-18, 29 (in Chinese)

邓国, 龚建东, 邓莲堂等. 2010. 国家级区域集合预报系统研发和性能检验. 应用气象学报, 21(5): 513-523. Deng G, Gong J D, Deng L T, et al. 2010. Development of mesoscale ensemble prediction system at national meteorological center. J Appl Meteor Sci, 21(5): 513-523 (in Chinese)

杜钧, 陈静. 2010. 单一值预报向概率预报转变的基础: 谈谈集合预报及其带来的变革. 气象, 36(11): 1-11. Du J, Chen J. 2010. The corner stone in facilitating the transition from deterministic to probabilistic forecasts-ensemble forecasting and its impact on numerical weather prediction. Meteor Mon, 36(11): 1-11 (in Chinese)

杜钧, 邓国. 2020. “预报挑战度”和“可预报性演变指数”简介. 气象科技进展, 10(2): 75-77. Du J, Deng G. 2020. An introduction to "measure of forecast challenge" and "predictability horizon diagram index". Adv Meteor Sci Technol, 10(2): 75-77 (in Chinese)

段晚锁, 丁瑞强, 周菲凡. 2013. 数值天气预报和气候预测可预报性研究的若干动力学方法. 气候与环境研究, 18(4): 524-538. Duan W S, Ding R Q, Zhou F F. 2013. Several dynamical methods used in predictability studies for numerical weather forecasts and climate prediction. Climatic Environ Res, 18(4): 524-538 (in Chinese)

冯汉中, 陈静, 何光碧等. 2006. 长江上游暴雨短期集合预报系统试验与检验. 气象, 32(8): 12-16. Feng H Z, Chen J, He G B, et al. 2006. Simulation and test of short-range ensemble prediction system for heavy rainfall in the upper reach of Changjiang River. Meteor Mon, 32(8): 12-16 (in Chinese)

高丽, 陈静, 郑嘉雯等. 2019. 极端天气的数值模式集合预报研究进展. 地球科学进展, 34(7): 706-716. Gao L, Chen J, Zheng J W, et al. 2019. Progress in researches on ensemble forecasting of extreme weather based on numerical models. Adv Earth Sci, 34(7): 706-716 (in Chinese)

韩雨盟, 陈静, 彭飞等. 2023. 全球集合预报位温系统偏差和随机误差结合的模式倾向扰动方法. 气象学报, 81(4): 592-604. Han Y M, Chen J, Peng F, et al. 2023. A model tendency perturbation method that combines systematic bias of potential temperature and random errors in global ensemble prediction. Acta Meteor Sinica, 81(4): 592-604 (in Chinese)

霍振华, 刘永柱, 陈静等. 2020. 热带气旋奇异向量在 GRAPES 全球集合预报中的初步应用. 气象学报, 78(1): 48-59. Huo Z H, Liu Y Z, Chen J, et al. 2020. The preliminary appliation of tropical cyclone targeted singular vectors in the GRAPES global ensemble forecasts. Acta Meteor Sinica, 78(1): 48-59 (in Chinese)

纪永明, 陈静, 矫梅燕等. 2011. 基于多中心 TIGGE 资料的区域 GRAPES 集合预报初步试验. 气象, 37(4): 392-402. Ji Y M, Chen J, Jiao M Y, et al. 2011. The preliminary experiment of GRAPES-MESO ensemble prediction based on TIGGE data. Meteor Mon, 37(4): 392-402 (in Chinese)

李翀. 2001. 长江流域实现可持续发展生态环境管理综合决策模型[D]. 北京: 中国水利水电科学研究院. Li C. 2001. An integrated decision-making model of ecological and environmental management for sustainable development in the Yangtze River Basin[D]. Beijing: China Institute of Water Resources and Hydropower Research (in Chinese)

李俊, 杜钧, 王明欢等. 2009. 中尺度暴雨集合预报系统研发中的初值扰动试验. 高原气象, 28(6): 1365-1375. Li J, Du J, Wang M H, et al. 2009. Experiments of perturbing initial conditions in the development of mesoscale ensemble prediction system for heavy rainstorm forecasting. Plateau Meteor, 28(6): 1365-1375 (in Chinese)

李俊, 杜钧, 刘羽. 2015. 北京“7.21”特大暴雨不同集合预报方案的对比试验. 气象学报, 73(1): 50-71. Li J, Du J, Liu Y. 2015. A comparison of initial condition-, multi-physics- and stochastic physics-based ensembles in predicting Beijing "7.21" excessive storm rain event. Acta Meteor Sinica, 73(1): 50-71 (in Chinese)

李俊, 杜钧, 刘羽等. 2017. 不同扰动方法集合离散度演变的异同性暨地形扰动初探. 气象学报, 75(1): 123-146. Li J, Du J, Liu Y, et al. 2017. Similarities and differences in the evolution of ensemble spread using various ensemble perturbation methods including topography perturbation. Acta Meteor Sinica, 75(1): 123-146 (in Chinese)

李小泉, 刘金达, 汪迎辉. 1997. 集合预报及其在中期天气预报中的应用. 气象, 23(8): 3-9. Li X Q, Liu J D, Wang Y H. 1997. The ensemble prediction and its application in medium range weather forecast. Meteor Mon, 23(8): 3-9 (in Chinese)

李晓莉, 刘永柱. 2019. GRAPES 全球奇异向量方法改进及试验分析. 气象学报, 77(3): 552-562. Li X L, Liu Y Z. 2019. The improvement of GRAPES global extratropical singular vectors and experimental study. Acta Meteor Sinica, 77(3): 552-562 (in Chinese)

李泽椿, 陈德辉. 2002. 国家气象中心集合数值预报业务系统的发展及应用. 应用气象学报, 13(1): 1-15. Li Z C, Chen D H. 2002. The development and application of the operational ensemble prediction system at National Meteorological Center. J Appl Meteor Sci, 13(1): 1-15 (in Chinese)

刘琳, 陈静, 汪娇阳. 2018. 基于 T639 集合预报的持续性强降水中期客观预报技术研究. 气象学报, 76(2): 228-240. Liu L, Chen J, Wang J Y.

2018. A study on medium-range objective weather forecast technology for persistent heavy rainfall events based on T639 ensemble forecast. Acta Meteor Sinica, 76(2): 228-240 (in Chinese)

刘永柱, 杨学胜, 王洪庆. 2011. GRAPES 奇异向量研究及其在暴雨集合预报中的应用. 北京大学学报(自然科学版), 47(2): 271-277. Liu Y Z, Yang X S, Wang H Q. 2011. Research on GRAPES singular vectors and application to heavy rain ensemble prediction. Acta Sci Nat Univ Pekin, 47(2): 271-277 (in Chinese)

刘永柱, 沈学顺, 李晓莉. 2013. 基于总能量模的 GRAPES 全球模式奇异向量扰动研究. 气象学报, 71(3): 517-526. Liu Y Z, Shen X S, Li X L. 2013. Researeh on the singular vector perturbation of the GRAPES global model based on the total energy norm. Acta Meteor Sinica, 71(3): 517-526 (in Chinese)

刘永柱, 张林, 金之雁. 2017. GRAPES 全球切线性和伴随模式的调优. 应用气象学报, 28(1): 62-71. Liu Y Z, Zhang L, Jin Z Y. 2017. The optimization of GRAPES global tangent linear model and adjoint model. J Appl Meteor Sci, 28(1): 62-71 (in Chinese)

龙柯吉, 陈静, 马旭林等. 2011. 基于集合卡尔曼变换的区域集合预报初步研究. 成都信息工程学院学报, 26(1): 37-46. Long K J, Chen J, Ma X L, et al. 2011. The preliminary study on ensemble prediction of GRAPES-meso based on ETKF. J Chengdu Univ Inf Technol, 26(1): 37-46 (in Chinese)

马清, 龚建东, 李莉等. 2008. 中尺度集合预报的二阶矩离散度订正研究. 气象, 34(11): 15-21. Ma Q, Gong J D, Li L, et al. 2008. Study on the 2nd moment spread-correction of mesoscale ensemble forecast system. Meteor Mon, 34(11): 15-21 (in Chinese)

马旭林, 薛纪善, 陆维松. 2008. GRAPES 全球集合预报的集合卡尔曼变换初始扰动方案初步研究. 气象学报, 66(4): 526-536. Ma X L, Xue J S, Lu W S. 2008. Preliminary study on ensemble transform Kalman filter-based initial perturbation scheme in GRAPES global ensemble prediction. Acta Meteor Sinica, 66(4): 526-536 (in Chinese)

马旭林, 计燕霞, 周勃旸等. 2018. GRAPES 区域集合预报尺度混合初始扰动构造的新方案. 大气科学学报, 41(2): 248-257. Ma X L, Ji Y X, Zhou B Y, et al. 2018. A new scheme of blending initial perturbation of the GRAPES regional ensemble prediction system. Trans Atmos Sci, 41(2): 248-257 (in Chinese)

马雅楠, 陈静, 徐致真等. 2023. GRAPES 对流尺度集合预报模式中不同尺度初始扰动能量的演变特征. 大气科学, 47(5): 1541-1556. Ma Y N, Chen J, Xu Z Z, et al. 2023. Evolution characteristics of initial perturbation energy at different scales in convection-permitting ensemble prediction of GRAPES. Chinese J Atmos Sci, 47(5): 1541-1556 (in Chinese)

穆穆, 陈博宇, 周菲凡等. 2011. 气象预报的方法与不确定性. 气象, 37(1): 1-13. Mu M, Chen B Y, Zhou F F, et al. 2011. Methods and uncertainties of meteorological forecast. Meteor Mon, 37(1): 1-13 (in Chinese)

潘贤, 王秋萍, 张瑜等. 2021. 分析约束的集合预报初始扰动构造方案的研究. 大气科学, 45(6): 1327-1344. Pan X, Wang Q P, Zhang Y, et al. 2021. Analysis constraints scheme of initial perturbation of ensemble prediction. Chinese J Atmos Sci, 45(6): 1327-1344 (in Chinese)

彭飞, 李晓莉, 陈静等. 2019. GRAPES 全球集合预报系统模式扰动随机动能补偿方案初步探究. 气象学报, 77(2): 180-195. Peng F, Li X L, Chen J, et al. 2019. A stochastic kinetic energy backscatter scheme for model perturbations in the GRAPES global ensemble prediction system. Acta Meteor Sinica, 77(2): 180-195 (in Chinese)

彭飞, 李晓莉, 陈静. 2020. GRAPES 全球集合预报系统不同随机物理扰动方案影响分析. 气象学报, 78(6): 972-987. Peng F, Li X L, Chen J. 2020. Impacts of different stochastic physics perturbation schemes on the GRAPES global ensemble prediction system. Acta Meteor Sinica, 78(6): 972-987 (in Chinese)

彭飞, 陈静, 李晓莉等. 2024. CMA-GEPS 极端温度预报指数及 2022 年夏季极端高温预报检验评估. 气象学报, 82(2): 190-207. Peng F, Chen J, Li X L, et al. 2024. Development of the CMA-GEPS extreme forecast index and its application to verification of summer 2022 extreme high temperature forecasts. Acta Meteor Sinica, 82(2): 190-207 (in Chinese)

齐倩倩, 朱跃建, 陈静等. 2022. 基于 GRAPES-GFS 次季节预报的误差诊断和预报能力分析. 大气科学, 46(2): 327-345. Qi Q Q, Zhu Y J, Chen J, et al. 2022. Error diagnosis and assessment of sub-seasonal forecast using GRAPES-GFS model. Chinese J Atmos Sci, 46(2): 327-345 (in Chinese)

沈学顺, 王建捷, 李泽椿等. 2020. 中国数值天气预报的自主创新发展. 气象学报, 78(3): 451-476. Shen X S, Wang J J, Li Z C, et al. 2020. China's independent and innovative development of numerical weather prediction. Acta Meteor Sinica, 78(3): 451-476 (in Chinese)

谭宁, 陈静, 田华. 2013. 两种模式随机扰动方案比较及扰动传播分析. 气象, 39(5): 543-555. Tan N, Chen J, Tian H. 2013. Comparison between two global model stochastic perturbation schemes and analysis of perturbation propagation. Meteor Mon, 39(5): 543-555 (in Chinese)

谭燕, 陈德辉. 2007. 基于非静力模式物理扰动的中尺度集合预报试验. 应用气象学报, 18(3): 396-406. Tan Y, Chen D H. 2007. Meso-scale ensemble forecasts on physical perturbation using a non-hydrostatic model. J Appl Meteor Sci, 18(3): 396-406 (in Chinese)

田华, 邓国, 胡江凯等. 2007. 全球 T213 数值集合预报业务系统简介//中国气象学会 2007 年年会天气预报预警和影响评估技术分会场论文集. 广州: 中国气象学会, 2658-2662. Tian H, Deng G, Hu J K, et al. 2007. Introduction to the global T213 numerical ensemble forecast service system//Proceedings of the 2007 Annual Meeting of the Chinese Meteorological Society on Weather Forecasting, Early Warning and Impact Assessment Technology. Guangzhou: Chinese Meteorological Society, 2658-2662 (in Chinese)

田伟红, 庄世宇. 2008. ETKF 方法在区域集合预报中的初步应用. 气象, 34(8): 35-39. Tian W H, Zhuang S Y. 2008. Application of ETKF method to regional ensemble forecasts. Meteor Mon, 34(8): 35-39 (in Chinese)

汪娇阳, 陈静, 刘琳等. 2014. 极端降水天气预报指数对气候累积概率分布

敏感性研究. 暴雨灾害, 33(4): 313-319. Wang J Y, Chen J, Liu L, et al. 2014. The sensitivity of the extreme precipitation forecast index on climatological cumulative probability distribution. Torrential Rain Disaster, 33(4): 313-319 (in Chinese)

王晨稀, 姚建群, 梁旭东. 2007. 上海区域降水集合预报系统改进的对比试验. 气象科学, 27(5): 481-487. Wang C X, Yao J Q, Liang X D. 2007. The comparing experiment of improving the operational ensemble prediction system for shanghai regional precipitation. Scientia Meteor Sinica, 27(5): 481-487 (in Chinese)

王婧卓, 陈静, 庄照荣等. 2018. GRAPES 区域集合预报模式的初值扰动增长特征. 大气科学, 42(2): 367-382. Wang J Z, Chen J, Zhuang Z R, et al. 2018. Characteristics of initial perturbation growth rate in the regional ensemble prediction system of GRAPES. Chinese J Atmos Sci, 42(2): 367-382 (in Chinese)

王秋萍, 潘贤, 周勃旸等. 2023. 区域集合预报系统的集合变换卡尔曼滤波初始扰动的余弦分析约束方案. 大气科学, 47(6): 1731-1745. Wang Q P, Pan X, Zhou B Y, et al. 2023. Cosine analysis constraint scheme based on ETKF initial perturbations in the GRAPES regional ensemble prediction system. Chinese J Atmos Sci, 47(6): 1731-1745 (in Chinese)

吴政秋, 张进, 陈静等. 2020. GRAPES 区域集合预报条件性台风涡旋重定位方法研究. 气象学报, 78(2): 163-176. Wu Z Q, Zhang J, Chen J, et al. 2020. The study on the method of conditional typhoon vortex relocation for GRAPES regional ensemble prediction. Acta Meteor Sinica, 78(2): 163-176 (in Chinese)

夏凡, 陈静. 2012. 基于 T213 集合预报的极端天气预报指数及温度预报应用试验. 气象, 38(12): 1492-1501. Xia F, Chen J. 2012. The research of extreme forecast index based on the T213 ensemble forecast and the experiment in predicting temperature. Meteor Mon, 38(12): 1492-1501 (in Chinese)

徐致真, 陈静, 王勇等. 2019. 中尺度降水集合预报随机参数扰动方法敏感性试验. 气象学报, 77(5): 849-868. Xu Z Z, Chen J, Wang Y, et al. 2019. Sensitivity experiments of a stochastically perturbed parameterizations (SPP) scheme for mesoscale precipitation ensemble prediction. Acta Meteor Sinica, 77(5): 849-868 (in Chinese)

杨绚, 代刊, 朱跃建. 2022. 深度学习技术在智能网格天气预报中的应用进展与挑战. 气象学报, 80(5): 649-667. Yang X, Dai K, Zhu Y J. 2022. Progress and challenges of deep learning techniques in intelligent grid weather forecasting. Acta Meteor Sinica, 80(5): 649-667 (in Chinese)

杨学胜, 陈德辉, 冷亭波等. 2002. 时间滞后与奇异向量初值生成方法的比较试验. 应用气象学报, 13(1): 62-66. Yang X S, Chen D H, Leng T B, et al. 2002. The comparison experiments of SV and LAF initial perturbation techniques used at the NMC ensemble prediction system. J Appl Meteor Sci, 13(1): 62-66 (in Chinese)

叶璐, 刘永柱, 陈静等. 2020. 集合预报多尺度奇异向量初值扰动方法研究. 气象学报, 78(4): 648-664. Ye L, Liu Y Z, Chen J, et al. 2020. A study on multi-scale singular vector initial perturbation method for ensemble prediction. Acta Meteor Sinica, 78(4): 648-664 (in Chinese)

袁月, 李晓莉, 陈静等. 2016. GRAPES 区域集合预报系统模式不确定性的随机扰动技术研究. 气象, 42(10): 1161-1175. Yuan Y, Li X L, Chen J, et al. 2016. Stochastic parameterization toward model uncertainty for the GRAPES mesoscale ensemble prediction system. Meteor Mon, 42(10): 1161-1175 (in Chinese)

张涵斌, 智协飞, 陈静等. 2017. 区域集合预报扰动方法研究进展综述. 大气科学学报, 40(2): 145-157. Zhang H B, Zhi X F, Chen J, et al. 2017. Achievement of perturbation methods for regional ensemble forecast. Trans Atmos Sci, 40(2): 145-157 (in Chinese)

智协飞, 季晓东, 张璟等. 2013. 基于 TIGGE 资料的地面气温和降水的多模式集成预报. 大气科学学报, 36(3): 257-266. Zhi X F, Ji X D, Zhang J, et al. 2013. Multimodel ensemble forecasts of surface air temperature and precipitation using TIGGE datasets. Trans Atmos Sci, 36(3): 257-266 (in Chinese)

智协飞, 王田, 季焱. 2020. 基于深度学习的中国地面气温的多模式集成预报研究. 大气科学学报, 43(3): 435-446. Zhi X F, Wang T, Ji Y. 2020. Multimodel ensemble forecasts of surface air temperature over China based on deep learning approach. Trans Atmos Sci, 43(3): 435-446 (in Chinese)

庄潇然, 闵锦忠, 武天杰等. 2017. 风暴尺度集合预报中不同初始扰动的多尺度发展特征研究. 高原气象, 36(3): 811-825. Zhuang X R, Min J Z, Wu T J, et al. 2017. Development mechanism of multi-scale perturbation based on different perturbation methods in convection-allowing ensemble prediction. Plateau Meteor, 36(3): 811-825 (in Chinese)

Arakawa A. 2004. The cumulus parameterization problem: Past, present, and future. J Climate, 17(13): 2493-2525

Bauer P, Thorpe A, Brunet G. 2015. The quiet revolution of numerical weather prediction. Nature, 525(7567): 47-55

Berner J, Shutts G J, Leutbecher M, et al. 2009. A spectral stochastic kinetic energy backscatter scheme and its impact on flow-dependent predictability in the ECMWF ensemble prediction system. J Atmos Sci, 66(3): 603-626

Berner J, Fossell K R, Ha S Y, et al. 2015. Increasing the skill of probabilistic forecasts: Understanding performance improvements from model-error representations. Mon Wea Rev, 143(4): 1295-1320

Bowler N E, Arribas A, Mylne K R, et al. 2008. The MOGREPS short-range ensemble prediction system. Quart J Roy Meteor Soc, 134(632): 703-722

Buizza R. 1997. Potential forecast skill of ensemble prediction, and spread and skill distributions of the ECMWF ensemble prediction system. Mon Wea Rev, 125(1): 99-119

Buizza R, Milleer M, Palmer T N. 1999. Stochastic representation of model uncertainties in the ECMWF ensemble prediction system. Quart J Roy Meteor Soc, 125(560): 2887-2908

Charron M, Pellerin G, Spacek L, et al. 2010. Toward random sampling of model error in the Canadian ensemble prediction system. Mon Wea Rev, 138(5): 1877-1901

Chen J, Xue J S, Yan H. 2004. Impacts of diabatic physics parameterization

schemes on mesoscale heavy rainfall shortrange simulation. J Meteor Res, 18(1): 51-72

Chen J, Wang J Z, Du J, et al. 2020. Forecast bias correction through model integration: A dynamical wholesale approach. Quart J Roy Meteor Soc, 146(728): 1149-1168

Chen X, Yuan H L, Xue M. 2018. Spatial spread-skill relationship in terms of agreement scales for precipitation forecasts in a convection-allowing ensemble. Quart J Roy Meteor Soc, 144(710): 85-98

Chen Y X, Chen J, Chen D H, et al. 2021. A simulated radar reflectivity calculation method in numerical weather prediction models. Wea Forecasting, 36(1): 341-359

Chou J F. 1986. Some general properties of the atmospheric model in H space, R space, point mapping, cell mapping//Proceedings of International Summer Colloquium on Nonlinear Dynamics of the Atmosphere. Beijing: Science Press, 187-189

Denis B, Côté J, Laprise R. 2002. Spectral decomposition of two-dimensional atmospheric fields on limited-area domains using the discrete cosine transform (DCT). Mon Wea Rev, 130(7): 1812-1829

Duan W S, Zhou F F. 2013. Non-linear forcing singular vector of a two-dimensional quasi-geostrophic model. Tellus, 65(1): 18452

Duan W S, Huo Z H. 2016. An approach to generating mutually independent initial perturbations for ensemble forecasts: Orthogonal conditional nonlinear optimal perturbations. J Atmos Sci, 73(3): 997-1014

Dutra E, Magnusson L, Wetterhall F, et al. 2013. The 2010-2011 drought in the horn of Africa in ECMWF reanalysis and seasonal forecast products. Int J Climatol, 33(7): 1720-1729

Epstein E S. 1969. Stochastic dynamic prediction. Tellus, 21(6): 739-759

Feng J, Ding R Q, Liu D Q, et al. 2014. The application of nonlinear local lyapunov vectors to ensemble predictions in lorenz systems. J Atmos Sci, 71(9): 3554-3567

Guan H, Zhu Y J. 2017. Development of verification methodology for extreme weather forecasts. Wea Forecasting, 32(2): 479-491

Hamill T M. 1999. Hypothesis tests for evaluating numerical precipitation forecasts. Wea Forecasting, 14(2): 155-167

Hamill T M, Juras J. 2006. Measuring forecast skill: is it real skill or is it the varying climatology?. Quart J Roy Meteor Soc, 132(621C): 2905-2923

Hersbach H, Mureau R, Opsteegh J D, et al. 2000. A short-range to early-medium-range ensemble prediction system for the European area. Mon Wea Rev, 128(10): 3501-3519

Hoffman R N, Kalnay E. 1983. Lagged average forecasting, an alternative to Monte Carlo forecasting. Tellus, 35(2): 100-118

Hohenegger C, Schar C. 2007. Atmospheric predictability at synoptic versus cloud-resolving scales. Bull Amer Meteor Soc, 88(11): 1783-1794

Hollingsworth A. 1979. An experiment in Monte Carlo forecasting// Proceedings of Workshop on Stochastic Dynamic Forecasting. Reading: ECMWF, 65-85

Houtekamer P L, Derome J. 1995. Methods for ensemble prediction. Mon Wea Rev, 123(7): 2181-2196

Houtekamer P L, Lefaivre L, Derome J, et al. 1996. A system simulation approach to ensemble prediction. Mon Wea Rev, 124(6): 1225-1242

Houtekamer P L, Mitchell H L. 2005. Ensemble Kalman filtering. Quart J Roy Meteor Soc, 131(613): 3269-3289

Isaksen L, Bonavita M, Buizza R, et al. 2010. Ensemble of data assimilations at ECMWF. Reading: ECMWF, 636

Jankov I, Berner J, Beck J, et al. 2017. A performance comparison between multiphysics and stochastic approaches within a north American RAP ensemble. Mon Wea Rev, 145(4): 1161-1179

Jankov I, Beck J, Wolff J, et al. 2019. Stochastically perturbed parameterizations in an HRRR-based ensemble. Mon Wea Rev, 147(7): 153-173

Ji L Y, Zhi X F, Simmer C, et al. 2020. Multimodel ensemble forecasts of precipitation based on an object-based diagnostic evaluation. Mon Wea Rev, 148(6): 2591-2606

Ji Y, Zhi X F, Ji L Y, et al. 2023. Conditional ensemble model output statistics for postprocessing of ensemble precipitation forecasting. Wea Forecasting, 38(9): 1707-1718

Jiao M Y. 2010. Progress on the key technology development in application of ensemble prediction products associated with TIGGE. J Meteor Res, 24(1): 136

Johnson A. 2014. Optimal design of a multi-scale ensemble system for convective scale probabilistic forecasts: Data assimilation and initial condition perturbation methods[D]. Norman: University of Oklahoma

Jolliffe I T, Stephenson D B. 2012. Forecast Verification: A Practitioner's Guide in Atmospheric Science. 2nd ed. Chichester: John Wiley & Sons, 274pp

Krishnamurti T N, Kishtawal C M, LaRow T E, et al. 1999. Improved weather and seasonal climate forecasts from multimodel superensemble. Science, 285(5433): 1548-1550

Lalaurette F. 2003. Early detection of abnormal weather conditions using a probabilistic extreme forecast index. Quart J Roy Meteor Soc, 129(594): 3037-3057

Leith C E. 1974. Theoretical skill of Monte Carlo forecasts. Mon Wea Rev, 102(6): 409-418

Leutbecher M, Lock S J, Ollinaho P, et al. 2017. Stochastic representations of model uncertainties at ECMWF: State of the art and future vision. Quart J Roy Meteor Soc, 143(707): 2315-2339

Li J P, Zeng Q C, Chou J F. 2000. Computational uncertainty principle in nonlinear ordinary differential equations (Ⅰ)—Numerical results. Sci China Ser E Technol Sci, 43(5): 449-460

Li X L, Charron M, Spacek L, et al. 2008. A regional ensemble prediction system based on moist targeted singular vectors and stochastic parameter perturbations. Mon Wea Rev, 136(2): 443-462

Liu X, Chen J, Liu Y Z, et al. 2024. An initial perturbation method for the multiscale singular vector in global ensemble prediction. Adv Atmos Sci,

41(3): 545-563

Lorenz E N. 1963. Deterministic nonperiodic flow. J Atmos Sci, 20(2): 130-141

Lyu Y, Zhu S P, Zhi X F, et al. 2023. Improving subseasonal-to-seasonal prediction of summer extreme precipitation over Southern China based on a deep learning method. Geophys Res Lett, 50(24): e2023GL106245

Molteni F, Buizza R, Palmer T N, et al. 1996. The ECMWF ensemble prediction system: Methodology and validation. Quart J Roy Meteor Soc, 122(529): 73-119

Mu M, Duan W S, Wang B. 2003. Conditional nonlinear optimal perturbation and its applications. Nonlinear Processes Geophys, 10(6): 493-501

Mylne K, Chen J, Erfani A, et al. 2022. Guidelines for Ensemble Prediction System. Geneva: WMO, 8-40

Nielsen E R. 2016. Using convection-allowing ensembles to understand the predictability of extreme rainfall[D]. Fort Collins: Colorado State University

Ono K, Kunii M, Honda Y. 2021. The regional model—based mesoscale ensemble prediction system, MEPS, at the Japan meteorological agency. Quart J Roy Meteor Soc, 147(734): 465-484

Palmer T N, Buizza R, Doblas-Reyes F, et al. 2009. Stochastic parametrization and model uncertainty. Reading: ECMWF

Pauluis O, Schumacher J. 2013. Radiation impacts on conditionally unstable moist convection. J Atmos Sci, 70(4): 1187-1203

Qiao X S, Wang S Z, Min J Z. 2017. A stochastic perturbed parameterization tendency scheme for diffusion (SPPTD) and its application to an idealized supercell simulation. Mon Wea Rev, 145(6): 2119-2139

Qiao X S, Wang S Z, Min J Z. 2018. The impact of a stochastically perturbing microphysics scheme on an idealized supercell storm. Mon Wea Rev, 146(1): 95-118

Raynaud L, Touzé B, Arbogast P. 2018. Detection of severe weather events in a high-resolution ensemble prediction system using the extreme forecast index (EFI) and shift of tails (SOT). Wea Forecasting, 33(4): 901-908

Sanchez C, Williams K D, Collins M. 2016. Improved stochastic physics schemes for global weather and climate models. Quart J Roy Meteor Soc, 142(694): 147-159

Shutts G. 2005. A kinetic energy backscatter algorithm for use in ensemble prediction systems. Quart J Roy Meteor Soc, 131(612): 3079-3102

Steinhoff J, Underhill D. 1994. Modification of the Euler equations for "vorticity confinement": Application to the computation of interacting vortex rings. Phys Fluids, 6(8): 2738-2744

Stensrud D J, Bao J W, Warner T T. 2000. Using initial condition and model physics perturbations in short-range ensemble simulations of mesoscale convective systems. Mon Wea Rev, 128(7): 2077-2107

Su X, Yuan H L, Zhu Y J, et al. 2014. Evaluation of TIGGE ensemble predictions of northern Hemisphere summer precipitation during 2008-2012. J Geophys Res Atmos, 119(12): 7292-7310

Tompkins, A M, Berner J. 2008. A stochastic convective approach to account for model uncertainty due to unresolved humidity variability. J Geophys Res Atmos, 113(9): D18101

Torn R D, Hakim G J. 2008. Performance characteristics of a pseudo-operational ensemble kalman filter. Mon Wea Rev, 136(10): 3947-3963

Toth Z, Kalnay E. 1993. Ensemble forecasting at NMC: The generation of perturbations. Bull Amer Meteor Soc, 74(12): 2317-2330

Tsonevsky I, Doswell III C A, Brooks H E. 2018. Early warnings of severe convection using the ECMWF extreme forecast index. Wea Forecasting, 33(3): 857-871

Wang L, Shen X S, Liu J J, et al. 2020. Model uncertainty representation for a convection-allowing ensemble prediction system based on CNOP-P. Adv Atmos Sci, 37(8): 817-831

Wang X G, Bishop C H. 2003. A comparison of breeding and ensemble transform Kalman filter ensemble forecast schemes. J Atmos Sci, 60(9): 1140-1158

Wang Y, Bellus M, Geleyn J F, et al. 2014. A new method for generating initial condition perturbations in a regional ensemble prediction system: Blending. Mon Wea Rev, 142(5): 2043-2059

Wei M Z, Toth Z, Wobus R, et al. 2006. Ensemble transform Kalman filter-based ensemble perturbations in an operational global prediction system at NCEP. Tellus, 58(1): 28-44

Wei M Z, Toth Z, Wobus R, et al. 2008. Initial perturbations based on the ensemble transform (ET) technique in the NCEP global operational forecast system. Tellus, 60(1): 62-79

Whitaker J S, Hamill T M. 2002. Ensemble data assimilation without perturbed observations. Mon Wea Rev, 130(7): 1913-1924

Wilks D S. 2011. Forecast verification. Int Geophys, 100: 301-394

Williams R M, Ferro C A T, Kwasniok F. 2014. A comparison of ensemble post-processing methods for extreme events. Quart J Roy Meteor Soc, 140(680): 1112-1120

Xia Y, Chen J, Du J, et al. 2019. A unified scheme of stochastic physics and bias correction in an ensemble model to reduce both random and systematic errors. Wea Forecasting, 34(6): 1675-1691

Xu Z Z, Chen J, Mu M, et al. 2022a. A nonlinear representation of model uncertainty in a convective-scale ensemble prediction system. Adv Atmos Sci, 39(9): 1432-1450

Xu Z Z, Chen J, Mu M, et al. 2022b. A stochastic and non-linear representation of model uncertainty in a convective-scale ensemble prediction system. Quart J Roy Meteor Soc, 148(746): 2507-2531

Yang M, Yu P L, Zhang L F, et al. 2024. Predictability of the 7·20 extreme rainstorm in Zhengzhou in stochastic kinetic-energy backscatter ensembles. Sci China Earth Sci, 67(7): 2226-2241

Yano J I, Ziemiański M Z, Cullen M, et al. 2018. Scientific challenges of convective-scale numerical weather prediction. Bull Amer Meteor Soc, 99(4): 699-710

Yuan H L, Mullen S L, Gao X G, et al. 2005. Verification of probabilistic quantitative precipitation forecasts over the southwest United States

during winter 2002/03 by the RSM ensemble system. Mon Wea Rev, 133(1): 279-294

Zhang F Q, Bei N F, Rotunno R, et al. 2007. Mesoscale predictability of moist baroclinic waves: Convection-permitting experiments and multistage error growth dynamics. J Atmos Sci, 64(10): 3579-3594

Zhang H, Duan W S, Zhang Y C. 2023. Using the orthogonal conditional nonlinear optimal perturbations approach to address the uncertainties of tropical cyclone track forecasts generated by the WRF model. Wea Forecasting, 38(10): 1907-1933

Zhang H B, Chen J, Zhi X F, et al. 2015. Study on multi-scale blending initial condition perturbations for a regional ensemble prediction system. Adv Atmos Sci, 32(8): 1143-1155

Zhang X Y, Min J Z, Wu T J. 2020. A study of ensemble-sensitivity-based initial condition perturbation methods for convection-permitting ensemble forecasts. Atmos Res, 234: 104741

Zhang Y C, Duan W S, Vannitsem S, et al. 2023. A new approach to represent model uncertainty in the forecasting of tropical cyclones: The orthogonal nonlinear forcing singular vectors. Quart J Roy Meteor Soc, 149(755): 2206-2232

Zhao X H, Torn R D. 2022. Evaluation of independent stochastically perturbed parameterization tendency (iSPPT) scheme on HWRF-based ensemble tropical cyclone intensity forecasts. Mon Wea Rev, 150(10): 2659-2674

Zhi X F, Qi H X, Bai Y Q, et al. 2012. A comparison of three kinds of multimodel ensemble forecast techniques based on the TIGGE data. Acta Meteor Sinica, 26(1): 41-51

Zhou X Q, Zhu Y J, Hou D C, et al. 2016. A comparison of perturbations from an ensemble transform and an ensemble Kalman filter for the NCEP global ensemble forecast system. Wea Forecasting, 31(6): 2057-2074

Zhou X Q, Zhu Y J, Hou D C, et al. 2017. Performance of the new NCEP global ensemble forecast system in a parallel experiment. Wea Forecasting, 32(5): 1989-2004

Zhou X Q, Zhu Y J, Hou D C, et al. 2022. The development of the NCEP global ensemble forecast system version 12. Wea Forecasting, 37(6): 1069-1084

Zhu S P, Zhi X F, Ge F, et al. 2021. Subseasonal forecast of surface air temperature using superensemble approaches: Experiments over northeast Asia for 2018. Wea Forecasting, 36(1): 39-51

Zhu Y J, Toth Z, Wobus R, et al. 2002. The economic value of ensemble-based weather forecasts. Bull Amer Meteor Soc, 83(1): 73-84

Zhuang X R, Xue M, Min J Z, et al. 2021. Error growth dynamics within convection-allowing ensemble forecasts over central U. S. regions for days of active convection. Mon Wea Rev, 149(4): 959-977